THE UNIVERSITY
OF BIRMINGHAM

New Mobile Positioning Techniques for LOS/NLOS Environments and Investigation of Topology Influence

Hao Li

A thesis submitted to the University of Birmingham for the degree of Doctor of Philosophy

School of Electronic, Electrical and System Engineering

The University of Birmingham

January 2015

Abstract

The advent of wireless location technology and the increase in location-based services has meant the need to investigate efficient network-based location methods becoming of paramount importance. Therefore, the interest in wireless positioning techniques has been increasing over recent decades. Among mobile positioning techniques, the Time of Arrival (TOA) and Time Difference of Arrival (TDOA) look promising. For the purpose of dealing with such technologies, some classic algorithms such as least square, most likelihood and Taylor method have been used to solve the estimation, which distinguishes the location. However, in real practice, there are certain factors that influence the level of location accuracy. The two most significant factors are cellular topologies and non-line-of-sight (NLOS) effect.

This thesis reviews existing approaches and suggests innovative methods for both line-of-sight (LOS) and NLOS scenarios. A simulation platform is designed to test and compare the performances of these algorithms. The results of the simulation compared with actual position measurements demonstrate that the innovative approaches have high positioning accuracy. Additionally, this thesis demonstrates different types of cellular topologies and develops a simulation to show how the cellular topology affects the positioning quality level. Finally, this thesis implements an experiment to exhibit how the innovative algorithms perform in the real world.

Acknowledgement

My first debt of gratitude must go to my supervisor Dr. Mourad Oussalah. He patiently provided the vision, encouragement and advice necessary for me to proceed through the doctoral program and complete my thesis. I want to thank him for his unflagging encouragement and serving as role models to me as a junior member of academia.

I would like to thank examiners of my thesis, Prof. Abdennour El Rhalibi and Dr. Alexandros Feresidis for accepting to examine this thesis. Their comments will be of paramount importance to improve the technical quality of this thesis.

I would also like to express my deep gratitude to my grandfather, Prof. Dekong Ding, who has been very supportive and generous in supervising me for the math problems, as well as encouraged me to be confident in PhD research.

I want to thank my best friends Miss Bing Hua for her editorial support.

Last but not least, I would like to thank my beloved parents, for their endless support, love and understanding.

Acronyms

2D	Two-Dimensional
A-GPS	Assisted Global Positioning System
AOA	Angle-of-Arrival
BS	Base Station
BSs	Base Stations
CARIN	CAR Information and Navigation system
CDF	Cumulative Distribution Function
CDMA	Code Division Multiple Access
Cell-ID	Cell Identity
CIS	Cybernetic Intelligent Systems
CLS	Constrained LS Algorithm and Quadratic Program
D-GPS	Differential Global Positioning System
FCC	Federal Communications Commission
GDIC	Gradient Descent Iteration – Combination Method
GDOP	Geometric Dilution of Precision
GLE	Geometry Constrained Location Estimation
GNSS	Global Navigation Satellite System
GPS	Global Positioning System
GSM	Global System for Mobile
IPO	Interior Point Optimization

LLS	Linear Least Squares
LMUS	Location Measurement Units
LOS	Line-of-Sight
MLE	Most Likelihood Estimation
MS	Mobile Station
NBS	Number of Base Stations
NLOS	Non-Line-Of-Sight
QP	Quadratic Programming
RF	Radio Frequency
RMSE	Root Mean Square Error
RSS	Received Signal Strength
TDOA	Difference of Arrival
TOA	Time of Arrival
UMTS	Universal Mobile Telecommunications System

Contents List

Figure Contents

Table Contents List

CHAPTER 1: INTRODUCTION

1.1 Background of Localization Issues in Mobile Network

With the development of wireless communication technology, wireless location and positioning play increasingly more important roles. Wireless positioning determines the position of a mobile station in a particular space using wireless communication signals to usually fixed base stations. This includes technology based on GSM, 3G and 4G networks, WiFi based positioning systems, Radio Frequency Identification (RFID), BlueTooth, microwave and Ultra Wide Band Frequency (UWBF). The space of the positioning system can either be local as in enterprise facility / warehouse, location with respect to a set of predefined landmarks in city, or global as in global positioning system (GPS). In both cases, the knowledge of the mobile location enables a vast number of location aware solutions, i.e., target advertising, route planner, emergency intervention. The latter has been recognized as a key in all cellular network operators, where regulator bodies constrained the mobile operators in order to achieve certain level of positioning accuracy regardless the availability of GPS signal. In this respect, one shall mention the location regulation named E911 [1], introduced by the United States Federal Communications Commission (FCC) in 1996. This service started officially in 1998 and has been improved since. Until 2001, E911 managed the basic requirement, but in that year, the FCC compelled all wireless

services to provide user location information with a location error of less than 125m for 67% of calls to the E911 public security service system. Similarly, the European Recommendation E112 requires that wireless providers are able to locate emergency callers within tens of meters [39].

There are several typical applications of mobile positioning, which include:

- **Automated Position Determination Service:** A road-side services that provide drivers with a quick and efficient emergency help on roads [13]
- **Traffic Routing & Scheduling:** It provides helpful fleet management for traffic routing and scheduling of vehicles in real time [13]
- **CAR Information and Navigation (CARIN) System:** It is an in-car navigation system that helps in finding direction from known positions to given destination (s) [37]
- **EasyLiving Project:** Part of Microsoft Research project, concerned with the development of architecture and technologies for intelligent environments which provide cellular phone-based location systems, proposed for determining driving directions and delivering reminders based on the user's location [33]
- **Facebook:** An online social networking service; one of its functions is to provide a wireless location service to online users [34]
- **Google Map:** A desktop and mobile web-mapping service, offering satellite imagery, street maps, and street view perspectives, as well as functions

such as a route planner for traveling by foot, car, bicycle (in beta test), or by public transport [35]

- **RADAR:** One of the first systems to use radio frequency (RF) signal intensity for location-sensing [36]

All these applications, among others, have dramatically improved our lives and wireless location technology has become part of our daily life. Wireless location technologies are also widely used in the military research. USA and Russia started to use global position systems in the 1960s to provide location and navigation services to ground staffs. By the middle of the 1970s, the second generation of global positioning technology was put into service. In the 1990s, Global Positioning System (GPS) [40] became widespread and has now been improved for much better performance and services. At the same time, Europe has moved forward with its own global Navigation Satellite System (GNSS) called Galileo [38]. The GNSS has better accuracy with an error measurement of 1m (as opposite to about 10 m for GPS). The Chinese government has developed an independent satellite navigation system, named BeiDou Navigation Satellite System. It may refer to either the first or second generation of the Chinese navigation system. By 2020, upon its completion, the BeiDou Navigation Satellite System will begin serving global customers.

The dramatic development of mobile communication technology has

encouraged widespread attention and initiated profound research. The next section reviews the various technologies and approaches employed by wireless location systems.

1.2 Wireless Location System

A wireless location system determines the actual location of a mobile station (MS) by testing the transmission signal measurements between the MS and several settled base stations (BSs). In modern wireless communication networks, wireless location system techniques/technologies can be divided into three main classes based on the dominant entity responsible for location processing: terminal-based, network-based and GPS location-based. These are detailed in the next section.

1.2.1 Terminal - Based Location System

In this case, the MS position is determined using the transmitted signal measurements from the surrounding BSs. Based on these measurements (e.g. signal strength, time of arrival, and time difference of arrival), the MS software works out the solution to the positioning problem using a particular algorithm [2]. Therefore, to the mobile terminal holders, terminal-based location is a kind of active location solution processed within the (software) resources implemented in the terminal only. A minimum configuration for the handset is required in order

to enable terminal based location system because of the amount of processing capabilities that maybe required. For example, a surveying instrument for position marking is a terminal-based location system.

1.2.2 Network - Based Location Systems

In contrast to terminal-based location, the network based location systems assume that the MS position is computed by an external entity and communicated back to the terminal. Typically, the signals from emitters to MS are collected and transmitted to some mobile location centre for processing. Once the MS location is estimated, it is sent back to the enquirers. Hence, to the mobile terminal holders, network-based location is a kind of passive location, where the mobile location centre does the work to find mobile terminal positions. This system is widely used in the emergency services. Additionally, some telecom operators, provide location services through a network-based location system. After the location estimation of MS is calculated, position information is sent back to the enquiring mobile set.[3] This system has the advantage that the MS handset does not take part in the location-finding process, thus, it is not necessary to modify the existing handset for a more advanced one to achieve mobile positioning.

1.2.3 Global Positioning System (GPS)

GPS can also be considered as a handset-based position system because most of the processing is performed by the GPS receiver installed on the handset but it is reported here as a separate class because of its restriction to satellite signals and its global nature. As shown in Fig. 1.1, the GPS comprises satellites which are circling the Earth in particular orbits, therefore, at any given moment, at least three satellites fall within LOS to any GPS receiver on Earth [4]. A wireless user must have a handset equipped with a GPS receiver. When the user requests a location, the GPS-enabled handset determines the phone's latitude and longitude based on the satellites' broadcast [4]. The biggest advantage of GPS is its high level of accuracy. However, GPS-enabled handsets are more expensive than normal handsets and furthermore, GPS must have a clear LOS between the receiver and the satellites. Therefore in situations of in urban areas with high building that may obscure the satellite signal as well as in case of indoor environment, GPS performance can deteriorate.

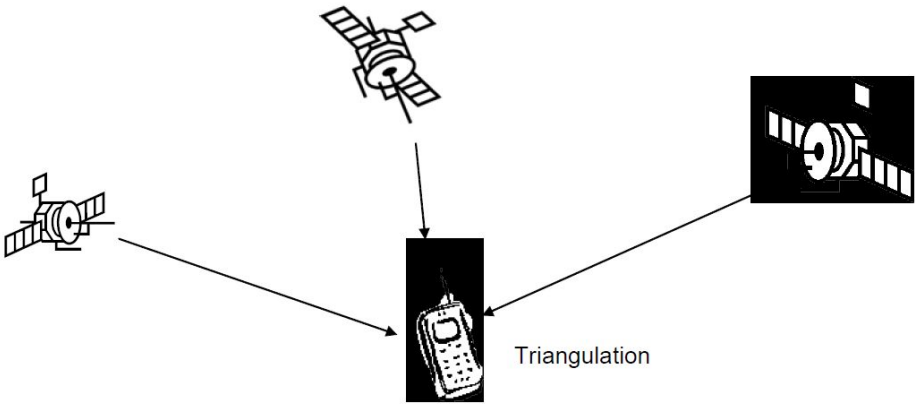

Figure 1.1: An Example of GPS [5]

There are some advanced GPS systems applying to the wireless positioning, which are:

- **Assisted Global Positioning System (A-GPS)** [7]: Another kind of handset-based technology which can be understood as an enhanced version of normal GPS. A-GPS uses both the GPS chipset in the mobile handset, and some assistance data sent from the mobile network to locate the mobile receiver
- **Differential Global Positioning System (D-GPS)**: Similar to A-GPS, this is also handset-based but requires a reference station (either ground-based or geosynchronous) to reduce location data error, so that, it can provide highly accurate location results [8].

1.3 Wireless Location Technologies

Location technologies are normally network-centric, where the mobile phone network has the function of locating the mobile devices, or station-centric, which requires some additional stations, such as satellites or additional radio transmitters, to help calculate the location.

1.3.1 Cell Identity (Cell-ID)

Compared to other location methods, Cell-ID [9] is the simplest positioning technology and it is network-centric. It can be either terminal-based or

network-based. It is also a mast-based location. The mobile network can measure the location of a registered mobile phone to a location area level and, when a call is in progress, the wireless network knows which one of the cells within this area is communicating with the calling handset. The cell centre is used to estimate the user location, see Fig. 1.3. The cell size will obviously define the resolution so the accuracy level for GSM 1800 (which has smaller cell size) is better than GSM 900. The third generation of mobile phones network, UMTS, will provide better results than GSM 1800, because it operates at 2000 MHz and has an even smaller cell size.

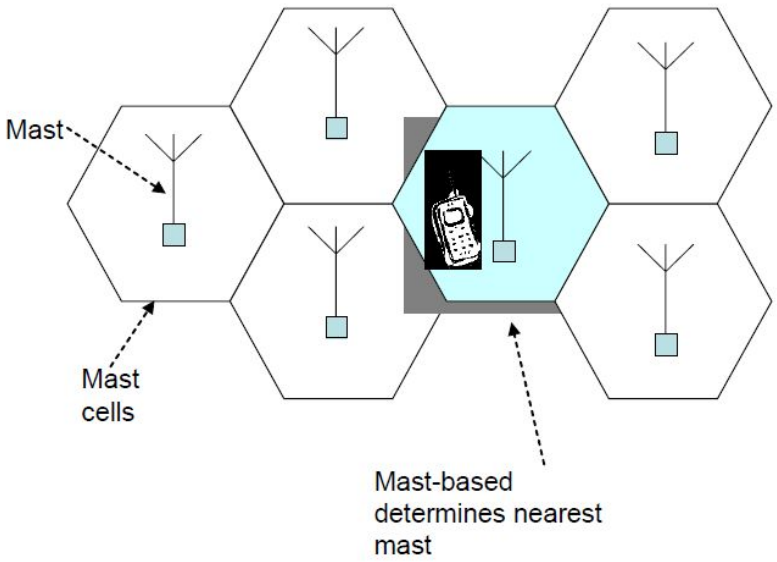

Figure 1.2: An Example of Cell-ID [9]

1.3.2 Time-of-Arrival (TOA)

This method measures the time spent by signals travelling between the MS and the BSs, calculating, in turn, the distance from MS to BS according to the

velocity of electromagnetic wave [10][11]. This method needs at least three location measurement units (LMUS) attached to the BS. In this algorithm, if at least three different receivers can receive the signal from the mobile station, then the 2D coordinates of the MS can be obtained as the intersections of the three circles whose centres coincide with the positions of the BS, and radiuses correspond to the distances from the BS to MS (see, Fig. 1.4). This method is also called the circular-circular-circular system [12]. However, the method requires a quite accurate timing reference at the MS which needs to be synchronised with the clock at the BS, which adds some burden cost to the handset.

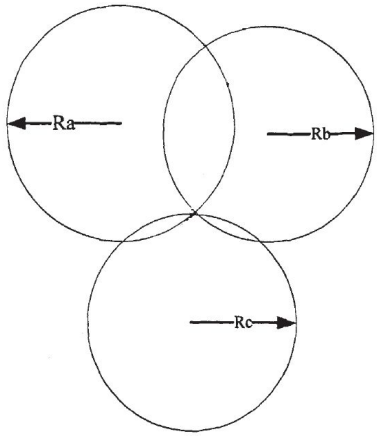

Figure 1.3: Illustration of Localisation in TOA

1.3.3 Time-Difference-of-Arrive (TDOA)

Unlike TOA, TDOA measurements [13] measure the time arrival difference of the signal between the MS to two different BS. Typically, one of these two BS is

taken as a constant and is referred to as reference base station. The method was actively in many indoor location systems as well as in CDMA systems. For generic solution, a hyperbola is drawn through the focus of two BSs and the focal length of the distance difference between the MS to two BSs. Next, the 2D coordinates of the MS can be measured by the intersection of the two hyperbolas. This kind of TDOA is also called a hyperbolic-hyperbolic system, see, Fig. 1.5.

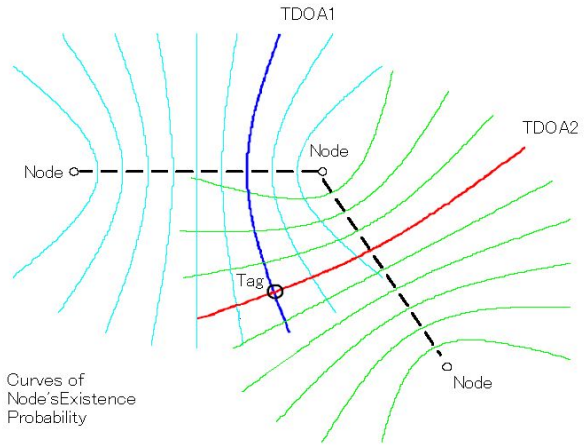

Figure 1.4: Illustration of Localisation in TDOA [14]

1.3.4 Angle-of-Arrival (AOA) [15]

This method makes use of the angle at which the signal arrives from the subscriber's handset. The angle measurements available at each base station are then sent to a central processing unit or a mobile switch where they are analysed and used to generate the approximate position of the MS. This assumes that the base stations are equipped with instruments that determine

the compass direction from which the user's signal is arriving. This ultimately increases the cost of implementation and maintenance. The advantage of AOA is that it is nearly always available and less subject to multiple reflection phenomenon, either in indoor or outdoor environments, and provides location data across all mobile handsets as the processing is done externally, see, Fig. 1.6, but at the cost of extra infrastructure requirements.

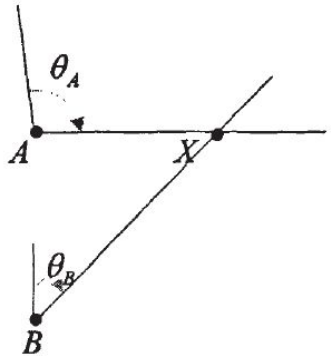

Figure 1.5: Illustration of Localisation in AOA [16]

1.3.5 Received Signal Strength (RSS)

RSS is a method for measuring the power received from an RSS indicator device [17]. The measured signal strength can be related to the distance by using the path loss model, which converts signal attenuation into distance. Traditional triangulation or any stochastic based method can be employed to derive the MS location. Besides, interestingly such processing can be implemented within the mobile handset itself, which explains its wide spread in

research community. The method is viewed as one of the cheapest positioning technique, although it is acknowledged for its lack of accuracy due to signal fluctuations as compared to AOA or TDOA based approach for instance. The method also requires the possibility of the MS to access neighbour base stations, which can easily be enabled through software based approach.

1.3.6 Comparison of Wireless Location Technologies

Table 1.1 summarizes the main wireless location technologies in terms of the dependence on extra infrastructure hardware, difficulty of implementation, cost and expected level of accuracy.

	Dependency on Synchronisation	Limitation of Number of BSs	Difficulty of Implementation	Cost	Accuracy
TOA	**Very High** [17]	**3**	**Very Difficult** [19]	**Expensive** [22]	**Very Accurate** [18] [20] [21]
TDOA	**Low**	**3**	**Easy** [13]	**Cheap** [19]	**Accurate** [23] [19]
AOA	**No**	**2** [15]	**Complicated** [29]	**Expensive** [29]	**Less Accurate** [29]
RSS	**No**	**3**	**Easy** [24][25]	**Cheap**[26]	**Poor** [27] [28]

Table 1.1: Comparison of Wireless Location Technologies

- TOA
  - ✓ TOA, in a synchronised location system, can obtain range measurements accurately.
  - ✓ TOA estimation is already implementable in existing timing-based multiple access scheme systems, such as in GSM or 3G (CDMA), providing high-accuracy TOA range estimation.
  - × The accuracy of TOA estimation is highly reliant on the synchronised location system, which is, hard to implement.
  - × Although a transceiver system is simpler to implement and costless, building up a synchronised location system is expensive.

- TDOA
  - ✓ By taking the difference between the arrival times of signals from two transmitters, the influence of the synchronised system is less than when using - TOA.
  - ✓ In TDOA, synchronising only those transmitters with known positions is much less expensive than synchronising the whole system, as in TOA.
  - ✓ The system is easy implemented.
  - × The range estimation accuracy can be less than that of a TOA system with the same system geometry, but is usually acknowledged to be of good accuracy in overall.
- AOA
  - ✓ The expensive time synchronisation system is not required in the AOA system.
  - ✓ Only two BSs are required to calculate the final position.
  - × An antenna array is required by AOA technique that is very expensive and difficult to implement.
  - × The antenna array increases the size of the device.
  - × In real world tests, the accuracy of AOA estimation is always challenged by landforms.

- RSS
  - ✓ RSS location system is very cheap and easy to implement.
  - ✓ Time synchronisation is not required.
  - × RSS-based positioning accuracy is usually much poorer.
  - × Determination of relevant parameters of the path loss model causes large errors.
  - × RSS is only good at short distance estimation. For long-distance, accuracy is usually much poorer, because such cases correspond to the flat tail area of the log-shaped pass-loss curve.

In this thesis, both the simulation and real time measurements are based on TDOA technology. This is motivated by the following:

- Measuring the difference in the times of arrival decreased the dependence on synchronised system.
- The TDOA technique system is easier and cheaper to implement than TOA.
- TDOA is better applied to CDMA systems because they employ spread-spectrum technology to spread deliberately in the frequency domain, resulting in a signal with a wider bandwidth, in order to have multipath interference mitigation. Besides, CDMA is known to be not a power sensitive system so that the signal attenuation has only a limited effect on the accuracy of difference time measurements.

- The use of TDOA allows us to compensate for any specific imperfections affecting any single timing measurement as we rather are interested in difference between two single timing measurements, so any constant bias or so occurring at a single timing measurement will get eliminated.
- There is increasing number of successful applications, especially in indoor environment, where the TDOA has been used as the main measurement framework. So, restricting our research to this framework allows us to match the current development stream in this field.

1.3.7 Parameters Influencing Positioning Techniques

- **Noise** – In positioning techniques, noise is a parameter which cannot be avoided. When taking distance measurements, measurements are always pervaded by noise. Although it is quite common to account for random noise through some Gaussian distribution whose parameters can be tuned to accommodate the larger possible perturbations that may affect the system, there are also other type of noise, which are not necessarily random, although by abuse many literature treat them as random. This includes:
  - **Thermal Noise**: An electronic noise, generated by the thermal agitation of the charge carriers inside an electrical conductor at equilibrium [42]
  - **Electromagnetic Interference Noise**: A disturbance that affects an

electrical circuit due to either electromagnetic induction or electromagnetic radiation emitted from an external source [43]

- **Random Noise**: Other kinds of system noise, which follow a random Gaussian distribution [44]

- **System Error** – Found in measurements that lead to measurable values being inconsistent when repeated measures of a constant attribute or quantity are taken. When parameters are measured, we cannot avoid errors due to method inherent limitation, operator expertise, environmental conditions, etc. Such errors are often included as part of the additive Gaussian noise pervading the measurements.
- **NLOS Bias** - Wireless location accuracy is subject to wireless transmission channel quality. If the signal between the MS and BS is LOS transmitting, wireless location accuracy is higher. If the LOS is blocked by large buildings or other barriers it becomes an NLOS, which means only signals that can reflect or diffract reach the MS, causing the NLOS errors in the TOA measurements. Because of this, we can establish that NLOS is a kind of positive error, which only makes the measurements larger than they really are, which introduces a constant (positive) bias to initial measurement. Accordingly, one split the main wireless location research trend into two directions: first, based on the measurements and the geometrical relationship between the MS and BS; second, based on the NLOS error's

statistical nature. Both trends aim to inhibit or reduce the effects of NLOS. There are many algorithms created to mitigate NLOS effects, which will be discussed in Chapters 5 and 6.

1.3.8 Monte-Carlo Simulations

Monte-Carlo [31] simulations are typical computational algorithms which use repeated random sampling to obtain a numerical result. The results are then generated over a long run of noise realizations. This kind of simulation runs many times in order to obtain the distribution of an unknown probabilistic entity. In this thesis, the system error was set as a Gaussian distribution with different standard deviations. Especially, throughout our analysis, each simulation was run 10,000 times for Monte-Carlo simulations. In each single simulation, a random sample of a Gaussian Noise is generated by Matlab, and added into the measurements assumption to start a positioning calculation. And then, the program repeated for 10,000 times for selecting different values of Gaussian Noise in order to generate a location error level.

1.4 Metrics of Positioning Evaluation

In order to judge the goodness of any estimation based location algorithm, a metric is required to quantify the quality of such estimation, especially given the

range of errors that pervade both the measurement and the estimation algorithm [32]. Three metrics are mentioned here.

1.4.1 Root Mean Square Error (RMSE)

In this thesis, the root mean square error (RMSE) was chosen as the main metric to evaluate location accuracy.

RMSE is a frequently-used method to obtain the differences between values predicted by a model or an estimator and the values actually observed. Because Monte-Carlo simulation was introduced in this thesis, each group of simulations was made up 10000 pairs of true and evaluated MS position. The RMSE was given as:

$$RMSE = \sqrt{\frac{\sum_{i=1}^{n} \left(\left(MSx_i - EMSx_i \right)^2 + \left(MSy_i - EMSy_i \right)^2 \right)}{n}}, \quad n=10000 \qquad (1.1)$$

Obviously, the smaller RMSE obtained, the better the location accuracy.

1.4.2 Cumulative Distribution Function (CDF)

CDF describes the probability of a positioning error which is under some threshold [41]. When we compare two positioning techniques, if they present similar accuracies, we prefer the system with the CDF graph, which reaches high probability values faster, because its distance error is concentrated in small values. In practice, CDF is described by the percentile format.

1.4.3 Geometric Dilution of Precision (GDOP)

GDOP is a term used in satellite navigation and geometrics engineering to specify the additional multiplicative effect of navigation satellite geometry on positional measurement precision. GDOP depends on the relative positions of the BS and the MS. When GDOP values are smaller than a threshold, they are usually preferable. Referring to GDOP in the literature [45], it can be defined as:

$$GDOP = \frac{RMSE_{loc}}{RMSE_{range}} = \frac{\delta_{loc}}{\delta} \tag{1.2}$$

where $RMSE_{loc}$ and $RMSE_{range}$ are the RMSE of the location estimate and the range estimate and σ_{loc} is the standard deviation of the location estimate. For identical noise variances $\sigma_i^2=\sigma^2$ at different BSs, while GDOP values are smaller than a threshold, normally three, are preferable, values larger than six may imply a very bad geometry of the BSs. The GDOP is given by

$$GDOP = \frac{\sqrt{trace\left[I^{-1}(X)\right]}}{\delta} = \sqrt{trace\left[\hat{I}^{-1}(X)\right]} \tag{1.3}$$

where $\hat{I}(x) = \begin{bmatrix} \sum_{i=1}^{N} \cos^2(\alpha_i) & \sum_{i=1}^{N} \cos(\alpha_i)\sin(\alpha_i) \\ \sum_{i=1}^{N} \cos(\alpha_i)\sin(\alpha_i) & \sum_{i=1}^{N} \sin^2(\alpha_i) \end{bmatrix}$

α_i defines the angle from the i^{th} BS to the MS

1.5 Contribution of the Thesis

The main contributions of this thesis can be summarised as below:

- A new review of LOS and NLOS localisation techniques is provided taking into account the algorithm complexity of the approach as well as environmental and inherent constraints of the various methods. This is highlighted in Chapter 2 for LOS positioning and Chapter 5 for NLOS techniques.
- A new positioning technique based on a new estimator, constructed as a convex combination of Chan and Taylor methods is put forward whose performances have been quantified using both simulated and real time measurements. The detailed description of the estimator is reported in Chapter 3, together with detailed simulation results. Experimental results are reported in Chapter 7.
- A new analysis of the network topology taking into account the possibility of BS signal failure is reported in Chapter 4. In this respect, a set of basic topology structures has been devised and comparison results have been initiated.
- A new estimator in case of NLOS scenario, based on gradient descent method-like optimisation is put forward in Chapter 6 where performance results in terms of RMSE are reported in the same chapter.

1.6 Organisation of the Thesis

The rest of the thesis is organised as follows:

Chapter 2 reviews the different location estimation algorithms in LOS scenario. The basic principles of maximum likelihood, least square, iterative like methods are discussed and analysed. The limitation and complexity of each algorithm are summarised.

In Chapter 3, an innovative combination algorithm for mobile positioning in LOS is presented. The chapter also reports on some Monte Carlo simulations results in typical LOS scenario where the performances of the various algorithms in terms of RMSE are examined.

Chapter 4 investigates the influences of network topology in terms of BS positioning that result from a failure of a given BS(s). A set of elementary topology structures has been designed and comparative and positioning accuracy of various methods with respect to each topology is examined.

Chapter 5 is dedicated to the different estimation algorithms in NLOS scenarios. The basic formulas of the mitigation algorithms are listed.

An innovative algorithm and optimisation used in NLOS, named the Gradient

Descent Iteration – Combination (GDIC) method, are provided in Chapter 6. Simulation results and comparison between each existing algorithm are shown in this chapter, while Chapter 7 describes a real world experiment in a residential area. The experiment performed wireless location in an MS-moving situation, based on the innovative algorithm described in Chapters 3 and 6.

The main conclusion of this thesis is given in Chapter 8. Perspective and future work are also presented.

The logical structure of this thesis is shown in Figure 1.7:

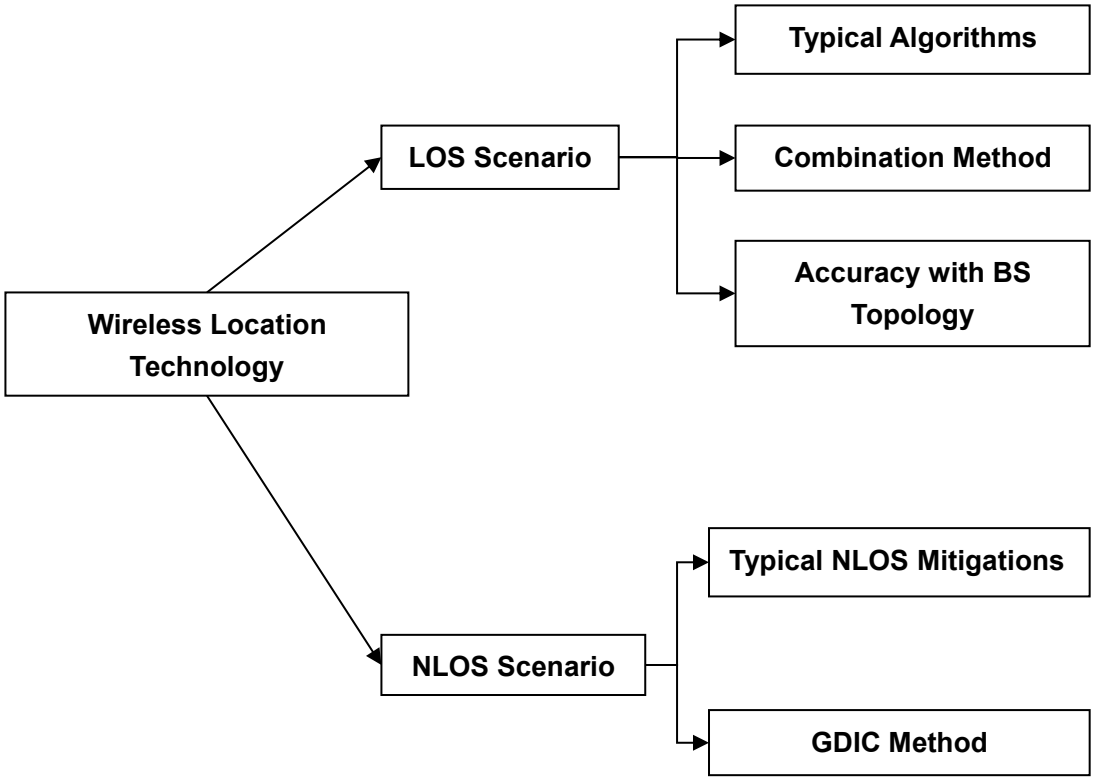

Figure 1.6: Logic Structure of Thesis

1.7 Reference

[1] C.C. Docket, “*Revision of the Commission rules to ensure compatibility with enhanced 911 emergency calling systems*”, RM-8143, Report No. 94-102, FCC, 1994

[2] Havinis T, Hayes S, Roel-Ng M. “*System and method for informing network of terminal-based positioning method capabilities: U.S. Patent*” 6,002,936[P]. 1999-12-14.

[3] A. H. Sayed, A. Tarighat and N. Khajehnouri, "*Network-based wireless location: challenges faced in developing techniques for accurate wireless location information*," Signal Processing Magazine, IEEE, vol. 22, pp. 24-40, 2005.

[4] Y. H. Ho, S. Abdullah and M. H. Mokhtar, "*Global positioning system (GPS) positioning errors modeling using global ionospheric scintillation model (GISM)*," in Space Science and Communication (IconSpace), 2013 IEEE International Conference on, 2013, pp. 33-38.

[5] http://www.how-gps-works.com/

[6] Guibin Zhu, Qiuhua Li, Peng Quan and JiuZhi Ye, "*A GPS-free localization scheme for wireless sensor networks*," in Communication Technology (ICCT), 2010 12th IEEE International Conference on, 2010, pp. 401-404.

[7] http://yorcshin.com/blog/nokia/nokiaagps.php

[8] Ching Tard Goh and Han Wang, "*State estimation for a golf buggy via differential global positioning system*," in Intelligent Transportation Systems, 1999. Proceedings. 1999 IEEE/IEEJ/JSAI International Conference on, 1999, pp. 649-654.

[9] J. G. Markoulidakis and C. Dessiniotis, "*Statistical terminal assisted mobile positioning technique*," Communications, IET, vol. 1, pp. 325-332, 2007.

[10] R. M. Vaghefi and R. M. Buehrer, "*Asynchronous time-of-arrival-based source localization*," in Acoustics, Speech and Signal Processing (ICASSP), 2013 IEEE International Conference on, 2013, pp. 4086-4090.

[11] Jiao Shuhong, Si Xicai and Kong Fanru, "*A time-of arrival location algorithm for maneuvering target on two-dimensional surface*," in Signal Processing Proceedings, 1998. ICSP '98. 1998 Fourth International Conference on, 1998, pp. 1700-1703 vol.2.

[12] S. R. Aedudodla and T. F. Wong, "*On time-of-arrival estimation in dense ultra-wideband channels*," in Communications, Circuits and Systems Proceedings, 2006 International Conference on, 2006, pp. 1315-1320.

[13] A. Abrardo, G. Benelli, C. Maraffon and A. Toccafondi, "*Performance of TDoA-based radiolocation techniques in CDMA urban environments*," in Communications, 2002. ICC 2002. IEEE International Conference on, 2002, pp. 431-435.

[14]http://www.intechopen.com/books/current-trends-and-challenges-in-rfid/iterative-delay-compensation-algorithm-to-mitigate-nlos-influence-for-positioning

[15] M. D. Zoltowski, "*Maximum likelihood based angle-of-arrival estimation in a diffuse multipath environment*," in Antennas and Propagation Society International Symposium, 1987, 1987, pp. 32-35.

[16]http://www.cisco.com/c/en/us/td/docs/solutions/Enterprise/Mobility/WiFiLBS-DG/wifich2.html

[17] N. Patwari, J. N. Ash, S. Kyperountas, A. O. Hero, R. L. Moses and N. S. Correal, "*Locating the nodes: cooperative localization in wireless sensor networks*," Signal

Processing Magazine, IEEE, vol. 22, pp. 54-69, 2005.

[18] Sunwoo Kim, T. Pals, R. A. Iltis and H. Lee, "*CDMA sparse channel estimation using a GSIC/AM algorithm for radiolocation*," in Signals, Systems and Computers, 2002. Conference Record of the Thirty-Sixth Asilomar Conference on, 2002, pp. 1473-1477 vol.2.

[19] Yilin Zhao, "*Standardization of mobile phone positioning for 3G systems*," Communications Magazine, IEEE, vol. 40, pp. 108-116, 2002.

[20] B. Ludden and L. Lopes, "*Cellular based location technologies for UMTS: A comparison between IPDL and TA-IPDL*," in Vehicular Technology Conference Proceedings, 2000. VTC 2000-Spring Tokyo. 2000 IEEE 51st, 2000, pp. 1348-1353 vol.2.

[21] J. Winter and C. Wengerter, "*High resolution estimation of the time of arrival for GSM location*," in Vehicular Technology Conference Proceedings, 2000. VTC 2000-Spring Tokyo. 2000 IEEE 51st, 2000, pp. 1343-1347 vol.2.

[22] F. Sivrikaya and B. Yener, "*Time synchronization in sensor networks: a survey*," Network, IEEE, vol. 18, pp. 45-50, 2004.

[23] Pratap Misra and Per Enge. "*Global Positioning System: Signals, Measurements, and Performances*". Ganga-Jamuna Press, second edition, 2006.

[24] T. Gigl, G. J. M. Janssen, V. Dizdarevic, K. Witrisal and Z. Irahhauten, "*Analysis of a UWB indoor positioning system based on received signal strength*," in Positioning, Navigation and Communication, 2007. WPNC '07. 4th Workshop on, 2007, pp. 97-101.

[25] Yihong Qi and H. Kobayashi, "*On relation among time delay and signal strength based geolocation methods*," in Global Telecommunications Conference, 2003. GLOBECOM '03.

IEEE, 2003, pp. 4079-4083 vol.7.

[26] G. Bellusci, G. J. M. Janssen, Junlin Yan and C. C. J. M. Tiberius, "*Novel ultra wideband low complexity ranging using different channel statistics*," in Wireless Communications and Networking Conference, 2008. WCNC 2008. IEEE, 2008, pp. 290-295.

[27] J. A. Dabin, Nan Ni, A. M. Haimovich, E. Niver and H. Grebel, "*The effects of antenna directivity on path loss and multipath propagation in UWB indoor wireless channels*," in Ultra Wideband Systems and Technologies, 2003 IEEE Conference on, 2003, pp. 305-309.

[28] T. Wakabayashi and H. Matsui, "*Omni-directional characteristics over frequency range for UWB of modified planar antenna with an elliptical element on the dielectric substrate*," in Wireless Communication Systems, 2009. ISWCS 2009. 6th International Symposium on, 2009, pp. 463-467.

[29] S. Gezici, Zhi Tian, G. B. Giannakis, H. Kobayashi, A. F. Molisch, H. V. Poor and Z. Sahinoglu, "*Localization via ultra-wideband radios: a look at positioning aspects for future sensor networks*," Signal Processing Magazine, IEEE, vol. 22, pp. 70-84, 2005.

[30] Li-Hong Huang, Sheng-Yu Tsai and Yuan-Hao Huang, "*Mobile positioning system based on virtual base station transform and convex optimization*," in Signal Processing Systems (SiPS), 2012 IEEE Workshop on, 2012, pp. 243-248.

[31] Zhang jian wu, Yu Cheng-lei and Ji Ying-ying, "*The performance analysis of chan location algorithm in cellular network*," in Computer Science and Information Engineering, 2009 WRI World Congress on, 2009, pp. 339-343.

[32] B. Sridhar and M. Z. Ali Khan, "*RMSE comparison of path loss models for UHF/VHF*

bands in india," in Region 10 Symposium, 2014 IEEE, 2014, pp. 330-335.

[33] B. Brumitt, B. Meyers, J. Krumm, A. Kern, and S. Shafer. "*EasyLiving: Technologies for intelligent environments*", Proceedings of the 2nd international symposium on Handheld and Ubiquitous Computing, Bristol, UK, 2000, pp.12-29

[34] http://www.Facebook.com

[35] http://maps.google.com

[36] P. Bahl and V. N. Padmanabhan. *Enhancements to the RADAR user location and tracking system*. Technical Report MSR-TR-2000-12, Microsoft Research, Feb. 2000

[37] http://www.wirelesscommunication.nl/reference/chaptr01/roadtrin/positi.htm

[38] Art. 2 Kooperationsabkommen über ein globales ziviles Satellitennavigationssystem (GNSS) zwischen der Europäischen Gemeinschaft und ihrer Mitgliedstaaten und der Ukraine vom 1. Dezember 2005, Bekanntmachung vom 20. Januar 2014 (BGBl. II S. 128)

[39]http://skynet.ee.ic.ac.uk/notes/MSc_C5_Arch_2005_Positioning_Architectures_in_Wireless_Networks.pdf

[40] A. N. Idris, A. M. Suldi, J. R. A. Hamid and D. Sathyamoorthy, "*Effect of radio frequency interference (RFI) on the global positioning system (GPS) signals*," in Signal Processing and its Applications (CSPA), 2013 IEEE 9th International Colloquium on, 2013, pp. 199-204.

[41] Hui Liu, H. Darabi, P. Banerjee and Jing Liu, "*Survey of Wireless Indoor Positioning Techniques and Systems*," Systems, Man, and Cybernetics, Part C: Applications and Reviews, IEEE Transactions on, vol. 37, pp. 1067-1080, 2007.

[42] D. C. Agouridis, "*Thermal Noise of Transmission Media*," Instrumentation and

Measurement, IEEE Transactions on, vol. 26, pp. 243-245, 1977.

[43] K. Borisov, H. L. Ginn and A. M. Trzynadlowski, "*Attenuation of Electromagnetic Interference in a Shunt Active Power Filter*," Power Electronics, IEEE Transactions on, vol. 22, pp. 1912-1918, 2007.

[44] A. Skiadopoulos and K. Gianikellis, "*Random error propagation analysis in center of pressure signal*," in Biomedical Robotics and Biomechatronics (2014 5th IEEE RAS & EMBS International Conference on, 2014, pp. 632-637.

[45] Sharp, Kegen Yu and Y. J. Guo, "*GDOP Analysis for Positioning System Design*," Vehicular Technology, IEEE Transactions on, vol. 58, pp. 3371-3382, 2009.

CHAPTER 2: WIRELESS LOCATION ALGORITHMS IN LOS SCENARIOS

2.1 Overview

Wireless location accuracy is subject to wireless transmission channel quality. Typically, if a LOS propagation exists between the MS and a group of BSs, high location accuracy can be achieved. In this chapter, we discuss the main methods of wireless location based on the TDOA [1], LOS situations.

This chapter is organised as follows: Section 2.2 reviews the basic three BSs algorithm, which is the foundation of wireless location methods. A more calculable algorithm, used in 3-BS, Fang's method, is represented in Section 2.3. In the rest of the chapter, Sections 2.4 to 2.7 are dedicated to the more than 3-BSs used for the MS positioning. Four algorithms, linear least squares, constrained weighted least squares, Chan's and Taylor's methods will be introduced in these sections. Section 2.8 provides some concluding remarks.

2.2 Basis of Geometric TDOA Positioning

The idea of TDOA is to determine the relative position of the mobile transmitter by examining the difference in time at which the signal arrives at multiple measuring units. Therefore, for each TDOA measurement, the transmitter must lie on a hyperboloid with a constant range difference between the two measuring

units (BSs). Commonly, one fixed BS acts as a servicing BS where the time differences are calculated with respect to the servicing BS. To illustrate the functioning of TDOA, Figure 2.1 provides an example with three BSs, A, B and C, where A acts as the servicing BS.

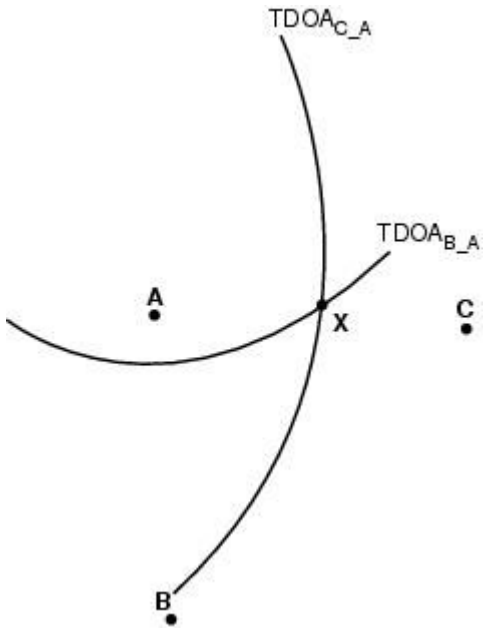

Figure 2.1: Examples of TDOA Measurements with Three Base Stations, A, B and C

The curve $TDOA_{B\_A}$ is the hyperbola of a set of points at a constant range difference from MS to BS A to BS B.

The curve $TDOA_{C\_A}$ is the hyperbola of a set of points at a constant range difference from MS to BS A and BS C. In 2D Cartesian space, let (x, y), (be the x-y coordinates of the MS, BS A, BS B and BS C, respectively.

Therefore, denoting by R_i the distance from the MS to the i^{th} BS (here i =A, B, C), and assuming *A* be the servicing BS, we have: [1]

$$R_i = \sqrt{(X_i - x)^2 + (Y_i - y)^2} \quad (2.1)$$

$$R_{B,A} = cT_{B,A} = R_B - R_A = \sqrt{(X_B - x)^2 + (Y_B - y)^2} - \sqrt{(X_A - x)^2 + (Y_A - y)^2} \quad (2.2)$$

$$R_{C,A} = cT_{C,A} = R_C - R_A = \sqrt{(X_C - x)^2 + (Y_C - y)^2} - \sqrt{(X_A - x)^2 + (Y_A - y)^2} \quad (2.3)$$

where $T_{B,A}$ and $T_{C,A}$ are the measured TDOA and *c* stands for the signal propagation speed, corresponding to the speed of light, e.g., $c \approx 3*10^8$ *m/s.*

The MS estimation consists of determining the coordinates (x, y) in equations (2.2-2.3). From a geometrical viewpoint, this boils down to the intersection of the two hyperbolas, which is the point “X” in the graph in Figure 2.1.

From equations (2.2-2.3), it is clear that at least three BSs, which yield two equations, are required to estimate the MS location in 2D space. Similarly, in 3D space, four BSs are required to estimate the (x, y, z) position of the MS.

Furthermore, when a higher number of BSs become available, and hence the number of equations is higher than the number of variables (only two), an approximate method, e.g. non-linear regression, is required to solve the problem. This chapter aims to review the main solutions and provides an original of their complexity analysis with respect to the number of BSs.

2.3 Three-Base Stations with Fang’s Location Algorithm

An analytical solution to (2.2-2.3) is not straightforward due to highly nonlinear terms, so a framework for an exact solution is provided by Fang [3], sometimes, known as Fang’s positioning method. This section presents an overview and

discusses this approach. For the sake of coherence, we shall employ notations from Figure 2.1 as a basis for our development. More formally, from (2.1),

$$R_i^2 = (X_i - x)^2 + (Y_i - y)^2 = X_i^2 - 2X_i x + x^2 + Y_i^2 - 2Y_i y + y^2 \quad (i=A,B,C) \quad (2.4)$$

Let

$$K_i = X_i^2 + Y_i^2 \qquad (i=A,B,C), \quad (2.5)$$

Putting (2.5) in (2.4) yields:

$$R_i^2 = K_i^2 - 2X_i x + x^2 - 2Y_i y + y^2 \quad (2.6)$$

Using $R_{i,j} = R_i - R_j$

$$R_B^2 = (R_{B,A} + R_A)^2 = R_{B,A}^2 + 2R_{B,A}R_A + R_A^2 = K_B - 2X_B x - 2Y_B y + x^2 + y^2 \quad (2.7)$$

$$R_C^2 = (R_{C,A} + R_A)^2 = R_{C,A}^2 + 2R_{C,A}R_A + R_A^2 = K_C - 2X_C x - 2Y_C y + x^2 + y^2 \quad (2.8)$$

Subtracting the quantity R_A^2 and its equivalent entity according to (2.6) in both terms of expressions (2.7-2.8) yields

$$R_{B,A}^2 + 2R_{B,A}R_A = K_B - 2X_{B,A}x - 2Y_{B,A}y - K_A \quad (2.9)$$

$$R_{C,A}^2 + 2R_{C,A}R_A = K_C - 2X_{C,A}x - 2Y_{C,A}y - K_A \quad (2.10)$$

where

$$X_{i,A} = X_i - X_A; \qquad Y_{i,A} = Y_i - Y_A; \quad (2.11)$$

Now, only *x, y,* R_A are unknown, which together with (2.4; 2.9-2.10), allows us to determine the location of the MS (x, y).

Following Fang's approach, a Cartesian frame can be chosen so that its origin will be the BS A (servicing BS) and so that one of the axis passes through another BS, say, B. This yields A(*0，0)*，B(X_B, *0)*，C(X_C, Y_C). Therefore, we have:

$$R_A = \sqrt{\left(X_A - x\right)^2 + \left(Y_A - y\right)^2} = \sqrt{x^2 + y^2} \tag{2.12}$$

$$R_{B,A}{}^2 + 2R_{B,A}R_A = K_B - 2X_{B,A}x - 2Y_{B,A}y - K_A$$

$$= X_B{}^2 + Y_B{}^2 - 2(X_B - X_A)x - 2(Y_B - Y_A)y - X_A - Y_A = X_B{}^2 - 2X_B x \tag{2.13}$$

$$\therefore R_A = \frac{R_{B,A}{}^2 - X_B{}^2 - 2X_B x}{-2R_{B,A}} \tag{2.14}$$

Using the same steps for C, one gets:

$$R_A = \frac{R_{C,A}{}^2 - \left(X_C{}^2 + Y_C{}^2\right) + 2X_C x + 2Y_C y}{-2R_{C,A}} \tag{2.15}$$

so,

$$\frac{R_{B,A}{}^2 - X_B{}^2 - 2X_B x}{-2R_{B,A}} = \frac{R_{C,A}{}^2 - \left(X_C{}^2 + Y_C{}^2\right) + 2X_C x + 2Y_C y}{-2R_{C,A}}$$

$$\frac{2Y_C y}{-2R_{C,A}} - \frac{R_{C,A}{}^2 - \left(X_C{}^2 + Y_C{}^2\right) + 2X_C x}{2R_{C,A}} = \frac{R_{B,A}{}^2 - X_B{}^2}{-2R_{B,A}} + \frac{2X_B x}{2R_{B,A}}$$

$$\frac{Y_C}{-R_{C,A}} y = \frac{R_{C,A}{}^2 - \left(X_C{}^2 + Y_C{}^2\right) + 2X_C x}{2R_{C,A}} + \frac{R_{B,A}{}^2 - X_B{}^2}{2R_{B,A}} + \frac{X_B}{R_{B,A}} x$$

$$\therefore y = \frac{X_B R_{C,A} - X_C R_{B,A}}{R_{B,A} Y_C} x + \frac{R_{B,A}{}^2 R_{C,A} - X_B{}^2 R_{C,A} - R_{C,A}{}^2 R_{B,A} + R_{B,A}\left(X_C{}^2 + Y_C{}^2\right)}{2R_{B,A} Y_C}$$

(2.16)

This can be written as:

$$y = g\ x + h$$

where

$$g = \frac{X_B R_{C,A} - X_C R_{B,A}}{R_{B,A} Y_C} = \frac{\frac{X_B R_{C,A}}{R_{B,A}} - X_C}{Y_C}$$

,

$$h = \frac{R_{B,A} R_{C,A}\left(1 - \left(\frac{X_B}{R_{B,A}}\right)^2\right) - R_{C,A} + \left(X_C{}^2 + Y_C{}^2\right)}{2Y_C}$$

Combining (2.12) and (2.14) and substituting y by its expression in (2.16) yields

a second order equation in x:

$$d\,x^2 + e\,x + f = 0 \tag{2.16}$$

where

$$d = -\left\{\left[1-\left(\frac{X_B}{R_{B,A}}\right)^2\right]+g^2\right\}$$

$$e = X_B \times \left[1-\left(\frac{X_B}{R_{B,A}}\right)^2\right]-2gh$$

$$f = \frac{R_{B,A}^2}{4}\times\left[1-\left(\frac{X_B}{R_{B,A}}\right)^2\right]^2-h^2$$

Solving the above polynomial equation yields:

$$x = \frac{-e \pm \sqrt{e^2-4df}}{2d}$$
$$y = g\,x + h \tag{2.17}$$

The existence of the solution can intuitively be proven through geometric construction; that is, the linear graph of (2.16) intersects with the hyperbola induced by the equations (2.12, 2.14) either on one or two Cartesian points.

Since there are two solution results of *x* according to (2.17), the use of some prior knowledge is required to exclude one solution. This includes, for instance, choosing a solution situated within a convex region generated by BSs A, B and C.

In the case where several BSs are employed (more than three), there are more equations in the sense of (2.7-2.8) than the number of variables (only two),

therefore a least-square like based approach is required. The next sections review such an approach.

2.4 Linear Least Squares Algorithm

2.4.1 Matrix Representation of the Non-Linear Model

Let us consider N BSs (i=1, 2,…,N) and let us assume without loss of generality that the first BS (i=1) acts as the servicing BS. Then the counterpart of (2.9-2.10) will be

$$\begin{aligned} K_2 - K_1 - R_{2,1}{}^2 &= 2X_{2,1}x + 2Y_{2,1}y + 2R_{2,1}R_1 \\ K_3 - K_1 - R_{3,1}{}^2 &= 2X_{3,1}x + 2Y_{3,1}y + 2R_{3,1}R_1 \\ &. \\ K_N - K_1 - R_{N,1}{}^2 &= +2X_{N,1}x + 2Y_{N,1}y + 2R_{N,1}R_1 \end{aligned} \tag{2.18}$$

with $R_1 = \sqrt{\left(X_1 - x\right)^2 + \left(Y_1 - y\right)^2}$

Assuming R_1 is a variable, then (2.18) shows a linear system in (x, y, R_1),

$$F = G\,z \tag{2.19}$$

where

$$F = \frac{1}{2}\begin{bmatrix} K_2 - K_1 - R_{2,1}^2 \\ K_3 - K_1 - R_{3,1}^2 \\ ..... \\ K_N - K_1 - R_{N,1}^2 \end{bmatrix}, \qquad G = \begin{bmatrix} X_{2,1} & Y_{2,1} & R_{2,1} \\ X_{3,1} & Y_{3,1} & R_{3,1} \\ ... & ... & ... \\ X_{M,1} & Y_{M,1} & R_{M,1} \end{bmatrix}, \quad z = \begin{bmatrix} x \\ y \\ R_1 \end{bmatrix} \tag{2.20}$$

The linear least square estimation of (2.19) is straightforwardly provided by

$$z = \frac{1}{2}\left(G^T G\right)^{-1} G^T F \tag{2.21}$$

The above equation, although simple, lacks consistency as the variable R_1 is

fully dependent on *x* and *y* variables. Therefore, solution (2.21) is not used to provide a correct solution but rather an initial location estimate to apply further algorithms.

2.4.2 Taylor's Location Algorithm

Taylor's location method starts with an initial guess (x_0,y_0) and computes the deviation of the position location estimation. It utilises Taylor-series expansion to linearize Equation (2.18) after substituting R_1 by its expression in terms of x and y variables. As a result, Taylor's location method starts with the initial guess, which would allow us to calculate the distances Ri (i=1,N) and uses the following equation to compute iteratively the final location MS(x, y) [11][12].

$$h_t = G_t \delta + \varepsilon \tag{2.22}$$

where,

$$h_t = \begin{bmatrix} R_{2,1} - (R_1 - R_2) \\ R_{3,1} - (R_1 - R_3) \\ \vdots \\ R_{N,1} - (R_1 - R_N) \end{bmatrix},$$

$$\delta = \begin{bmatrix} \Delta X \\ \Delta Y \end{bmatrix} \quad G_t = \begin{bmatrix} \frac{X_1 - X_0}{R_1} - \frac{X_2 - X_0}{R_2} & \frac{Y_1 - Y_0}{R_1} - \frac{Y_2 - Y_0}{R_2} \\ \frac{X_1 - X_0}{R_1} - \frac{X_3 - X_0}{R_3} & \frac{Y_1 - Y_0}{R_1} - \frac{Y_3 - Y_0}{R_3} \\ \vdots & \vdots \\ \frac{X_1 - X_0}{R_1} - \frac{X_N - X_0}{R_N} & \frac{Y_1 - Y_0}{R_1} - \frac{Y_N - Y_0}{R_N} \end{bmatrix}$$

ε stands for TDOA measurements errors, which are assumed zero-mean and covariance Q.

$$\delta = \begin{bmatrix} \Delta x \\ \Delta y \end{bmatrix} = \left(G_t{}^T Q^{-1} G_t \right)^{-1} G_t{}^T Q^{-1} h_t$$

(2.23)

Typically, from $x = X_0$; $y = Y_0$, in the next iteration using (2.23), we update the location as

$$\begin{aligned} X' &= X + \Delta x \\ Y' &= Y + \Delta y \end{aligned} \qquad (2.24)$$

The method repeats the steps above until $\Delta x \Delta y$ is smaller than some predefined threshold: $|\Delta x| + |\Delta y| < \alpha$. The result of the last iteration is then supposed to be the position estimate.

Taylor's method can accommodate any number of BSs but requires a relatively good initialisation; otherwise it may lead to local minima and divergence. Besides, it may require a high number of iteration in order to achieve the difference between two estimate being less than threshold α, which makes the solution computationally very intensive.

2.4.3 Chan's Location Algorithm

Chan's method [2] [10] uses a two-step estimation procedure. In the first step, assuming that R_1 is independent of x and y, a weighted linear least square is used to get an initial estimate of the position, which is then refined in the next

stage using another weighted least square approach. More specifically, the method assumes a system (2.19) with added random perturbations as:

(2.25)

where the perturbation is rooted to individual TDOA measurements distinguishing noise-free measurements (or equivalently,), the covariance matrix:

$$\psi = E\left[\varepsilon\ \varepsilon^T\right] = c^2 BQB \tag{2.26}$$

where

$$B = diag\left(R_2^0, R_3^0, ..., R_N^0\right) \tag{2.27}$$

Q is the Covariance matrix of TDOA measurements

$$Q = diag\left(\sigma_1^2, \sigma_2^2, ..., \sigma_M^2\right)$$

The first solution of (2.25) assumes non-correlation of x, y and R_1 is given by (using a (weighted) least square approach):

$$z = \left(G^T \psi^{-1} G\right)^{-1} G^T \psi^{-1} F \tag{2.28}$$

Nevertheless, (2.28) requires the B that contains the true distances from the MS to the BSs but is unknown. (2.28) is approximated by

$$z = \left(G^T Q^{-1} G\right)^{-1} G^T Q^{-1} F \tag{2.29}$$

Its covariance matrix is estimated using the perturbation approach by

$$cov(z) = \left(G^{0T} \psi^{-1} G^0\right)^{-1} \tag{2.30}$$

where G^0 stands for the non-noisy decomposition of *G* that accommodates true distance $d_{i,1}^0$ ($G = G^0 + \Delta G$).

Next, in order to account for the fact that *z* contains dependent variables, e.g., the fact that R_1 is dependent on *x* and *y*, the components of z are separated from their noisy part and the relationship of the third component with the two others is taken into account as

$$z_1 = x^0 + e_1 \qquad z_2 = y^0 + e_2 \qquad z_3 = R_1^{\,0} + e_3$$

where $e_1,\ e_2,\ e_3$ are the error estimates of *z*.

The error vector of a *z* is expressed as:

$$\psi' = h' - Gz' \tag{2.31}$$

where

$$h' = \begin{bmatrix} (z_1 - X_1)^2 \\ (z_2 - Y_1)^2 \\ z_3^2 \end{bmatrix} \qquad G' = \begin{bmatrix} 1 & 0 \\ 0 & 1 \\ 1 & 1 \end{bmatrix} \qquad z' = \begin{bmatrix} (x - X_1)^2 \\ (y - Y_1)^2 \end{bmatrix}$$

The associated covariance matrix of (2.31) is given by

$$\phi = E\left[\psi'\psi'^{T}\right] = 4B'\,cov(z)\,B' \tag{2.32}$$

where $B' = diag\left(x^0 - X_1, y^0 - Y_1, R_1^0\right)$

Finally, using the maximum likelihood or equivalently weighted least square, the estimation of z' is given by

$$z' = \left(G'^{T}\,\phi^{-1}G'\right)^{-1} G'^{T}\,\phi^{-1}h' \tag{2.33}$$

At last, the final result of MS positioning is that:

$$\begin{bmatrix} x \\ y \end{bmatrix} = \pm\sqrt{z'} + \begin{bmatrix} X_1 \\ Y_1 \end{bmatrix} \tag{2.34}$$

A priori knowledge about the environment should be used to ensure a single

solution in (2.34)

2.4.4 Alternative Least Square Approaches

So far in the previous approaches, the row measurements are the standard TDOA measurements. Nevertheless, other approaches have been developed by relaxing such constraints. More specifically, instead of the difference in timing with respect to the servicing BS, we consider the difference of squared time, e.g. $d_i^2 - d_j^2$. From an implementation perspective, this requires further processing capabilities. Still, this is also considered by many authors as part of TDOA measurements. On the other hand, some of these approaches also question the choice of a specific servicing BS as will be detailed later on.

2.4.4.1 LLS – 1 Solution

Given a set of measurements $d'_{i,1} = d_i^2 - d_1^2$ (assuming the first BS be the servicing BS), the LLS-1 estimator is constructed in the following way [5]:

From (2.6):

$$R_i^2 = K_i^2 - 2X_i x + x^2 - 2Y_i y + y^2 \qquad \text{(i=1, N)} \qquad (2.35)$$

For i=1, it holds

$$R_1^2 = K_1^2 - 2X_1 x + x^2 - 2Y_1 y + y^2 \qquad (2.36)$$

Subtracting (2.36) to (2.35) for i=2=N, yields

$$d'_{i,1} = R_i^2 - R_1^2 = K_i^2 - K_1^2 - 2(X_i - X_1)x - 2(Y_i - Y_1)y \quad \text{(i=2, N)} \qquad (2.37)$$

This can be written as

$$p_{LS1} = A_{LS1}\begin{bmatrix} x \\ y \end{bmatrix} \qquad (2.38)$$

where

$$A_{LS1} = \begin{bmatrix} X_2 - X_1 & Y_2 - Y_1 \\ X_3 - X_1 & Y_3 - Y_1 \\ \vdots & \vdots \\ X_N - X_1 & Y_N - Y_1 \end{bmatrix} \qquad p_{LS1} = \frac{1}{2}\begin{bmatrix} d'_{2,1} + K_1 - K_2 \\ d'_{3,1} + K_1 - K_3 \\ \vdots \\ d'_{N,1} + K_1 - K_N \end{bmatrix} \qquad (2.39)$$

yielding the location of the MS as:

$$EMS = \begin{bmatrix} x \\ y \end{bmatrix} = \frac{1}{2}\left({A_{LS1}}^T A_{LS1} \right)^{-1} {A_{LS1}}^T p_{LS1} \qquad (2.40)$$

2.4.4.2 LLS – 2 Solution

Another approach, referred to as LLS2 proposed in [6], assumes that any BS can be a referencing BS. More specifically, the counterpart of (2.37) will be:

$$d'_{i,j} = R_i^2 - R_j^2 = K_i^2 - K_j^2 - 2(X_i - X_j)x - 2(Y_i - Y_j)y \quad \text{(j < i)} \qquad (2.41)$$

yielding N(N-1)/2 linear equations in the form (2.41). So similar to LLS-1, the solution is in the form

$$EMS = \begin{bmatrix} x \\ y \end{bmatrix} = \frac{1}{2}\left({A_{LS2}}^T A_{LS2} \right)^{-1} {A_{LS2}}^T p_{LS2} \qquad (2.42)$$

where

$$p_{LS2}=\frac{1}{2}\begin{bmatrix} d'_{2,1}+K_1-K_2 \\ d'_{3,1}+K_1-K_3 \\ \vdots \\ d'_{N,1}+K_1-K_N \\ d'_{3,2}+K_2-K_3 \\ d'_{4,2}+K_2-K_4 \\ . \\ . \\ d'_{N,2}+K_2-K_N \\ . \\ d'_{N,N-1}+K_{N-1}-K_N \end{bmatrix}, \quad A_{LS2}=\begin{bmatrix} X_2-X_1 & Y_2-Y_1 \\ X_3-X_1 & Y_3-Y_1 \\ \vdots & \vdots \\ X_N-X_1 & Y_N-Y_1 \\ X_3-X_2 & Y_3-Y_2 \\ X_4-X_2 & Y_4-Y_2 \\ . & \\ X_N-X_2 & Y_N-Y_2 \\ . & \\ X_N-X_{N-1} & Y_N-Y_{N-1} \end{bmatrix} \tag{2.43}$$

2.4.4.3 LLS –3 Solution

In the proposal suggested in [7] the reference BS is not one of the original BSs but assumes a processing unit that calculates the average timing from all BSs. In other words, given

$$\overline{R}^2=\frac{1}{N}\sum_{k=1}^{N}R_k^2=\frac{1}{N}\sum_{k=1}^{N}K_k^2+(x^2+y^2)-2x\frac{1}{N}\sum_{k=1}^{N}X_k-2y\frac{1}{N}\sum_{k=1}^{N}Y_k \tag{2.44}$$

subtracting (2.44) from each equation (2.35) where i=1, N, yielding the solution

$$EMS=\frac{1}{2}\left(A_{LS3}{}^{T}A_{LS3}\right)^{-1}A_{LS3}{}^{T}p_{LS3}, \tag{2.45}$$

where

$$A_{LS3}=\begin{bmatrix} X_1-\frac{1}{N}\sum_{j=1}^{N}X_j & Y_1-\frac{1}{N}\sum_{j=1}^{N}Y_j \\ X_2-\frac{1}{N}\sum_{j=1}^{N}X_j & Y_1-\frac{1}{N}\sum_{j=1}^{N}Y_j \\ \vdots & \vdots \\ X_N-\frac{1}{N}\sum_{j=1}^{N}X_j & Y_N-\frac{1}{N}\sum_{j=1}^{N}Y_j \end{bmatrix}, \quad p_{LS3}=\frac{1}{2}\begin{bmatrix} d'_{1,-}+\frac{1}{N}\sum_{i=1}^{N}K_i-K_1 \\ d'_{2,-}+\frac{1}{N}\sum_{i=1}^{N}K_i-K_2 \\ \vdots \\ d'_{N,-}+\frac{1}{N}\sum_{i=1}^{N}K_i-K_N \end{bmatrix}, \tag{2.46}$$

$$d'_{i,-} = R_i^2 - \frac{1}{N}\sum_{k=1}^{N} R_k^2 \qquad (2.47)$$

2.4.4.4 LLS – RS Solution

In [8], a new variation of the least square solution is presented by considering that the reference BS is usually associated with the smallest distance; namely,

$$r = arg\min_{i=1,N}\{R_i\}. \qquad (2.48)$$

Similar to LLS1, the solution reads

$$EMS = \frac{1}{2}\left(A_{RS}{}^{T} A_{RS}\right)^{-1} A_{RS}{}^{T} p_{RS}$$

with $(r \neq 1, r \neq 2, r \neq N)$

$$A_{RS} = \begin{bmatrix} X_1 - X_r & Y_1 - Y_r \\ X_2 - X_r & Y_2 - Y_r \\ \vdots & \vdots \\ X_N - X_r & Y_N - Y_r \end{bmatrix}, \; p_{RS} = \frac{1}{2}\begin{bmatrix} d'_{1,r} + K_r - K_1 \\ d'_{2,r} + K_r - K_2 \\ \vdots \\ d'_{N,r} + K_r - K_N \end{bmatrix} \qquad (2.49)$$

2.4.4.5 Most Likelihood Estimation - MLE

Similarly to (2.25), we can also consider the case where the measurements are noisy with known statistics. In this case, the counterpart for (2.25) is

$$p_{RS} = A_{RS}\begin{bmatrix} x \\ y \end{bmatrix} + \varepsilon$$

Where, unlike the RS method, r can stand for any BS among the set of initial BSs, while ε is a random noise with known covariance matrix C. The solution is therefore equivalent to weighted least square [9]:

$$EMS = \frac{1}{2}\left(A_{RS}{}^{T} C^{-1} A_{RS} \right)^{-1} A_{RS}{}^{T} C^{-1} p_{RS}$$

Such a solution is also equivalent to a maximum likelihood solution. An approximation of C has been given in [9] as:

$$C = 4d_r{}^2\sigma^2 + 2\sigma^4 + diag\left\{4\sigma^2 d_1^2 + 2\sigma^4 \quad \ldots \quad 4\sigma^2 d_i^2 + 2\sigma^4 \quad \ldots \quad 4\sigma^2 d_N^2 + 2\sigma^4 \right\}$$

2.5 Comparison of Location Algorithms' Performances in LOS Scenarios

2.5.1 Complexity Analysis

First, it is required that, for an n x n matrix, good algorithmic complexity for the matrix inversion is given by an optimised C-W-like algorithm [12], which reported $O(n^{2.373})$. Multiplication of n x m and m x p matrices has complexity O(nmp), which can be reduced to $O(n^{2.373})$ if n=m=p.

In this case, we compare the previous LOS localisation algorithms with respect to the number of BSs N.

Method	Complexity
Fang	O(1) -restricted to three base stations only
LLS-1	O(8(N-1))
LLS-2	$O(N^2)$
LLS-3	O(8N)
LLS-RS	O(8(N-1))
ML	$O((N-1)^2)$
Taylor	$O(p(N-1)^2)$ - with p number of iterations
Chan	$O(N^2)$

Table 2.1: Complexity of Each Algorithm

2.5.2 Simulation Conditions of Comparison

In this section, we demonstrate the comparison of each location algorithm performance in the LOS environment with different conditions. The comparison has many aspects, such as the limitation of how many BSs are used, accuracy variations with the number of BSs used, accuracy variation with noise added and RMSE in different environments. In order to hold this comparison on a strictly fair platform, in each comparison, only one input condition is changed, all the algorithms share the rest of the conditions, such as the same topology of BSs used (shown in *Figure 2.2*), the same random Gaussian noise added (with standard deviations values 0.1us, 0.15us, 0.2us, 0.25us, 0.3us, 0.35us, 0.4us, 0.45us, 0.5us) or the same initial MS position, and the same radius of cells (*radius = 3000m*). The comparison is presented in turn with a different number of BSs (NBS) (3, 4, 5, 6 and 7). All the performances were qualified by using RMSE evaluation.

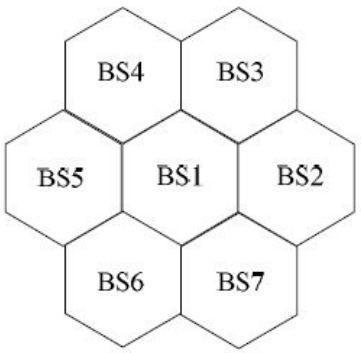

Figure 2.2: The Topology of a Cellular System

2.5.3 Algorithm Limitation of Number of Base Stations Used

In this section, Tables 2.2 and 2.3 introduce the limitation of each algorithm in different simulation conditions. Some of algorithms have usage limitations that otherwise would make the matrix close to singular or non-scaled. The reference BS chosen and noise added to measurements also affects location accuracy.

Algorithms	Influence of Gaussian Noise Added - Change Rate of RMSE (m) with σ (us)			
	NBS=7	NBS=6	NBS=5	NBS=4
LLS-1	85 m/us	101 m/us	128 m/us	214.6 m/us
LLS-2	86 m/us	90.5 m/us	116.8 m/us	79.6 m/us
LLS-3	86 m/us	84.6 m/us	91.1 m/us	104.5 m/us
LLS-RS	86 m/us	151.5 m/us	261.2 m/us	270.4 m/us
MLE	40.3 m/us	94.85 m/us	214.5 m/us	250.8 m/us
Chan	202.3 m/us	197.9 m/us	210.4 m/us	187.5 m/us
Taylor	218 m/us	197.5 m/us	236.3 m/us	263.7 m/us

Table 2.2: Variation of Location Accuracy with Noise Added

The ratio of RMSE with Gaussian noise deviation (**σ**) gives the anti-interference ability of the algorithm system from the noise. Therefore, the larger the slope stands the weaker anti-interference ability. From Table 2.2, nearly all the algorithms were affected by reducing of number of BSs used. When we used seven BSs, least square algorithms presented impressive anti-interference ability compared with the two-step most likelihood method (Chan) and Taylor's iteration estimators. When the use of BSs is decreased, compared to the Chan and Taylor estimators, least square methods become dramatically weaker in mitigating the noise. During this process, Chan's method and Taylor's method showed their stability in the variety of how many BSs were used in the simulation.

Hence, we can summarise that least square methods are less stable with a variation of the number of BSs used, and Chan's and Taylor's methods presents good characteristics of stability.

However, when the number of BSs achieved the limit, which was four, Chan's method gave a good performance along with some of the other algorithms, so there are other conditions that might affect the positioning result. We have the simulation result in Table 2.3:

Algorithms	Limitation of Number of BSs	Influence of Initialization or Reference BS Chosen	Influence of Variation of Number of BSs Used
Fang	Min=3; Max=3	No	Less Stable
LLS-1	Min=3; Max=∞	Very Sensitive	Less Stable
LLS-2	Min=3; Max=∞	Moderate	Stable
LLS-3	Min=3; Max=∞	Less Sensitive	Stable
LLS-RS	Min=3; Max=∞	Moderate	Less Stable
MLE	Min=3; Max=∞	Very Sensitive	Stable
Chan	Min=4; Max=∞	Moderate	Very Stable
Taylor	Min=3; Max=∞	Very Sensitive	Stable

Table 2.3: Limitation of Each Location Algorithm

Some of the algorithms need a very appropriate reference BS or initial guess to obtain an approximate solution. Taylor, LLS-1, MLE only provide an approximate location result whose accuracy relies on the quality of the reference chosen. LLS-3 and LLS-RS and Chan's approaches have their own step to pick out or create an appropriate reference BS, so they do not suffer from initialisation or the reference BS chosen.

2.5.4 Execution time & Complexity Analysis

When implementing each algorithm in Matlab, different location methods spend different times on calculations. By increasing the number of BSs used for getting the measurements, the execution time increases. In this section, the comparison is dedicated to the complexity of each algorithm by analysing the programme running speed. The comparison result is shown in Table 2.4.

	Execution Time for 3BSs (s)	Execution Time for 4BSs (s)	Execution Time for 5BSs (s)	Execution Time for 6BSs (s)	Execution Time for 7BSs (s)
Fang	**0.598342**	**–**	**–**	**–**	**–**
LLS-1	**0.813218**	**0.865838**	**0.933085**	**0.996357**	**1.052122**
LLS-2	**0.902780**	**1.037191**	**1.172237**	**1.341021**	**1.509134**
LLS-3	**2.264266**	**3.052388**	**3.803990**	**4.597497**	**5.374518**
LLS-RS	**0.901795**	**0.931641**	**0.951766**	**0.976715**	**0.996259**
MLE	**1.064748**	**1.201628**	**1.310236**	**1.395390**	**1.511204**
Chan	**–**	**2.117430**	**2.296203**	**2.474040**	**2.608051**
Taylor	**4.379776**	**4.791822**	**5.180560**	**5.564169**	**5.930608**

Table 2.4: Complexity Analysis of Each Location Method

Each of the algorithms has an execution time when simulated. This is also considered in this thesis. Compared with Taylor, the iterative method and the least square approaches are more direct. The time spent is less than 5 seconds.

2.6 Conclusion

In Chapter 2, we discussed several algorithms used in the LOS scenario. Through simulations both respectively and together, we can clearly understand

the advantages and limitations of each algorithm.

- If we do not have many BSs to allocate, we prefer to choose Chan's and Taylor's methods for their anti-interference ability from noise.
- If we do not have good priori information with which to choose a reference or initial guess, LLS-3, LLS-RS and Chan's are the best choices.
- If we require estimating speed, some of the algorithms without the iteration step can be trusted.

In order to search a good algorithm for real life positioning, we have to research external factors which can affect the location quality of algorithms (such as the topology of BSs in Section 2.7.1). In the following chapters, we will research some of the external factors affecting location accuracy, and show an innovation algorithm.

2.7 Reference

[1] A. Abrardo, G. Benelli, C. Maraffon and A. Toccafondi, "*Performance of TDoA-based radiolocation techniques in CDMA urban environments*," in Communications, 2002. ICC 2002. IEEE International Conference on, 2002, pp. 431-435.

[2] Zhang jian wu, Yu Cheng-lei and Ji Ying-ying, "*The performance analysis of chan location algorithm in cellular network*," in Computer Science and Information Engineering, 2009 WRI World Congress on, 2009, pp. 339-343.

[3] B. T. Fang, "*Simple solutions for hyperbolic and related position fixes*," Aerospace and

Electronic Systems, IEEE Transactions on, vol. 26, pp. 748-753, 1990.

[4] K. W. Cheung, H. C. So, W. -. Ma and Y. T. Chan, "*Least squares algorithms for time-of-arrival-based mobile location*," Signal Processing, IEEE Transactions on, vol. 52, pp. 1121-1130, 2004.

[5] S. Gezici, I. Guvenc and Z. Sahinoglu, "*On the performance of linear least-squares estimation in wireless positioning systems*," in Communications, 2008. ICC '08. IEEE International Conference on, 2008, pp. 4203-4208.

[6] S. Venkatesh and R. M. Buehrer, "*A linear programming approach to NLOS error mitigation in sensor networks*," in Information Processing in Sensor Networks, 2006. IPSN 2006. the Fifth International Conference on, 2006, pp. 301-308.

[7] Zang Li, W. Trappe, Y. Zhang and B. Nath, "*Robust statistical methods for securing wireless localization in sensor networks*," in Information Processing in Sensor Networks, 2005. IPSN 2005. Fourth International Symposium on, 2005, pp. 91-98.

[8] I. Guvenc, S. Gezici, F. Watanabe and H. Inamura, "*Enhancements to linear least squares localization through reference selection and ML estimation*," in Wireless Communications and Networking Conference, 2008. WCNC 2008. IEEE, 2008, pp. 284-289.

[9] S. M. Kay, Fundamentals of Statistical Signal Processing: Estimation Theory. Upper Saddle River, NJ: Prentice Hall, Inc., Volume I: Estimation Theory, 1993.

[10] Y. T. Chan and K. C. Ho, "*A simple and efficient estimator for hyperbolic location*," Signal Processing, IEEE Transactions on, vol. 42, pp. 1905-1915, 1994.

[11] Wuk Kim, Jang Gyu Lee and Gyu-In Jee, "*The interior-point method for an optimal treatment of bias in trilateration location*," Vehicular Technology, IEEE Transactions on, vol. 55, pp. 1291-1301, 2006.

[12] W. H. Foy, "*Position-Location Solutions by Taylor-Series Estimation*," Aerospace and Electronic Systems, IEEE Transactions on, vol. AES-12, pp. 187-194, 1976.

CHAPTER 3: COMBINATION OF TAYLOR'S AND CHAN'S METHODS FOR MOBILE POSITIONING

3.1 Overview

After reviewing the main mobile positioning approaches employed in LOS scenarios where the raw measurements are comprised of TDOA due to their proven efficiency and relatively easy implementation, a new method based on an optimal statistical combination of Chan's and Taylor's methods is proposed in this chapter. In particular, a linear combination of the two estimators that minimises variance is proposed as suggested in [1].

This chapter is organised as follows: Section 3.2 gives the motivation for creating the combination method. The new combination method is presented in Section 3.3. The performances of the new estimator in terms of RMSE metrics are summarised in Section 3.4, while comparisons with other positioning methods are presented in Section 3.5. Section 3.6 provides some conclusions.

3.2 Motivation Grounds for the Combination Method

The idea of combining Taylor's and Chan's estimators has several intuitive grounds. First, it is accepted that once the initial guess is near to the true position of MS, then, provided that computational cost is not a big issue, Taylor's estimation provides plenty good results. Similarly, the accuracy of the

approximate solution provided by Chan's algorithm relies mainly on the quality of the a priori information employed to solve the underlying maximum likelihood estimation problem. Consequently, a combination of the two estimators is worth considering. Intuitively, a possible combination scenario of the two estimators consists of using Chan's estimator to initialise Taylor's estimator. Nevertheless, we consider a combined estimate which minimises the variance in the light of the pioneering work of Franklin and Graybilland [1], such that the combination is more linear where the underlying estimator has minimal variance.

3.3 Combination of Chan and Taylor Method

3.3.1 Linear Combination of Chan-Taylor Method

Typically, let Z_1 and Z_2 stands for the estimates using Chan and Taylor's estimations, respectively. The new estimate Z is obtained as a linear combination of the above two estimates and unbiased [7]:

$$Z = \lambda_1 Z_1 + \lambda_2 Z_2 \tag{3.1}$$

According to the fact that the two estimators are both unbiased and the linearity of the expectation, we obtained:

$$E[Z] = \lambda_1 E[Z_1] + \lambda_2 E[Z_2] \tag{3.2}$$

This yields

$1 = \lambda_1 + \lambda_2$, or, equivalently, $\lambda_1 = 1 - \lambda_2$

The rationale behind the preceding calculation is to assume that the two existing

estimators only provide an approximate estimate of the true position, which can be reached asymptotically. This justifies the fact that the two estimators have the same mean on average as the combined estimator Z. [7]

As regards the covariance matrix, by using Equation (3.1), we obtain:

$$\begin{aligned} Var(Z) &= E\left[(Z - E[Z])^2\right] = E\left[(Z - E[Z])^2\right] \\ &= E\left[\left(\lambda_1 Z_1 + \lambda_2 Z_2 - E\left[\lambda_1 Z_1 + \lambda_2 Z_2\right]\right)^2\right] \\ &= E\left[\left((\lambda_1 Z_1 - \lambda_1 E[Z_1]) + (\lambda_2 Z_2 - \lambda_2 E[Z_2])\right)^2\right] \\ &= {\lambda_1}^2 E\left[\left(Z_1 - E[Z_1]\right)^2\right] + {\lambda_2}^2 E\left[\left(Z_2 - E[Z_2]\right)^2\right] \end{aligned} \quad (3.3)$$

Equation (3.3) can be rewritten as

$$Var(Z) = \lambda^2 . Var(Z_1) + (1-\lambda)^2 . Var(Z_2) \quad (3.4)$$

Particularly, given that the output of Z_1 and Z_2 is 2-dimensional (latitude and longitude coordinates), the method is to take the norm of (3.4), yielding

$$Var(Z) = \lambda^2 . |Var(Z_1)| + (1-\lambda)^2 . |Var(Z_2)| \quad (3.5)$$

To minimise *Var(Z)*, one can set the derivative of |*Var(Z)*| expression with respect to λ to zero, which yields

$$\lambda = \frac{P_{Taylor}(1,1)^2 + P_{Taylor}(2,2)^2}{P_{Taylor}(1,1)^2 + P_{Taylor}(2,2)^2 + P_{Chan}(1,1)^2 + P_{Chan}(2,2)^2} \quad (3.6)$$

Consequently, the combined estimator presents as

$$Z = \lambda \begin{bmatrix} x_{Chan} \\ y_{Chan} \end{bmatrix} + (1-\lambda) \begin{bmatrix} x_{Taylor} \\ y_{Taylor} \end{bmatrix} \quad (3.7)$$

3.3.2 Formulation of Chan's and Taylor's Hyperbolic Estimator Combination

Because Taylor algorithm needs an initial value near the MS to make sure of Taylor series convergence, so Chan's method [2][3] is used to calculate the initial position that will be employed in Taylor's [4][5] method, which avoids taking an initial value at random.

Assume $z_a = \begin{bmatrix} z_p{}^T & R_1 \end{bmatrix}^T$ is the unknown vector, where $z_p = \begin{bmatrix} x & y \end{bmatrix}^T$

First, an approximation of the solution can be provided by

$$\begin{bmatrix} x \\ y \\ R_1 \end{bmatrix} = \left(G_a{}^T Q^{-1} G_a \right)^{-1} G_a{}^T Q^{-1} F \qquad (3.8)$$

with $G_a = -\begin{bmatrix} X_{2,1} & \mathrm{Y}_{2,1} & \mathrm{R}_{2,1} \\ X_{3,1} & \mathrm{Y}_{3,1} & \mathrm{R}_{3,1} \\ . & & \\ X_{M,1} & \mathrm{Y}_{M,1} & \mathrm{R}_{M,1} \end{bmatrix}$ and $F = \frac{1}{2}\begin{bmatrix} R_{2,1}^2 - K_2^2 + K_1^2 \\ R_{3,1}^2 - K_3^2 + K_1^2 \\ ..... \\ R_{M,1}^2 - K_M^2 + K_1^2 \end{bmatrix}$

Let us denote by $R_{i,1}^0$ the noise-free measurement from $R_{i,1}$; namely, $R_{i,1} = R_{i,1}^0 + n_{i,1}$, where $n_{i,1}$ stands for zero-meanGaussian noise, while the noise vector n has a known variance-covariance matrix Q, which allows full noise reconstruction. This yields the following:

$$R_{i,1} = R_i^0 - R_1^0 + n_{i,1} \qquad \text{(i=2 to M)} \qquad (3.9)$$

Denote

$$B = \begin{pmatrix} R_1^0 & 0 & 0..0 \\ 0 & R_2^0 & 0..0 \\ . & & \\ 0 & 0 & ..0 \; R_M^0 \end{pmatrix}$$

A second update of estimation in (3.8) is given by

$$\begin{bmatrix} x \\ y \\ R_1 \end{bmatrix} = \left(G_a{}^T \psi^{-1} G_a{}^T \right)^{-1} G_a{}^T \psi^{-1} h \tag{3.10}$$

with

$$\Psi = c^2 BQB \tag{3.11}$$

On the other hand, using the covariance matrix

$$\mathrm{cov}([x \;\; \mathrm{y} \; R_1]^T) \approx (G_a \Psi^{-1} G_a)^{-1}, \tag{3.12}$$

we can construct the noise-free estimate of *x*, *y* and R_1; namely,

$$x = x^0 + v_x, \; \mathrm{y} = y^0 + v_y, \; \mathrm{R}_1 = R_1{}^0 + v_r, \tag{3.13}$$

where v is zero-mean Gaussian noise with variance-covariance matrix given by expression (3.12), and [*x y* R_1] is provided by (3.10). Let

$$S = \begin{pmatrix} x^0 - x_1 & 0 & 0 \\ 0 & \mathrm{y}^0 - y_1 & 0 \\ 0 & 0 & R_1^0 \end{pmatrix} \tag{3.14}$$

Then, the final estimate is given by

$$\begin{bmatrix} x_{Chan} \\ y_{Chan} \end{bmatrix} = \begin{bmatrix} x_1 \\ y_1 \end{bmatrix} \pm \sqrt{\left(G^T \psi^{-1} G \right)^{-1} G^T \psi^{-1} H} \tag{3.15}$$

with

$$G = \begin{bmatrix} 1 & 0 \\ 0 & 1 \\ 1 & 1 \end{bmatrix}, \qquad H = \begin{bmatrix} (x - x_1)^2 \\ (y - y_1)^2 \\ R_1^2 \end{bmatrix}$$

$$\psi = 4S(G_a \Psi^{-1} G_a)^{-1} S$$

and its associated variance-covariance:

$$P_{Chan} = \mathrm{cov}\left([x \; y]^T\right) \approx c^2 (B' G^T S^{-1} G^T B^{-1} Q^{-1} B^{-1} G S^{-1} G B')^{-1} \tag{3.16}$$

with

$$B' = \begin{bmatrix} x^0 - x_1 & 0 \\ 0 & y^0 - y_1 \end{bmatrix}, \qquad z_a = \begin{bmatrix} (x - x_1)^2 \\ (y - y_1)^2 \end{bmatrix},$$

When the Chan location part finished, the Taylor series starts from $\begin{bmatrix} x_{Chan} \\ y_{Chan} \end{bmatrix}$

$$\delta = \begin{bmatrix} \Delta x \\ \Delta y \end{bmatrix} = \left(G_t^{\,T} Q^{-1} G_t\right)^{-1} G_t^{\,T} Q^{-1} h_t \tag{3.17}$$

With

$$h_t = \begin{bmatrix} R_{2,1} - (R_1 - R_2) \\ R_{3,1} - (R_1 - R_3) \\ . \\ R_{M,1} - (R_1 - R_M) \end{bmatrix}$$

$$G_t = \begin{bmatrix} \frac{X_1 - x}{R_1} - \frac{X_2 - x}{R_2} & \frac{Y_1 - y}{R_1} - \frac{Y_2 - y}{R_2} \\ \frac{X_1 - x}{R_1} - \frac{X_3 - x}{R_3} & \frac{Y_1 - y}{R_1} - \frac{Y_3 - y}{R_3} \\ . & \\ . & \\ \frac{X_1 - x}{R_1} - \frac{X_M - x}{R_M} & \frac{Y_1 - y}{R_1} - \frac{Y_M - y}{R_M} \end{bmatrix}$$

The solution is elaborated as follows:

- Initialise *(x, y)* as with $x = x_{Chan}$; $y = y_{Chan}$
- Use expression (3.17) to calculate variations Δx and Δy.
- In the next recursion use $x = x_{Chan} + \Delta x$ and $y = y_{Chan} + \Delta y$
- Repeat the steps above until Δx and Δy get smaller than some threshold α: $|\Delta x| + |\Delta y| < \alpha$
- Afterword, we can estimate the MS in $\begin{bmatrix} x_{Taylor} \\ y_{Taylor} \end{bmatrix}$
- The variance-covariance matrix of the estimate is

$$P_{Taylor} = \left(G_t^{\ T} Q^{-1} G_t \right)^{-1} \tag{3.18}$$

Based on equations (3.16) and (3.18), the final combination estimator reading will be (3.19):

$$\begin{bmatrix} x \\ y \end{bmatrix} = \lambda \begin{bmatrix} x_{Chan} \\ y_{Chan} \end{bmatrix} + (1-\lambda) \begin{bmatrix} x_{Taylor} \\ y_{Taylor} \end{bmatrix} \tag{3.19}$$

where

$$\lambda = \frac{P_{Taylor}(1,1)^2 + P_{Taylor}(2,2)^2}{P_{Taylor}(1,1)^2 + P_{Taylor}(2,2)^2 + P_{Chan}(1,1)^2 + P_{Chan}(2,2)^2}$$

The flow chart of the Chan-Taylor Combination method is presented as follows:

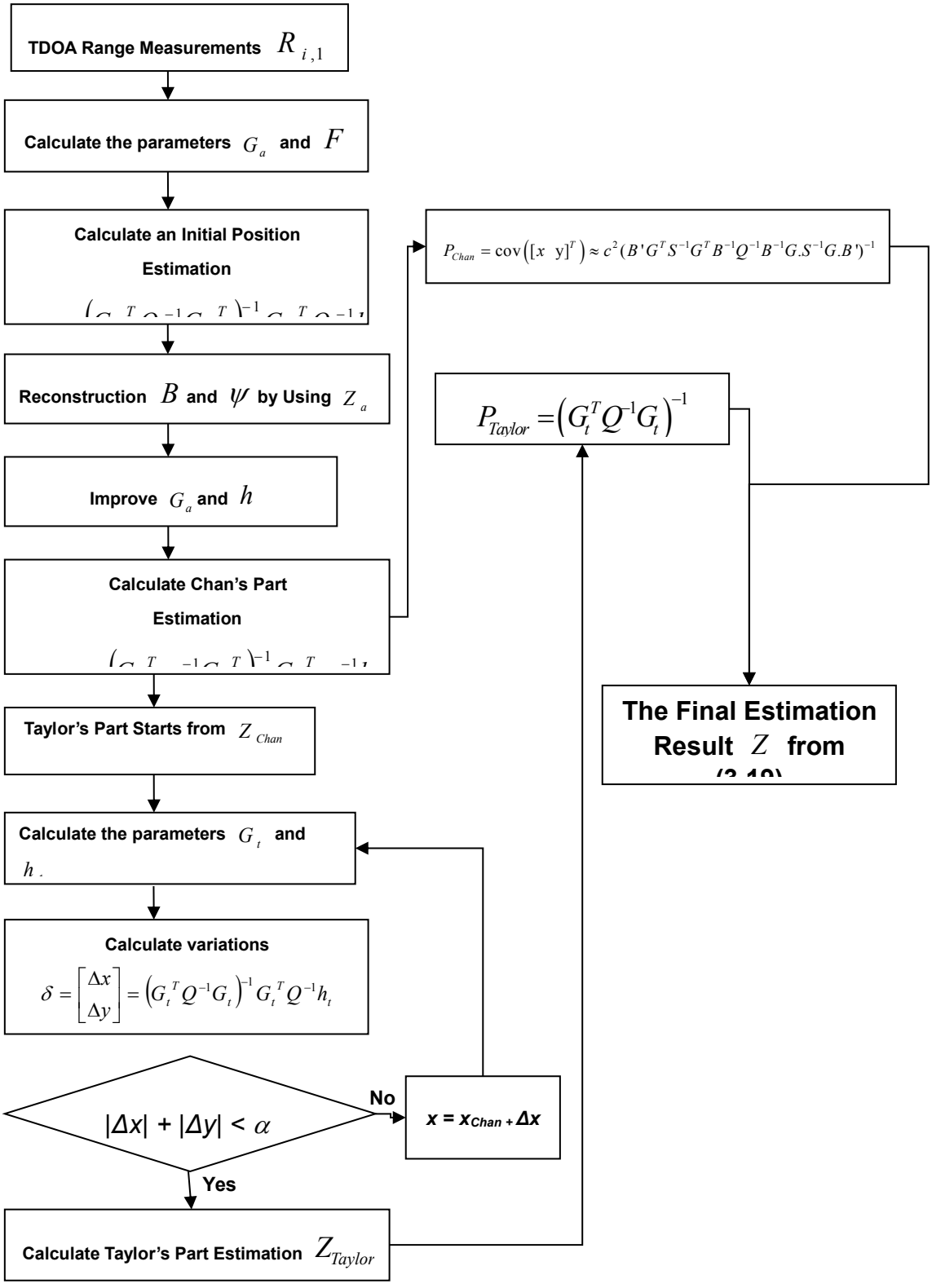

Figure 3.1: RMSE Result of Combination Location Method

3.4 Simulation of Location Performance by Combination Estimator

In this section, we reproduce the simulation setting of Section 2.5.2 [6]. The positioning performance is assessed both in terms of RMSE metric and direct-viewing on 2D coordinates. Perturbations pervading the measurements are modelled as zero-mean additive Gaussian noise whose standard deviation values range from 0.1us to 0.5us, and with a different number of BSs (NBS) (4, 5, 6 and 7).

The simulation result presented in Figure 3.1 exhibits the accuracy of the combination algorithm with respect to noise intensity as quantified by the standard deviation of Gaussian random noise from 0.1us to 0.5us. The Y-axis presents the RMSE values. The results when using four, five, six and seven BSs are highlighted.

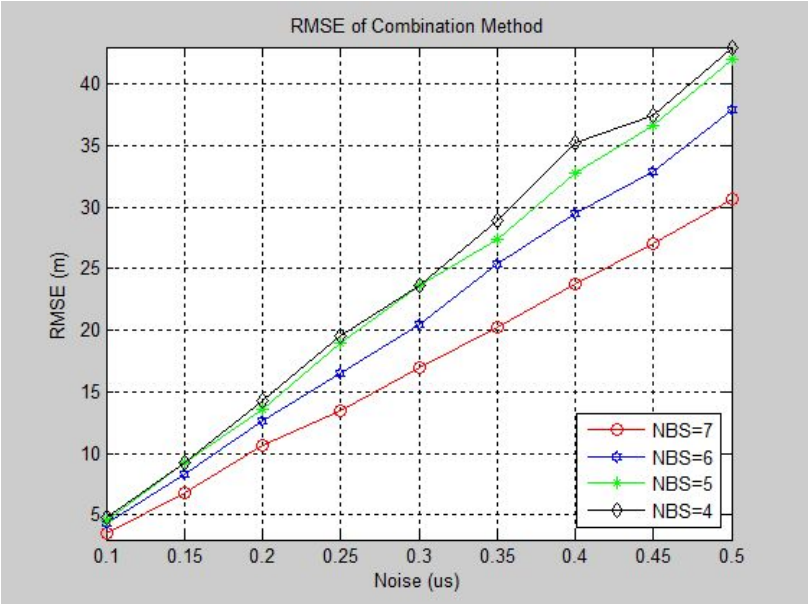

Figure 3.2: RMSE Result of Combination Location Method

Results highlighted in Figure 3.2 show that the performances of the hybrid estimator are affected by the number of BSs employed, in the sense that the higher the number of stations, the better is the performance in terms of RMSE values. On the other hand, the graph exhibits roughly a linear relationship between the noise intensity in terms of standard deviation of noise and the location accuracy (RMSE). Intuitively, the ratio of RMSE with Gaussian noise deviation (**σ**) also provides an indication of the anti-interference ability of the algorithm.

Figures 3.3, 3.4, 3.5 and 3.6 show 2D examples of the hybrid estimator with 7, 6, 5 and 4 BSs, respectively. In these figures, blue stars stand for BS locations; the red circle stands for the true position of the MS, while the green points correspond to location estimation results for different noise realisations. For each figure, a zoom around the true position is also depicted.

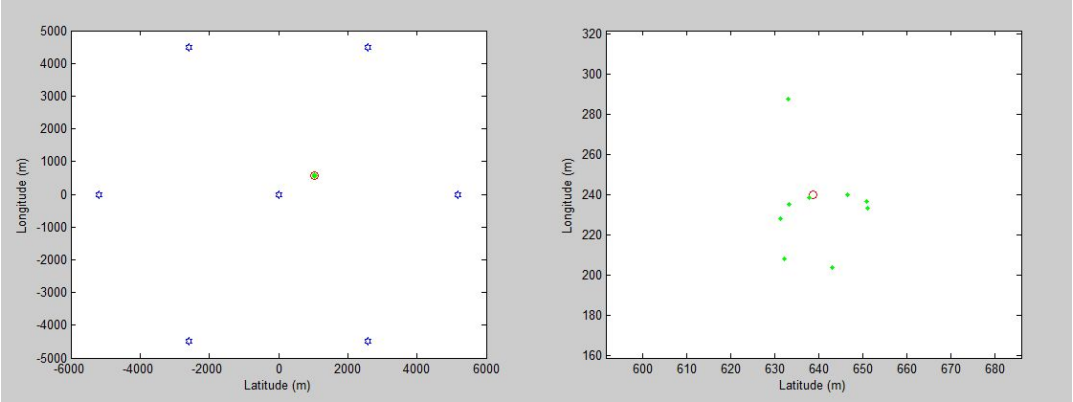

(a) ***(b)***

Figure 3.3 (a): Combination Location Estimator Performance in NBS=7.

(b): A Zoom Around of True Position

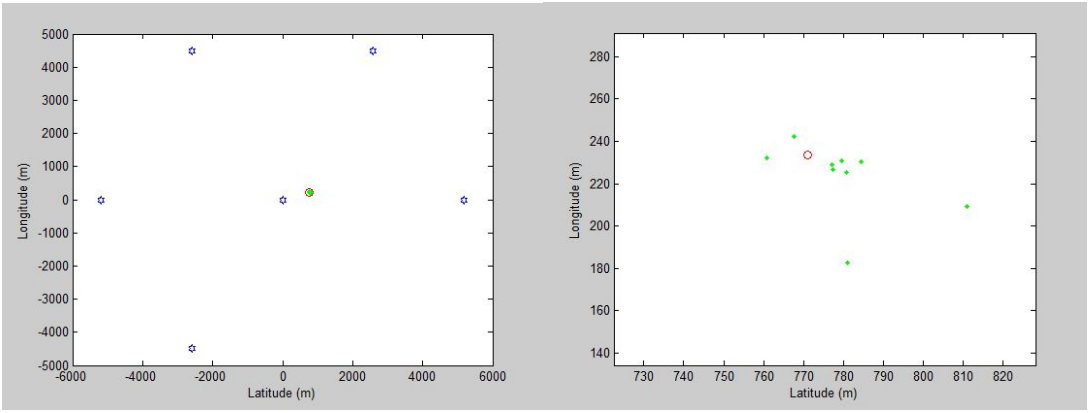

(a) ***(b)***

Figure 3.4 (a): Combination Location Estimator Performance in NBS=6

(b): A Zoom Around of True Position

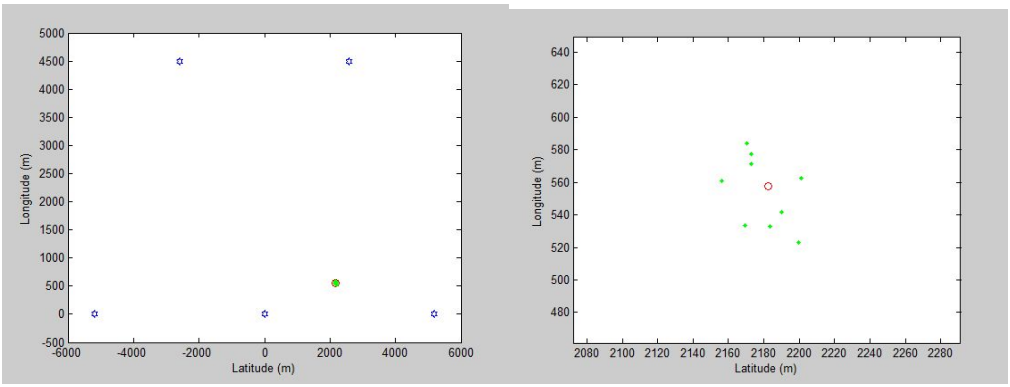

(a) ***(b)***

Figure 3.5 (a): Combination Location Estimator Performance in NBS=5

(b): A Zoom Around of True Position

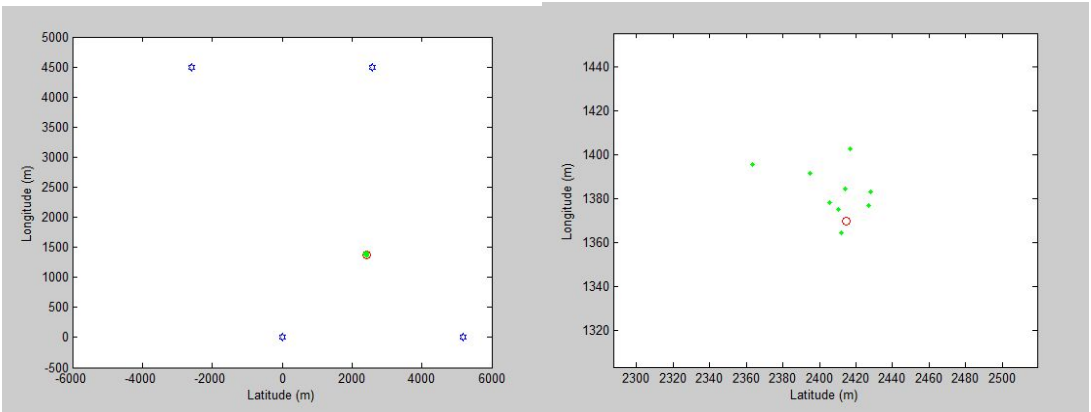

(a) *(b)*

Figure 3.6 (a): Combination Location Estimator Performance in NBS=4

(b): A Zoom Around of True Position

The simulation results provide a visual representation of the 2D mobile estimation with respect to the number of BSs employed. It is typically found that all estimated results are allocated close to the true position with acceptable errors. Furthermore, the visual representations also support the evidence gathered from Figure 3.1 that quality of estimation increases with the number of BSs employed, but decreases with noise intensity.

3.5 Comparison of Combination Algorithms with Classic Algorithms

In this section, a fair comparison between the hybrid method and some classic methods described in Chapter 2 is demonstrated. The simulation input conditions are strictly held as in Section 2.8.1. The comparison is carried out with respect to the number of BSs (NBS) (4, 5, 6 and 7), where the performance is quantified using RMSE evaluation. Meanwhile, the ratio of RMSE with standard deviation (**σ**) is also reported. The smaller this ratio, the stronger is the anti-interference ability of the system.

3.5.1 Simulation Using 7 Base Stations

Since, from Table 2.1 of the previous chapter for the case NBS=7, the LLS algorithms, LLS-2, LLS-3 and LLS-RS provided almost the same location quality, therefore, in this section, we only compare the hybrid method with LLS-1, LLS-2, MLE, Chan and Taylor.

NBS=7	Average RMSE (m) in Different Standard Deviations σ (us)									Change Rate of
	0.1us	0.15us	0.2us	0.25us	0.3us	0.35us	0.4us	0.45us	0.5us	RMSE with σ
Combination	3.69m	7.43m	10.25m	15.24m	19.26m	23.36m	25.42m	30.03m	33.08m	73.5 m/us
LLS-1	8.59m	13.81m	17.03m	21.83m	26.01m	29.96m	36.81m	38.47m	42.59m	85 m/us
LLS-2	8.74m	14.04m	17.27m	22.14m	26.54m	30.44m	37.49m	39.06m	43.14m	86 m/us
LLS-3	8.74m	14.04m	17.27m	22.14m	26.54m	30.44m	37.49m	39.06m	43.14m	86 m/us
LLS-RS	8.74m	14.04m	17.27m	22.14m	26.54m	30.44m	37.49m	39.06m	43.14m	86 m/us
MLE	4.15m	6.76m	8.29m	10.75m	12.13m	14.31m	17.58m	19.34m	20.30m	40.3 m/us
Chan	21.19m	32.60m	40.22m	51.66m	65.70m	73.11m	89.31m	92.62m	102.12m	202.3 m/us
Taylor	22.10m	34.26m	42.73m	55.15m	69.56m	78.67m	95.42m	98.61m	109.48m	218 m/us

Table 3.1: Performance of Location Algorithms Using 7 BSs

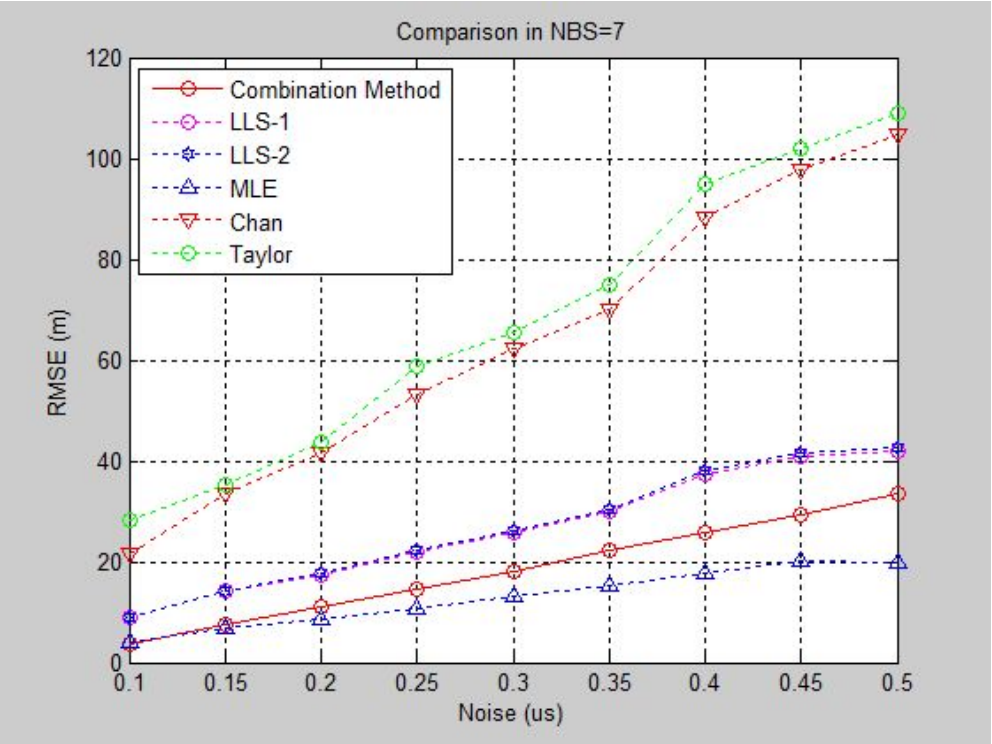

Figure 3.7: RMSE Result of Location Algorithms Using 7 BSs

The simulation result, in Figure 3.7, presents MLE as providing the best performance, while the hybrid method provides the second best performance.

3.5.2 Simulation Using 6 Base Stations

In this section, we repeated the previous simulations when the NBS is reduced to six. The relative position of the MS and the topology of the BSs were shown in unsymmetrical shape. The RMSE result is presented in Table 3.2:

NBS=6	Average RMSE (m) in Different Standard Deviations σ (us)									Change Rate of RMSE with σ
	0.1us	0.15us	0.2us	0.25us	0.3us	0.35us	0.4us	0.45us	0.5us	
Combination	3.52m	7.08m	10.30m	14.07m	17.44m	21.55m	25.00m	28.72m	31.56m	**70.1 m/us**
LLS-1	11.02m	16.30m	21.52m	26.66m	30.38m	38.67m	41.07m	49.06m	51.42m	**101 m/us**
LLS-2	9.92m	14.64m	19.32m	23.91m	27.27m	34.84m	36.88m	44.21m	46.11m	**90.5 m/us**
LLS-3	9.28m	13.72m	18.10m	22.53m	25.56m	32.88m	34.74m	41.58m	43.13m	**84.6 m/us**
LLS-RS	16.68m	24.57m	32.45m	39.51m	46.15m	55.74m	60.21m	72.64m	77.29m	**151.5 m/us**
MLE	10.75m	16.08m	21.07m	25.76m	30.52m	34.34m	38.26m	46.58m	48.69m	**94.85 m/us**
Chan	20.82m	30.65m	40.29m	49.82m	57.82m	68.97m	74.96m	89.44m	99.99m	**197.9 m/us**
Taylor	21.68m	32.01m	42.46m	51.66m	60.44m	72.61m	78.72m	94.26m	100.70m	**197.5 m/us**

Table 3.2: Performance of Location Algorithms Using 6 BSs

From Figure 3.8, we can observe that, in a six BSs network, the combination method shows the best performance both in accuracy and interference mitigating skill. In the RMSE analysis, the combination method shows an obvious gap to with rest of the algorithms.

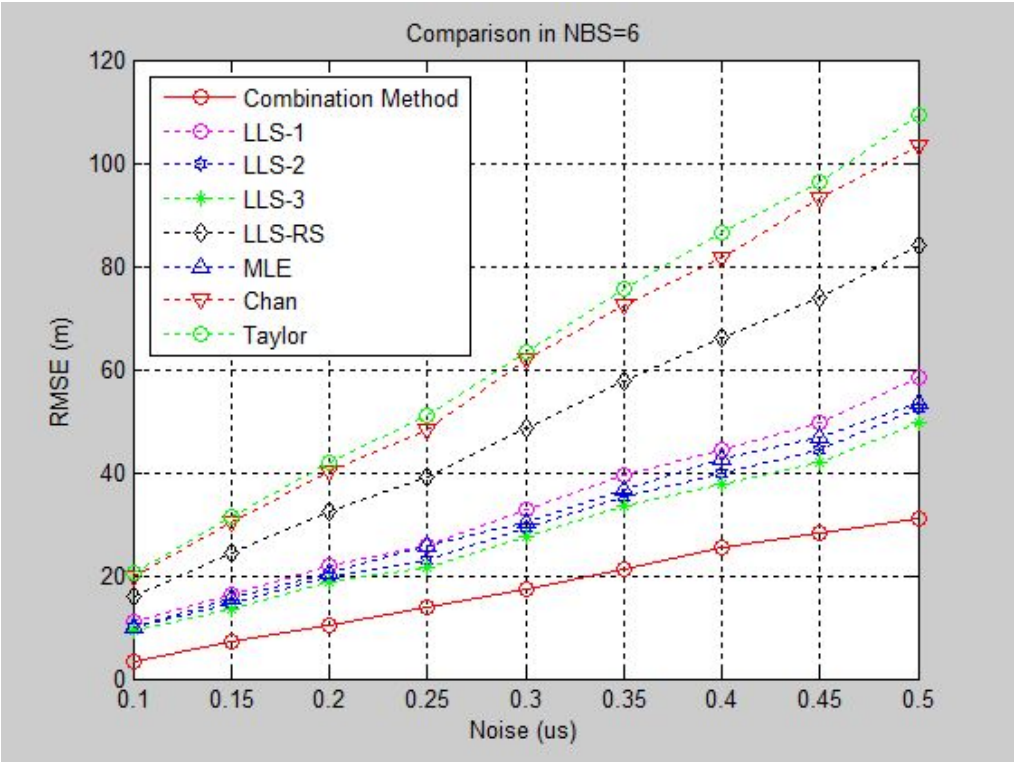

Figure 3.8: RMSE Result of Location Algorithms Using 6 BSs

3.5.3 Simulation Using 5 Base Stations

Continually taking out one BS from the system, the RMSE result is presented in Table 3.3:

NBS=5	Average RMSE (m) in Different Standard Deviations σ (us)									Change Rate of RMSE with σ
	0.1us	0.15us	0.2us	0.25us	0.3us	0.35us	0.4us	0.45us	0.5us	
Combination	4.01m	7.79m	12.08m	16.24m	20.11m	24.10m	28.11m	31.80m	36.48m	81.2 m/us
LLS-1	13.23m	19.28m	25.20m	30.72m	38.56m	42.69m	53.73m	57.22m	64.63m	128 m/us
LLS-2	12.22m	17.61m	23.25m	28.37m	35.33m	39.75m	49.22m	52.82m	58.96m	116.8 m/us
LLS-3	9.27m	13.64m	17.57m	21.29m	27.25m	29.33m	37.89m	40.23m	45.72m	91.1 m/us
LLS-RS	27.74m	39.26m	53.36m	65.41m	79.14m	93.25m	110.38m	119.77m	132.19m	261.2 m/us
MLE	23.31m	32.41m	45.17m	55.20m	65.75m	79.97m	91.46m	100.76m	109.12m	214.5 m/us
Chan	24.32m	34.81m	46.53m	55.48m	66.55m	76.33m	93.76m	95.57m	108.49m	210.4 m/us
Taylor	24.72m	35.75m	47.52m	58.27m	71.44m	81.47m	99.35m	107m	119.26m	236.3 m/us

Table 3.3: Performance of Location Algorithms Using 5 BSs

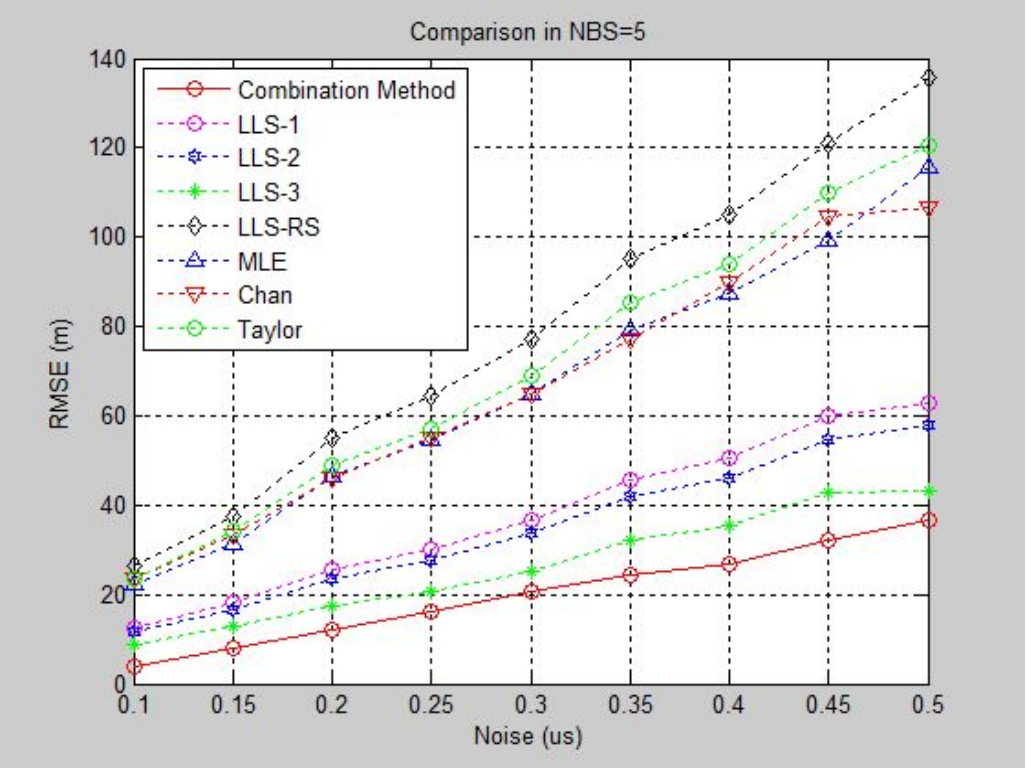

Figure 3.9: RMSE Result of Location Algorithms Using 5 BSs

Removing one of the BS from the system, the location quality from all the algorithms was affected, but the combination algorithm again shows the best positioning estimation. Compared to how some of the LLS algorithms' location quality changed, the combination estimator gives obvious performance stability.

3.5.4 Simulation Using 4 Base Stations

The RMSE result is presented in Table 3.4:

NBS=4	Average RMSE (m) in Different Standard Deviations σ (us)									Change Rate of RMSE with σ
	0.1us	0.15us	0.2us	0.25us	0.3us	0.35us	0.4us	0.45us	0.5us	
Combination	3.71m	7.44m	11.12m	14.37m	18.54m	22.04m	26.72m	30.59m	32.32m	**71.5 m/us**
LLS-1	20.90m	31.71m	44.97m	54.72m	63.18m	78.48m	87.27m	99.08m	106.74m	**214.6 m/us**
LLS-2	19.39m	29.50m	41.80m	50.81m	58.55m	72.69m	80.79m	91.87m	98.98m	**79.6 m/us**
LLS-3	10.38m	15.54m	22.25m	27.11m	30.89m	39m	43.28m	49.29m	52.20m	**104.5 m/us**
LLS-RS	26.29m	40.07m	56.66m	68.84m	79.65m	98.61m	109.66m	124.61m	134.46m	**270.4 m/us**
MLE	24.41m	37.35m	52.78m	63.98m	73.86m	91.39m	101.46m	115.7m	124.73m	**250.8 m/us**
Chan	21.1m	30.77m	43.95m	51.33m	62.33m	73.92m	81.7m	92.56m	96.12m	**187.5 m/us**
Taylor	22.88m	38.78m	53.89m	74.23m	72.33m	98.48m	103.11m	112.42m	128.35m	**263.7 m/us**

Table 3.4: Performance of Location Algorithms Using 4 BSs

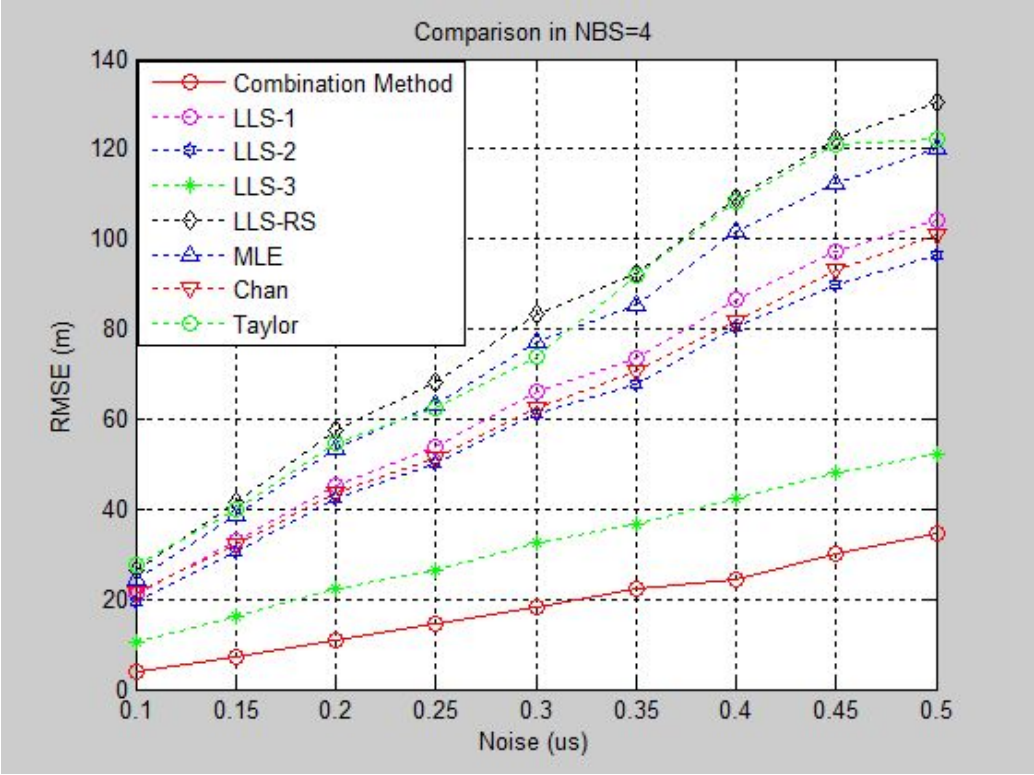

Figure 3.10: RMSE Result of Location Algorithms Using 4 BSs

Here, only four BSs left. All the algorithms are obviously affected yet, even in this kind of situation, the combination model do not show itself to be largely influenced. Compared with the other algorithms, the combination method is

credible.

3.5.5 Execution time & Complexity Analysis

Since the convex method is combined two algorithms, the execution time is longer than the previous methods. And the combination method is also affected from the number of BSs used. By increasing the number of BSs used for getting the measurements, the programme running time increases. The comparison result is shown in Table 3.5.

	Execution Time for 3BSs (s)	Execution Time for 4BSs (s)	Execution Time for 5BSs (s)	Execution Time for 6BSs (s)	Execution Time for 7BSs (s)
Fang	**0.598342**	**–**	**–**	**–**	**–**
LLS-1	**0.813218**	**0.865838**	**0.933085**	**0.996357**	**1.052122**
LLS-2	**0.902780**	**1.037191**	**1.172237**	**1.341021**	**1.509134**
LLS-3	**2.264266**	**3.052388**	**3.803990**	**4.597497**	**5.374518**
LLS-RS	**0.901795**	**0.931641**	**0.951766**	**0.976715**	**0.996259**
MLE	**1.064748**	**1.201628**	**1.310236**	**1.395390**	**1.511204**
Chan	**–**	**2.117430**	**2.296203**	**2.474040**	**2.608051**
Taylor	**4.379776**	**4.791822**	**5.180560**	**5.564169**	**5.930608**
Combination	**-**	**5.974747**	**7.567572**	**8.062854**	**8.831231**

Table 3.5: Complexity Analysis of Each Location Method

3.6 Conclusion

This chapter introduced a combination put forward using a linear combination of the two estimators that most improve location quality. A simulation platform using Monte Carlo simulations was designed to test the performance of the estimators under different noise intensity scenarios and using a range of known BSs. The results shown conform to intuition and are widely in agreement with the current

accuracy level observed in mobile location services.

3.7 Reference

[1] A. Franklin, R. Graybilland and B. Deal, Combining unbiased estimators, Biometrics, 15(4), 1959, pp. 543-550.

[2] Zhang jian wu, Yu Cheng-lei and Ji Ying-ying, "*The performance analysis of chan location algorithm in cellular network*," in Computer Science and Information Engineering, 2009 WRI World Congress on, 2009, pp. 339-343.

[3] Y. T. Chan and K. C. Ho, "*A simple and efficient estimator for hyperbolic location*," Signal Processing, IEEE Transactions on, vol. 42, pp. 1905-1915, 1994.

[4] Wuk Kim, Jang Gyu Lee and Gyu-In Jee, "*The interior-point method for an optimal treatment of bias in trilateration location*," Vehicular Technology, IEEE Transactions on, vol. 55, pp. 1291-1301, 2006.

[5] W. H. Foy, "*Position-Location Solutions by Taylor-Series Estimation*," Aerospace and Electronic Systems, IEEE Transactions on, vol. AES-12, pp. 187-194, 1976.

[6] Zhang jian wu, Yu Cheng-lei and Ji Ying-ying, "*The performance analysis of chan location algorithm in cellular network*," in Computer Science and Information Engineering, 2009 WRI World Congress on, 2009, pp. 339-343.

[7] Hao Li, M. Oussalah, "*Combination of Taylor and Chan method in mobile positioning*," in Cybernetic Intelligent Systems (CIS), 2011 IEEE 10th International Conference on, 2011, pp. 104-110.

CHAPTER 4: TDOA WIRELESS LOCALISATION COMPARISON INFLUENCE OF NETWORK TOPOLOGIES

4.1 Overview

The analysis of the previous sections assumes that the MS is receiving signals from all the surrounding BSs. Nevertheless, some failure cannot be fully avoided, yielding various cellular topologies which, in turn, would likely influence the accuracy of positioning. Unfortunately less work has been achieved from a wireless positioning accuracy perspective, although intuitively this would significantly contribute towards the E911 [1] [2], for instance. This motivates the current work where some commonly employed techniques involving TDOA and TOA technologies are contrasted and investigated with respect to the geometrical disposition of the antennas. More specifically, the approximated least square solutions (LLS-1 [3], LLS-2 [4], LLS-3 [5], LLS-RS [6]), MLE [7] [8], Chan's [9], Taylor's[10] described in Chapter 2 and the newly introduced combination of Chan-Taylor [11] introduced in Chapter 3 are compared while considering several antenna topologies. Four main types of cellular topologies are investigated: balanced, circular, U-shape and linear, which can be inferred from a balanced topology structure. Such topologies can straightforwardly be inferred from regular (optimal) cellular disposition when blocking occurs, disabling some BSs. The Section 4.2 of this chapter presents the structure of the four types of network topologies. Section 4.3 gives the main setup parameters in

simulations and Section 4.4 highlights the simulation platform and comments on the obtained results. Section 4.5 gives a summary of comparisons. Finally, some conclusive remarks are reported in Section 4.6.

4.2 Network Topologies

In this section, several network topologies are exhibited. Each topology is presented with a 2D graph and coordinates. We consider here four different topologies: balanced, circular, U-shape, and linear for analysing and simulating. Furthermore, we consider a vehicle moving at a constant speed in one direction.

4.2.1 Balanced Topology

A generic simulation platform is shown in Figure 4.1. As in practical implementations, the cells have hexagonal shapes in order to restrict the interference between cells so no overlapping region exists. We shall refer to such situation as a balanced topology.

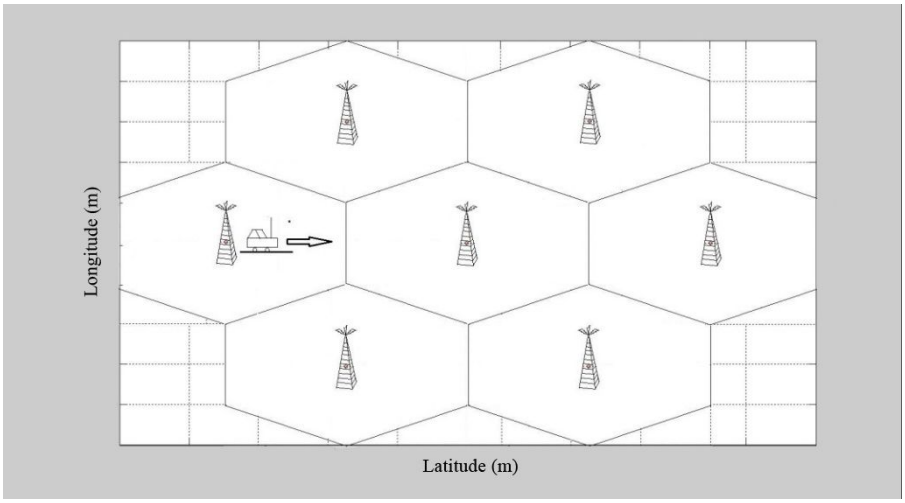

Figure 4.1: Balanced Topology

The coordinates of each BS presented are given as:

$$BalanceTop = \begin{bmatrix} BS_1 & BS_2 & BS_3 & BS_4 & BS_5 & BS_6 & BS_7 \\ 0 & 5196.15 & 2598.07 & -2598.07 & -5196.15 & -2598.07 & 2598.07 \\ 0 & 0 & 4500 & 4500 & 0 & -4500 & -4500 \end{bmatrix} \quad (4.1)$$

4.2.2 Circular Topology

A circular topology assumes that the set of BSs form a circular shape. In our study we focus on an example involving eight BS, allocated as in Figure 4.2. The coordinates of each base station are given in the following matrix CircularTop:

$$CircularTop = \begin{bmatrix} BS_1 & BS_2 & BS_3 & BS_4 & BS_5 & BS_6 & BS_7 & BS_8 \\ 5515.4 & 3900 & 0 & -3900 & -5515.4 & -3900 & 0 & 3900 \\ 0 & 3900 & 5515.4 & 3900 & 0 & -3900 & -5515.4 & 3900 \end{bmatrix} \quad (4.2)$$

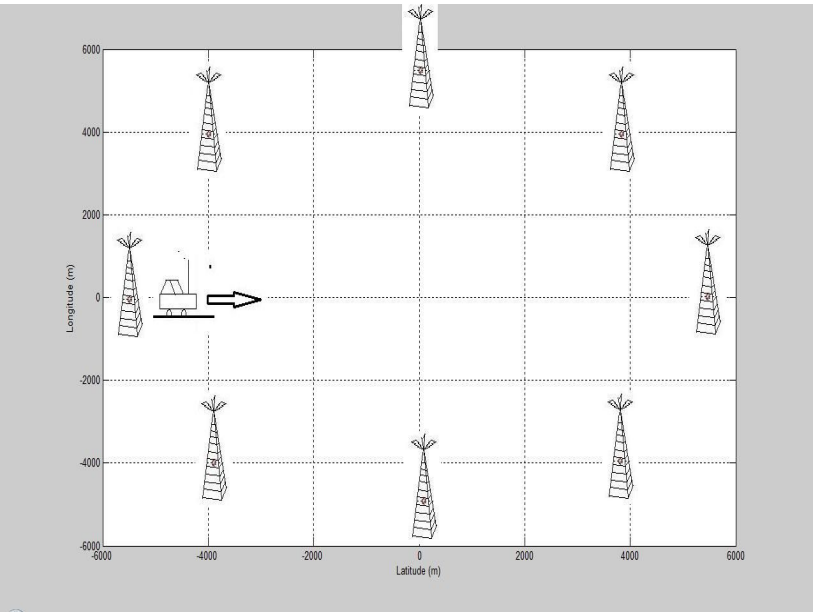

Figure 4.2: Circular Topology

4.2.3 U-shaped Topology

This topology assumes that the geometrical shape formed by the distribution of the Base Stations in the environment looks like a U-shape. Roughly speaking, this confines a scenario where one extreme base station is failed.

In our case the U-shape topology uses 7 Base Stations distributed as in Figure 4.3. The coordinates of each base station are summarized in the following matrix U-Top:

$$U-Top=\begin{bmatrix} BS_1 & BS_2 & BS_3 & BS_4 & BS_5 & BS_6 & BS_7 \\ 0 & 500 & 1000 & 1500 & 500 & 1000 & 1500 \\ 0 & 500 & 500 & 500 & -500 & -500 & -500 \end{bmatrix} \quad (4.3)$$

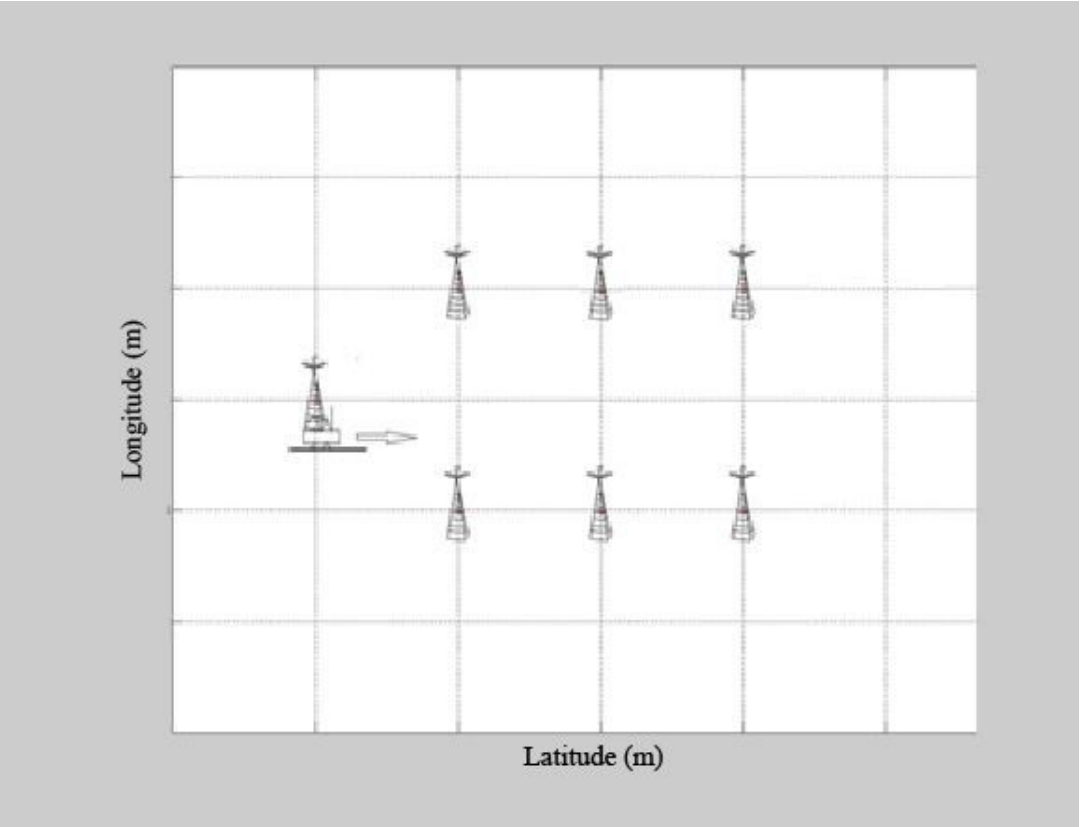

Figure 4.3: U-shaped Topology

4.2.4 Linear Topology

Similarly to the above, this topology assumes the locations of the BSs are linearly distributed in 2D space.

Figure 4.4 shows an example of seven BSs whose coordinates are given by the matrix LinearTop:

$$LinearTop = \begin{bmatrix} BS_1 & BS_2 & BS_3 & BS_4 & BS_5 & BS_6 & BS_7 \\ 0 & 500 & 1000 & 1500 & 2000 & 2500 & 3000 \\ 500 & 500 & 500 & 500 & 500 & 500 & 500 \end{bmatrix} \quad (4.4)$$

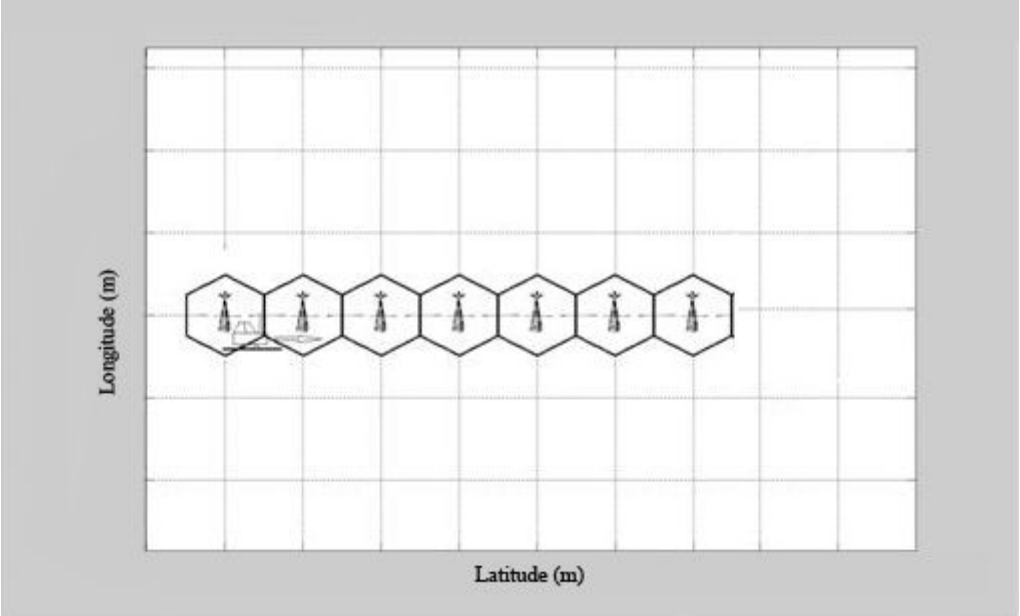

Figure 4.4: Linear Topology

4.3 Simulation Parameters Setup

In order to investigate both the effects of varying the location of the BSs and the topology on the accuracy of the positioning technique, we assume a vehicle moving at a constant speed in one direction from an initial position close to the location of the far left BS and moving towards the right direction. Table 4.1 contains the details of the simulation parameters for each topology.

We therefore, compute for each localisation technique the positioning accuracy with respect to a set of Monte Carlo simulations (as in Chapter 3).

BS Topology	Cell Radius	Noise Standard Deviation	MS Starting Position	Moving Distance	Time	Constant Velocity	Freq. of Sampling
Balanced	3000 m	0.1 us	[-5000, 1]	10000 m	50 s	200 m/s	Once / second
Circular	3000 m	0.1 us	[-5000, 1]	10000 m	50 s	200 m/s	Once / second
U-Shaped	3000 m	0.1 us	[0, 1]	1500 m	50 s	30 m/s	Once / second
Linear	3000 m	0.1 us	[1, 450]	3000 m	50 s	60 m/s	Once / second

Table 4.1: Parameters of the Simulation Setup

Typically, to the initial true mobile position is added a random perturbation generated by a zero-mean Gaussian noise with a given standard deviation. A pseudo-code highlighting the functioning of the simulation is described in Figure 4.5.

```
[MS, RMSE] =LOCATION_ESTIMATION (TOPOLOGY)
    RETRIEVE BSi, Vehicle Movement direction, Std σ, Initial MS0
    FOR EACH sampling interval k
        FOR EACH Monte Carlo iteration
            MS = ComputePosition (MS0, k)
            Generate a realization of Noise = (0,σ)
            FOR EACH BS
                Calculate distance  d_i = sqrt((BS_i x − MSx)^2 + (BS_i y − MSy)^2) + Noise
            END FOR
            Estimate Position MS= LocationAlgorithm (d, BS, Noise)
        END FOR
        Calculate RMSE of current MS
    END
END
```

Figure 4.5: Pseudo-code of Simulation

In order to quantify the performance of the eight localisation techniques, at each

sampling interval along the trajectory of the vehicle, the RMSE of the averaged MS estimation over the 1000 Monte Carlo simulations is calculated for each location technique:

$$RMSE(t)=\sqrt{\frac{\sum_{i=1}^{n}\left((x_{True}(t)-x_i(t))^2+(y_{True}(t)-y_i(t))^2\right)}{n}},$$

where $(x_i(t), y_i(t))$ stands for MS (x, y) estimation at the i^{th} Monte Carlo simulation and t sampling interval and n=1000.

4.4 Simulation Results

4.4.1 Simulation Using Balanced Topology

Figure 4.6 highlights the configuration of the BSs, shown as blue stars, and the true position of the MS shown as red star. The results of the simulation for various input parameters are summarised in Table 4.2.

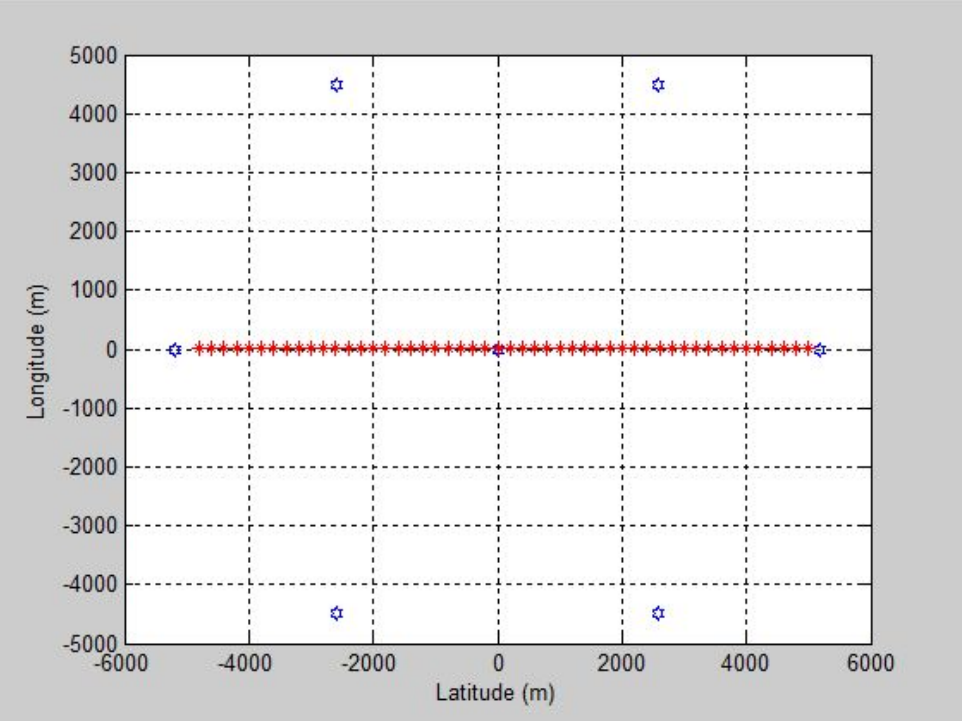

Figure 4.6: Vehicle Moving Track in Balanced Topology

The RMSE in each sampling is presented in Table 4.2:

Cellular Topology	Average RMSE (m) at Different Moving Moment (s)									
	1s	2s	3s	4s	5s	6s	7s	8s	9s	10s
Combination	13.71m	13.23m	12.91m	12.19m	12.55m	12.83m	12.91m	12.45m	12.67m	13.17m
LLS-1	23.74m	22.20m	21.83m	20.71m	18.98m	17.49m	16.84m	16.30m	15.14m	14.91m
LLS-2	25.78m	24.29m	24.07m	23.01m	21.25m	19.75m	19.15m	18.67m	17.45m	17.24m
LLS-3	25.38m	24.34m	24.52m	22.07m	21.64m	20.91m	19.61m	19.16m	17.68m	16.27m
LLS-RS	30.46m	28.83m	28.67m	25.44m	24.59m	23.39m	21.59m	20.73m	18.79m	16.95m
MLE	31.50m	29.38m	28.69m	24.93m	23.50m	21.71m	19.37m	17.88m	15.47m	13.21m
Chan	26.71m	24.05m	24.32m	22.74m	23.8m	22.94m	23.06m	22.89m	21.36m	21.29m
Taylor	23.65m	22.91m	24.59m	23.99m	25.52m	25.48m	26.03m	26.12m	25.24m	25.16m

	11s	12s	13s	14s	15s	16s	17s	18s	19s	20s
Combination	12.65m	12.21m	12.43m	12.47m	12.13m	12.01m	11.89m	11.56m	11.61m	11.14m
LLS-1	13.84m	12.48m	11.80m	11.48m	10.48m	10.39m	9.88m	9.61m6	10.38m	10.89m
LLS-2	16.01m	14.36m	13.40m	12.72m	11.14m	10.35m	8.97m	7.67m	6.99m	5.90m
LLS-3	15.54m	14.53m	12.84m	12.62m	11.57m	10.25m	9.08m	8.08m	6.82m	5.73m
LLS-RS	15.84m	14.47m	12.84m	12.62m	11.57m	10.25m	9.08m	8.08m	6.82m	5.73m
MLE	11.56m	9.73m	7.54m	6.26m	4.57m	2.91m	1.45m	0.25m	0.90m	1.69m
Chan	22.92m	20.45m	21.96m	19.98m	21.62m	20.10m	19.60m	20.12m	21.10m	21.69m
Taylor	26.19m	25.65m	25.38m	23.91m	24.36m	24.13m	22.56m	22.44m	23.65m	22.26m
	21s	**22s**	**23s**	**24s**	**25s**	**26s**	**27s**	**28s**	**29s**	**30s**
Combination	11.31m	10.31m	10.55m	10.03m	10.01m	9.98m	10.32m	10.39m	10.77m	10.76m
LLS-1	11.24m	12.26m	12.95m	14.11m	14.81m	14.73m	15.29m	15.00m	15.45m	15.97m
LLS-2	4.63m	3.55m	2.33m	1.17m	0.05m	1.13m	2.33m	3.38m	4.55m	5.75m
LLS-3	4.58m	3.42m	2.26m	1.22m	0.05m	1.15m	2.39m	3.49m	4.42m	5.59m
LLS-RS	4.58m	3.42m	2.26m	1.22m	0.05m	1.15m	2.39m	3.49m	4.42m	5.59m
MLE	2.12m	2.14m	1.75m	1.10m	0.05m	1.04m	1.87m	2.18m	2.03m	1.64m
Chan	19.07m	20.72m	19.35m	21.15m	19.68m	19.71m	21.35m	20.87m	20.46m	19.75m
Taylor	21.84m	21.69m	20.68m	21.38m	20.06m	20.23m	20.93m	21.76m	21.11m	21.07m
	31s	**32s**	**33s**	**34s**	**35s**	**36s**	**37s**	**38s**	**39s**	**40s**
Combination	11.29m	11.30m	11.52m	11.31m	11.55m	11.64m	12.26m	12.71m	12.41m	12.96m
LLS-1	16.13m	16.99m	17.59m	17.72m	18.23m	19.14m	18.97m	20.24m	21.25m	22.05m
LLS-2	6.77m	8.07m	9.23m	10.0m	11.11m	12.34m	12.83m	14.26m	15.49m	16.56m
LLS-3	6.87m	8.33m	9.03m	9.91m	11.29m	11.83m	13.58m	14.57m	15.83m	16.36m
LLS-RS	6.87m	8.33m	9.03m	9.91m	11.29m	11.83m	13.58m	14.51m	16.14m	17.04m
MLE	0.91m	0.28m	1.42m	2.81m	4.45m	5.88m	7.96m	9.75m	11.77m	13.29m
Chan	18.40m	19.46m	20.33m	19.40m	20.27m	21.74m	20.11m	21.79m	21.09m	21.93m
Taylor	20.74m	22.19m	22.98m	22.22m	23.22m	23.91m	23.35m	24.61m	24.14m	25.19m
	41s	**42s**	**43s**	**44s**	**45s**	**46s**	**47s**	**48s**	**49s**	**50s**
Combination	12.87m	12.89m	12.90m	12.92m	12.53m	13.30m	12.56m	13.19m	13.65m	16.68m
LLS-1	23.56m	24.13m	24.61m	25.02m	25.05m	28.63m	28.17m	28.17m	29.29m	31.02m
LLS-2	18.14m	18.99m	19.73m	20.39m	20.71m	23.96m	23.84m	24.06m	25.22m	26.91m
LLS-3	17.06m	18.62m	20.00m	20.22m	21.76m	22.51m	23.55m	25.55m	24.97m	25.76m
LLS-RS	18.13m	20.15m	22.01m	22.62m	24.72m	25.96m	27.53m	30.27m	29.97m	31.30m
MLE	14.93m	17.38m	19.75m	21.00m	23.63m	25.44m	27.56m	30.84m	31.00m	32.77m
Chan	20.10m	22.82m	22.28m	22.99m	23.99m	23.68m	24.31m	26.19m	26.48m	27.86m
Taylor	24.57m	26.21m	24.80m	25.75m	25.77m	24.48m	25.96m	24.06m	24.57m	25.59m

Table 4.2: RMSEs in Each Sampling Moment in Balanced Topology

Figure 4.7 exhibits localisation errors in terms of RMSE of the eight localisation techniques when using balanced topology

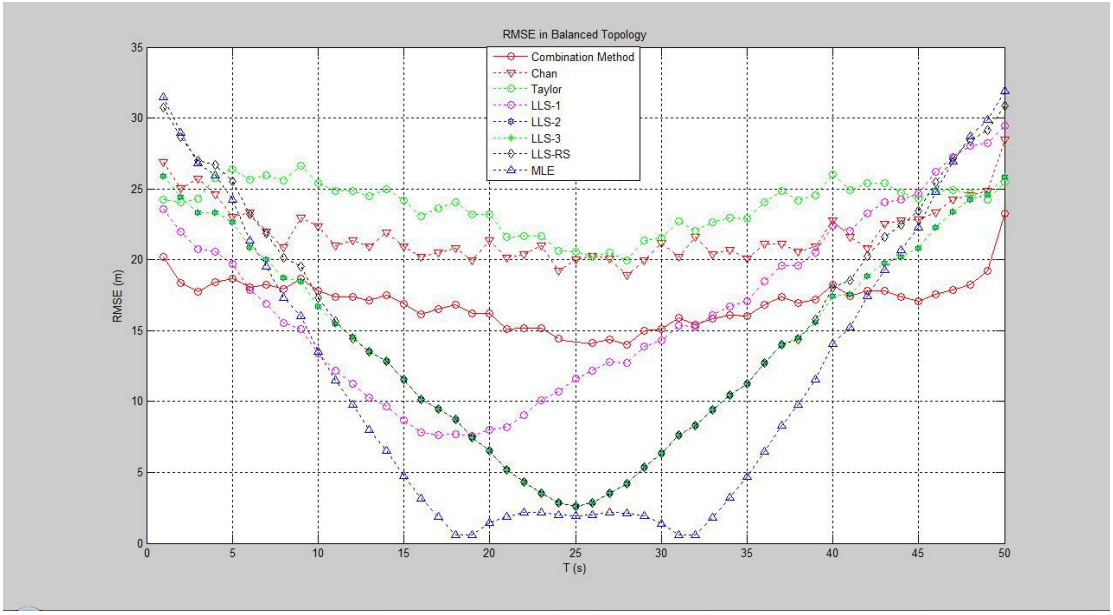

Figure 4.7: RMSE Value in Case of Balanced Topology

According to the Figure 4.7, the combination, Chan, Taylor methods are not obviously impacted by the movement of the MS. The combination algorithm gives a better performance than the Chan or Taylor method. Compared with these three methods, the least linear square methods present a quite different result. RMSE results of LLS-2, 3 and the RS algorithms give the impression that when the MS is approaching the centre BS, the location quality is greatly improved. The best location output happens at the position closest to the central BS. The MLE also shows a similar characteristic, but the difference is that the best location performance happens in the area MS moving towards or away from the centre of the topology.

4.4.2 Simulation Using Circular Topology

Similarly to Section 4.4.1, Figure 4.8 highlights the configuration of the BSs, shown as blue stars, and the true position of the MS shown as red stars. The results of the simulation for various input parameters are summarised in Table 4.3

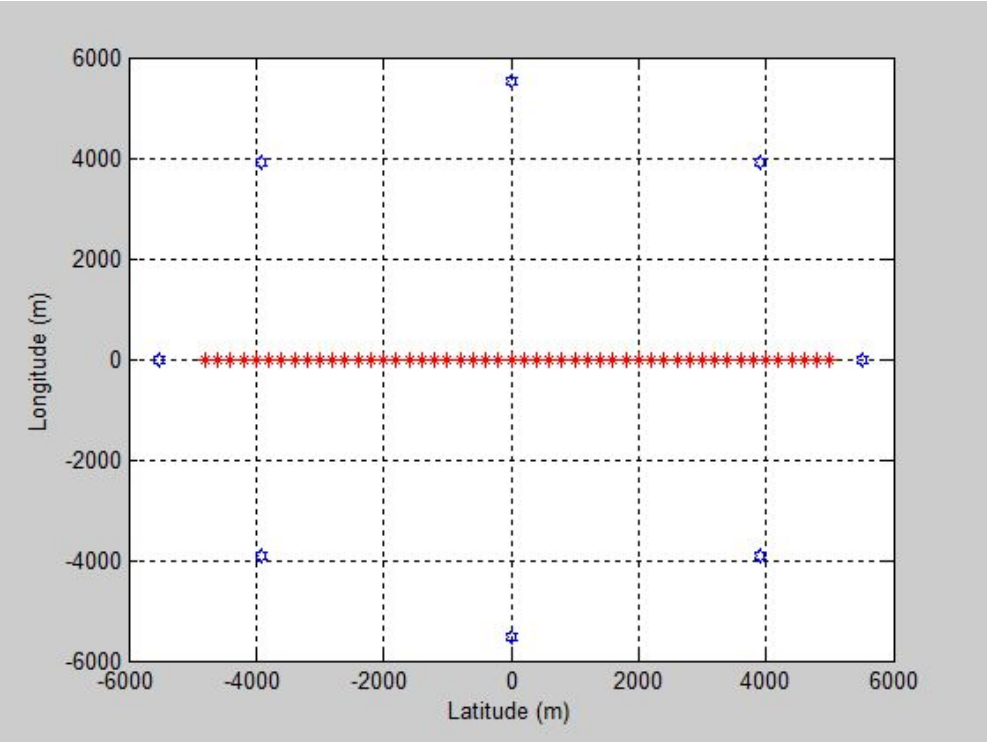

Figure 4.8: Vehicle Moving Track in Circular Topology

The RMSE in each sampling is presented in Table 4.3:

Cellular Topology	Average RMSE (m) in Different Moving Moment (s)									
	1s	2s	3s	4s	5s	6s	7s	8s	9s	10s
Combination	19.63m	18.67m	18.25m	17.48m	17.89m	18.63m	18.31m	17.84m	17.87m	17.41m
LLS-1	21.32m	20.15m	20.19m	19.32m	19.10m	18.06m	16.38m	16.03m	15.18m	14.70m
LLS-2	23.53m	22.18m	22.16m	21.15m	20.84m	19.65m	17.76m	17.32m	16.34m	15.77m
LLS-3	24.67m	23.22m	23.17m	22.08m	21.73m	20.46m	18.47m	17.98m	16.94m	16.32m
LLS-RS	29.01m	27.04m	26.72m	25.22m	24.59m	22.94m	20.52m	19.82m	18.51m	17.69m
MLE	31.28m	28.78m	28.08m	26.15m	25.16m	23.17m	20.51m	19.61m	18.17m	17.26m
Chan	22.31m	20.23m	20.96m	20.47m	21.31m	19.47m	18.81m	18.52m	19.28m	18.91m
Taylor	26.68m	25.82m	26.42m	26.80m	27.81m	27.22m	27.06m	26.44m	26.03m	25.85m
	11s	12s	13s	14s	15s	16s	17s	18s	19s	20s
Combination	17.08m	17.85m	17.74m	17.03m	16.96m	16.88m	16.84m	16.84m	15.46m	15.02m
LLS-1	13.87m	13.09m	11.68m	11.03m	10.00m	9.34m	8.17m	7.21m	6.17m	5.05m
LLS-2	14.82m	13.94m	12.39m	11.65m	10.52m	9.78m	8.52m	7.49m	6.38m	5.18m
LLS-3	15.31m	14.37m	12.76m	11.97m	10.78m	10.01m	8.70m	7.63m	6.48m	5.26m
LLS-RS	16.47m	15.35m	13.53m	12.60m	11.29m	10.41m	9.00m	7.85m	6.64m	5.36m
MLE	16.00m	14.85m	13.06m	12.16m	10.89m	10.06m	8.70m	7.61m	6.45m	5.23m
Chan	18.75m	17.95m	18.15m	17.14m	19.44m	17.80m	17.44m	17.59m	17.69m	18.83m
Taylor	25.88m	25.57m	24.76m	24.42m	24.14m	23.73m	22.86m	23.61m	22.98m	22.36m
	21s	22s	23s	24s	25s	26s	27s	28s	29s	30s
Combination	15.71m	14.49m	14.73m	14.67m	14.55m	14.07m	14.02m	14.08m	14.61m	14.82m
LLS-1	4.33m	3.20m	2.15m	1.08m	0.439m	1.07m	2.17m	3.26m	4.55m	5.56m
LLS-2	4.43m	3.25m	2.17m	1.09m	0.44m	1.07m	2.15m	3.20m	4.43m	5.39m
LLS-3	4.48m	3.28m	2.18m	1.09m	0.29m	1.06m	2.13m	3.17m	4.38m	5.30m
LLS-RS	4.55m	3.31m	2.20m	1.09m	0.79m	1.07m	2.17m	3.26m	4.55m	5.57m
MLE	4.45m	3.26m	2.17m	1.09m	0.44m	1.07m	2.15m	3.21m	4.46m	5.44m
Chan	18.17m	16.39m	17.80m	17.49m	17.46m	16.53m	17.33m	17.10m	16.65m	17.70m
Taylor	22.08m	20.79m	20.38m	21.36m	19.97m	19.64m	20.45m	20.06m	20.49m	20.78m
	31s	32s	33s	34s	35s	36s	37s	38s	39s	40s
Combination	15.80m	15.61m	16.25m	15.72m	16.07m	16.13m	17.01m	16.63m	17.17m	17.73m
LLS-1	6.78m	7.89m	9.05m	9.84m	11.77m	12.47m	14.13m	15.36m	16.16m	17.11m
LLS-2	6.52m	7.54m	8.59m	9.26m	10.99m	11.55m	12.99m	14.00m	14.59m	15.32m
LLS-3	6.39m	7.36m	8.34m	8.96m	10.59m	11.08m	12.39m	13.29m	13.78m	14.38m
LLS-RS	6.78m	7.91m	9.07m	9.86m	11.80m	12.50m	14.18m	15.41m	16.22m	17.18m
MLE	6.60m	7.67m	8.78m	9.53m	11.39m	12.07m	13.69m	14.92m	15.74m	16.76m
Chan	17.75m	17.53m	18.41m	18.71m	18.21m	18.89m	17.72m	17.40m	18.07m	18.70m
Taylor	22.00m	22.03m	22.13m	22.93m	22.57m	24.41m	24.28m	23.03m	24.68m	25.79m

	41s	42s	43s	44s	45s	46s	47s	48s	49s	50s
Combination	17.65m	18.35m	17.66m	18.13m	17.99m	17.01m	17.98m	18.35m	19.97m	24.11m
LLS-1	19.07m	20.39m	22.05m	23.57m	24.09m	26.39m	26.31m	27.39m	29.30m	30.65m
LLS-2	16.91m	17.90m	19.17m	20.29m	20.53m	22.26m	21.96m	22.61m	23.94m	24.77m
LLS-3	15.79m	16.61m	17.68m	18.59m	18.68m	20.11m	19.70m	20.13m	21.15m	21.72m
LLS-RS	19.16m	20.49m	22.16m	23.70m	24.23m	26.55m	26.48m	27.57m	29.51m	30.87m
MLE	18.81m	20.27m	22.14m	23.94m	24.78m	27.52m	27.81m	29.36m	31.81m	33.66m
Chan	19.92m	18.83m	20.47m	18.68m	19.33m	19.70m	20.26m	20.72m	21.99m	22.29m
Taylor	26.36m	26.30m	26.26m	26.52m	26.55m	26.75m	26.97m	26.20m	26.11m	26.01m

Table 4.3: RMSEs at Each Sampling Moment in Circular Topology

Figure 4.9 exhibits localisation errors in terms of RMSE of the eight localisation techniques when using circular topology:

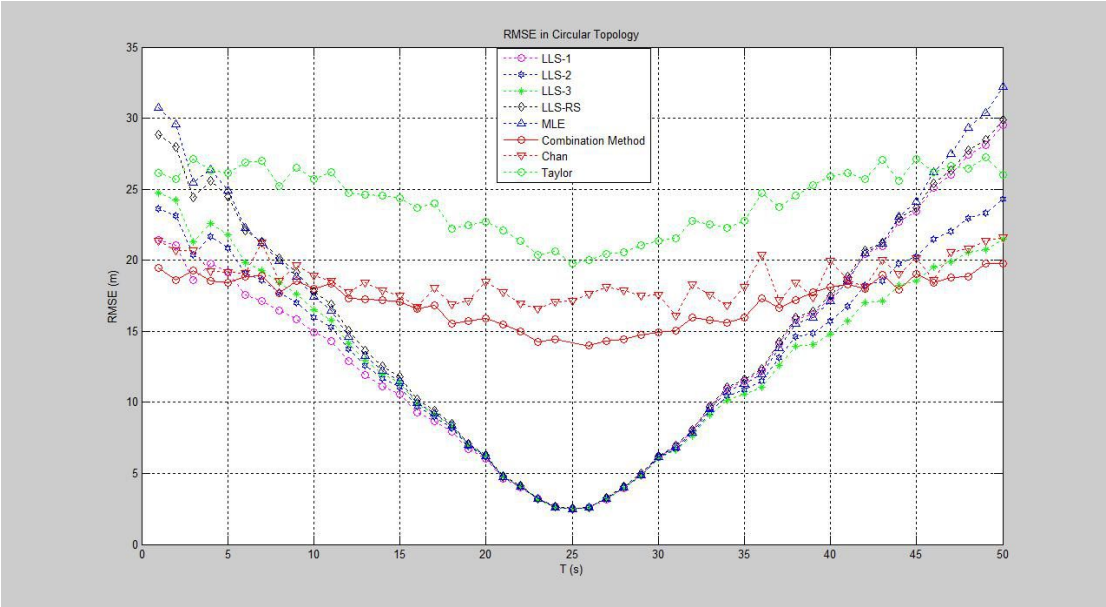

Figure 4.9: RMSE Value in Case of Circular Topology

From Figure 4.9, as in the balanced topology, the combination, Chan, Taylor methods are not obviously impacted by the movement of the MS. The combination algorithm gives a better performance than the Chan or Taylor. Additionally, in this topology, all the least linear square methods give similar

performances that when the MS is approaching the centre of network topology, the location quality is largely improved. The best location output happens at the position closest to the central network.

4.4.3 U-shaped Topology

Similarly to previous sections, Figure 4.10 highlights the configuration of the BSs, shown as blue stars, and the true position of the MS shown as red stars. The results of the simulation for various input parameters are summarised in Table 4.4:

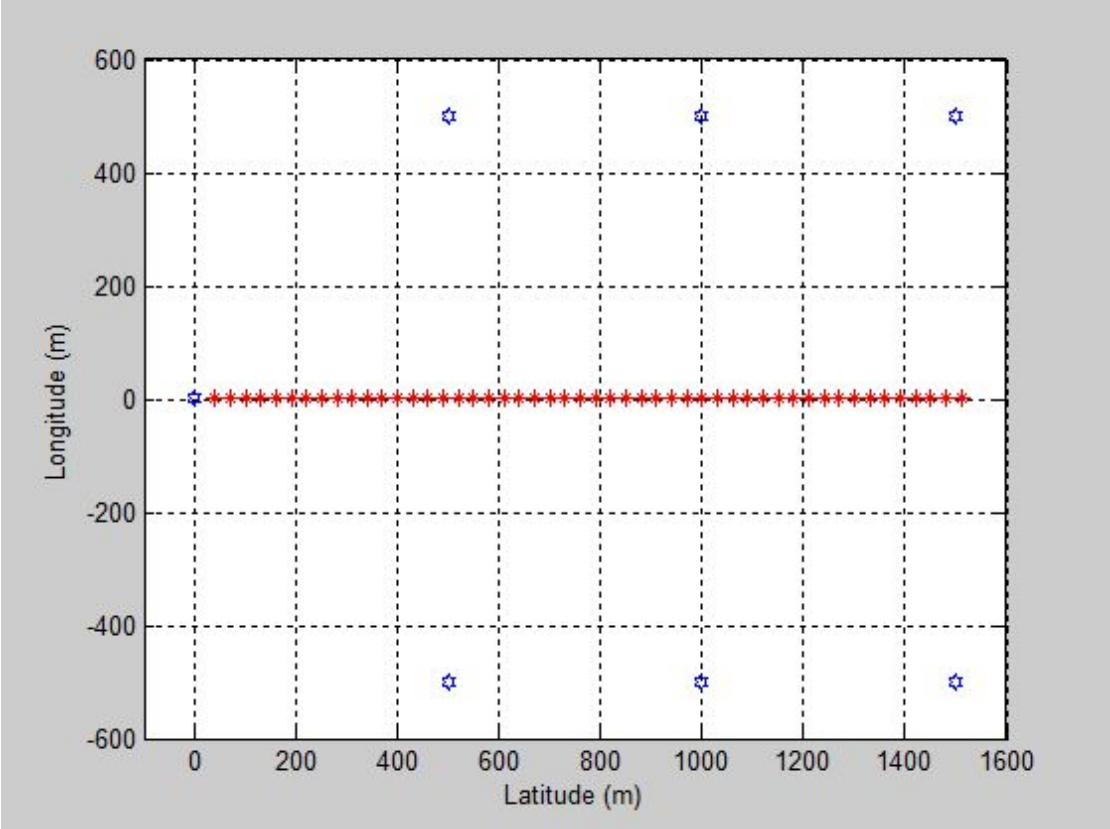

Figure 4.10: Vehicle Moving Track in U-shape Topology

The RMSE in each sampling is presented in Table 4.4:

Cellular Topology	Average RMSE (m) in Different Moving Moment (s)									
	1s	**2s**	**3s**	**4s**	**5s**	**6s**	**7s**	**8s**	**9s**	**10s**
Combination	3.36m	3.37m	3.21m	3.42m	3.25m	3.35m	3.42m	3.50m	3.53m	3.46m
LLS-1	31.25m	29.54m	26.61m	26.13m	26.36m	23.36m	22.17m	21.10m	19.07m	17.93m
LLS-2	28.33m	27.36m	25.20m	25.35m	26.23m	23.89m	23.35m	22.93m	21.43m	20.89m
LLS-3	26.26m	25.78m	24.15m	24.72m	26.02m	24.13m	24.02m	24.04m	22.91m	22.78m
LLS-RS	30.65m	29.13m	26.38m	26.07m	26.46m	23.62m	22.59m	21.68m	19.78m	18.77m
MLE	32.04m	30.17m	27.08m	26.47m	26.56m	23.45m	22.20m	21.12m	19.15m	18.14m
Chan	9.21m	8.62m	8.22m	7.96m	7.39m	7.48m	7.52m	7.51m	7.32m	7.43m
Taylor	17.27m	16.96m	16.07m	17.12m	16.29m	16.80m	17.14m	17.50m	17.69m	17.31m
	11s	**12s**	**13s**	**14s**	**15s**	**16s**	**17s**	**18s**	**19s**	**20s**
Combination	3.63m	3.65m	3.77m	3.79m	3.79m	3.92m	3.83m	3.84m	4.00m	4.08m
LLS-1	16.45m	13.96m	12.80m	11.52m	10.18m	8.86m	7.50m	6.42m	5.20m	4.39m
LLS-2	19.96m	17.69m	17.00m	16.14m	15.15m	14.09m	12.87m	12.00m	10.67m	9.84m
LLS-3	22.21m	20.11m	19.77m	19.20m	18.47m	17.63m	16.57m	15.93m	14.66m	14.07m
LLS-RS	17.42m	14.97m	13.90m	12.70m	11.42m	10.11m	14.11m	13.31m	11.99m	11.23m
MLE	16.85m	14.62m	13.75m	12.89m	11.92m	10.99m	9.97m	9.24m	8.19m	7.52m
Chan	6.91m	7.05m	6.49m	6.94m	7.21m	6.67m	7.32m	6.64m	6.62m	6.61m
Taylor	18.17m	18.29m	18.86m	18.99m	18.97m	19.64m	19.16m	19.21m	20.01m	20.39m
	21s	**22s**	**23s**	**24s**	**25s**	**26s**	**27s**	**28s**	**29s**	**30s**
Combination	4.06m	4.22m	4.21m	4.23m	4.52m	4.42m	4.59m	4.69m	4.80m	4.84m
LLS-1	3.68m	3.19m	3.34m	4.04m	4.64m	5.38m	6.63m	7.31m	8.21m	9.14m
LLS-2	8.73m	7.23m	6.22m	5.38m	4.06m	2.85m	1.82m	0.62m	0.50m	1.63m
LLS-3	13.06m	11.43m	10.52m	9.94m	8.46m	7.14m	6.32m	4.89m	3.68m	2.47m
LLS-RS	10.14m	8.59m	7.60m	6.84m	5.48m	4.96m	5.06m	4.96m	5.27m	5.79m
MLE	6.62m	5.44m	4.64m	3.96m	2.91m	1.97m	1.16m	0.26m	0.58m	1.40m
Chan	7.08m	6.78m	7.31m	6.58m	6.30m	6.38m	6.84m	6.35m	6.75m	6.87m
Taylor	20.36m	21.16m	21.08m	21.19m	22.63m	22.13m	22.95m	23.44m	24.03m	24.21m
	31s	**32s**	**33s**	**34s**	**35s**	**36s**	**37s**	**38s**	**39s**	**40s**
Combination	5.18m	5.22m	5.36m	5.60m	5.52m	5.56m	6.07m	6.17m	6.17m	6.38m
LLS-1	9.93m	11.11m	12.37m	12.83m	14.27m	14.09m	15.03m	15.42m	16.41m	17.34m
LLS-2	2.71m	3.91m	5.18m	6.12m	7.53m	8.08m	9.22m	10.02m	11.21m	12.37m
LLS-3	1.24m	0.04m	1.22m	2.42m	3.81m	4.75m	6.01m	7.04m	8.34m	9.63m
LLS-RS	6.36m	7.29m	8.36m	8.94m	10.24m	10.41m	11.40m	11.99m	13.06m	14.10m
MLE	2.17m	3.02m	3.93m	4.58m	5.62m	5.99m	6.86m	7.51m	8.48m	9.49m
Chan	7.05m	6.65m	6.97m	6.59m	7.04m	6.93m	6.77m	6.73m	7.46m	6.76m

Taylor	25.89m	26.04m	26.76m	27.89m	27.42m	27.58m	30.09m	30.48m	30.48m	31.40m
	41s	**42s**	**43s**	**44s**	**45s**	**46s**	**47s**	**48s**	**49s**	**50s**
Combination	6.78m	6.76m	7.14m	7.39m	7.45m	8.19m	8.23m	8.60m	9.07m	9.63m
LLS-1	18.00m	18.37m	20.23m	19.63m	20.19m	20.31m	20.98m	21.91m	22.00m	22.92m
LLS-2	13.34m	14.09m	15.98m	15.94m	16.79m	17.27m	18.18m	19.32m	19.71m	20.82m
LLS-3	10.78m	11.73m	13.65m	13.91m	14.94m	15.61m	16.67m	17.92m	18.48m	19.70m
LLS-RS	14.93m	12.45m	14.33m	14.46m	15.41m	15.99m	16.99m	18.19m	18.69m	19.86m
MLE	10.39m	11.16m	12.91m	13.08m	14.06m	14.67m	15.70m	16.95m	17.57m	18.79m
Chan	7.06m	7.09m	7.52m	7.55m	7.70m	7.73m	7.59m	8.57m	8.85m	9.73m
Taylor	33.28m	33.03m	34.71m	35.82m	35.92m	39.20m	39.01m	40.57m	42.30m	44.19m

Table 4.4: RMSEs at Each Sampling Moment in Circular Topology

Figure 4.11 gives localisation errors in terms of RMSE of the seven localisation techniques when using U-shaped topology:

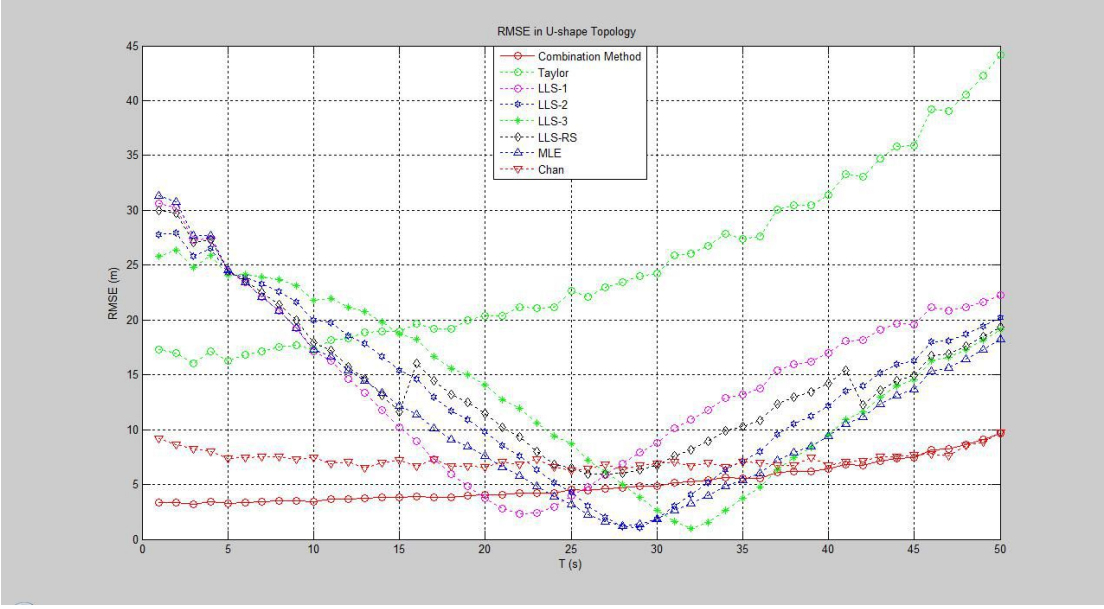

Figure 4.11: RMSE Value in Case of U-shaped Topology

Based on Figure 4.11, the combination, Chan methods give excellent location performance and also combination and Chan are not impacted obviously by the movement of the MS, but the RMSE of the Taylor method increases when the MS moves away from the start point. The combination algorithm gives a better

performance than the Chan or Taylor. Additionally, in this topology, since the topology of the BSs is no longer symmetrically distributed, the least linear square methods give different performances from previous results. However, all the least linear square algorithms exhibit location quality increasing when MS is approaching to the reference BS in each algorithm. In this scenario, the Taylor presents a constantly increasing RMSE, which because in the U shape topology, the 1st BS with following BSs building up a relatively closing area at beginning of the vehicle starts to move; then, in the other side of the topology, the structure is becoming open, therefore, a highly relying on a initial guess (randomly choose) algorithm, Taylor, in a relatively closing network area usually gives a better estimating than in a open structure.

4.4.4 Simulation Using Linear Topology

Similarly to previous sections, Figure 4.12 highlights the configuration of the BSs, shown as blue stars, and the true position of the MS shown as red stars. The results of the simulation for various input parameters are summarised in Table 4.5:

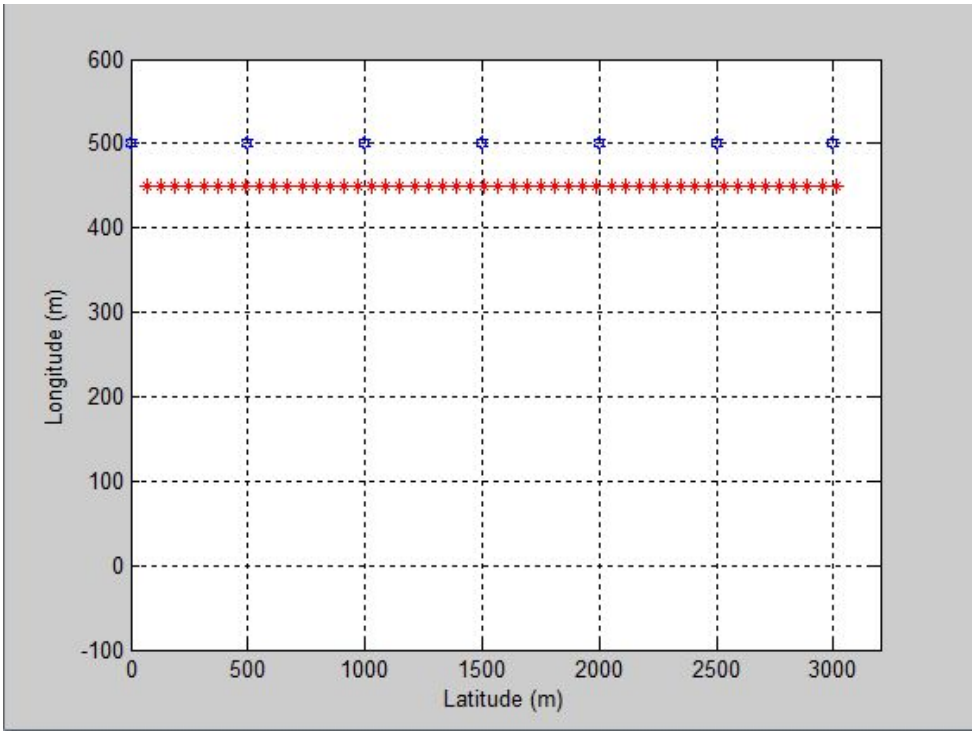

Figure 4.12: Vehicle Moving Track in Linear Topology

The RMSE in each sampling is presented in Table 4.5:

Cellular Topology	Average RMSE (m) at Different Moving Moment (s)									
	1s	**2s**	**3s**	**4s**	**5s**	**6s**	**7s**	**8s**	**9s**	**10s**
Combination	94.91m	85.50m	83.34m	86.40m	83.95m	82.57m	86.09m	81.82m	81.67m	81.35m
LLS-1	45.18m	57.20m	70.53m	84.91m	101.20m	116.98m	137.21m	148.98m	164.30m	155.60m
LLS-2	45.22m	57.25m	70.59m	84.99m	101.31m	117.15m	137.52m	149.79m	166.86m	160.13m
LLS-3	45.22m	57.25m	70.59m	84.99m	101.31m	117.15m	137.52m	149.79m	166.86m	160.13m
LLS-RS	45.22m	57.25m	70.59m	84.71m	100.90m	116.50m	136.24m	146.28m	155.58m	140.03m
MLE	45.11m	57.09m	70.37m	84.68m	100.84m	116.37m	135.91m	145.23m	151.98m	133.79m
Chan	192.73 m	176.14 m	168.29 m	161.73 m	152.93 m	145.25 m	146.62 m	144.82 m	135.47 m	138.18 m
Taylor	161.81 m	159.22 m	161.38 m	170.46 m	166.79 m	164.59 m	171.94 m	163.47 m	163.17 m	162.55 m
	11s	**12s**	**13s**	**14s**	**15s**	**16s**	**17s**	**18s**	**19s**	**20s**
Combination	83.43m	83.93m	85.46m	80.97m	82.25m	79.15m	74.46m	77.07m	77.20m	75.60m
LLS-1	164.41m	163.14m	166.18m	171.89m	176.44m	184.71m	180.05m	172.27m	169.43m	160.84m
LLS-2	171.46m	172.35m	177.74m	186.03m	193.15m	204.56m	202.28m	197.01m	197.53m	191.37m
LLS-3	171.46m	172.35m	177.74m	186.03m	193.15m	204.56m	202.28m	197.01m	197.53m	191.37m

LLS-RS	140.07m	131.34m	228.50m	247.95m	265.68m	288.14m	285.11m	271.68m	264.78m	248.59m
MLE	132.39m	127.82m	137.12m	159.37m	189.72m	225.40m	235.37m	225.66m	214.23m	194.79m
Chan	141.67 m	143.11 m	142.94 m	132.20 m	141.38 m	142.45 m	132.29 m	132.83 m	129.64 m	140.94 m
Taylor	166.70 m	167.65 m	170.74 m	161.80 m	164.45 m	158.24 m	148.91 m	154.02 m	154.37 m	151.32 m
	21s	**22s**	**23s**	**24s**	**25s**	**26s**	**27s**	**28s**	**29s**	**30s**
Combination	72.50m	75.43m	69.16m	68.85m	67.99m	67.16m	68.29m	67.78m	68.42m	70.40m
LLS-1	154.36m	151.36m	147.81m	132.77m	129.30m	124.38m	118.64m	103.88m	94.76m	91.87m
LLS-2	187.62m	188.13m	188.06m	173.12m	173.00m	171.12m	168.35m	152.58m	144.64m	146.42m
LLS-3	187.62m	188.13m	188.06m	173.12m	173.00m	171.12m	168.35m	152.58m	144.64m	146.42m
LLS-RS	291.65m	305.42m	318.37m	304.56m	311.82m	308.14m	300.04m	268.28m	250.34m	177.07m
MLE	183.88m	188.44m	207.85m	222.45m	253.78m	268.97m	265.84m	229.45m	204.24m	198.31m
Chan	134.07 m	138.66 m	130.32 m	129.99 m	128.59 m	117.44 m	128.79 m	134.23 m	134.47 m	132.82 m
Taylor	145.01 m	151.10 m	138.29 m	136.87 m	130.06 m	131.51 m	135.72 m	135.18 m	136.89 m	140.87 m
	31s	**32s**	**33s**	**34s**	**35s**	**36s**	**37s**	**38s**	**39s**	**40s**
Combination	72.63m	72.82m	74.07m	74.47m	78.77m	82.05m	79.64m	84.06m	82.32m	84.50m
LLS-1	80.65m	69.93m	64.83m	57.33m	51.21m	45.17m	41.36m	35.38m	32.39m	29.79m
LLS-2	134.93m	123.47m	121.01m	112.05m	104.23m	95.69m	90.97m	80.00m	73.61m	65.26m
LLS-3	134.93m	123.47m	121.01m	112.05m	104.23m	95.69m	90.97m	80.00m	73.61m	65.26m
LLS-RS	167.04m	156.63m	156.87m	146.47m	136.22m	124.76m	118.15m	65.38m	57.11m	47.95m
MLE	187.60m	193.44m	227.47m	248.10m	252.38m	234.89m	216.76m	176.69m	153.35m	138.58m
Chan	132.39 m	130.67 m	132.63 m	139.05 m	147.31 m	137.50 m	140.22 m	151.14 m	138.39 m	151.02 m
Taylor	145.28 m	145.62 m	148.04 m	148.91 m	157.47 m	164.04 m	159.23 m	168.00 m	164.57 m	168.93 m
	41s	**42s**	**43s**	**44s**	**45s**	**46s**	**47s**	**48s**	**49s**	**50s**
Combination	86.70m	85.90m	87.84m	84.87m	84.21m	87.89m	83.02m	86.64m	93.94m	116.40 m
LLS-1	29.88m	28.95m	29.74m	30.48m	29.33m	31.68m	29.74m	29.55m	28.69m	29.24m
LLS-2	59.75m	51.46m	47.51m	43.87m	38.08m	37.28m	32.15m	30.06m	28.41m	29.01m
LLS-3	59.75m	51.46m	47.51m	43.87m	38.08m	37.28m	32.15m	30.06m	28.41m	29.01m
LLS-RS	42.10m	36.42m	35.13m	34.35m	31.78m	52.94m	41.10m	34.00m	29.14m	28.92m
MLE	145.60m	160.37m	182.61m	198.94m	175.62m	160.21m	107.07m	71.08m	40.60m	30.04m

Chan	149.49 m	161.97 m	163.21 m	152.46 m	156.90 m	163.45 m	165.53 m	175.33 m	189.73 m	225.11 m
Taylor	173.35 m	171.84 m	175.79 m	169.91 m	168.41 m	175.41 m	164.13 m	167.48 m	171.11 m	179.75 m

Table 4.5: RMSEs in Each Sampling Moment in Linear Topology

Figure 4.13 gives localisation errors in terms of RMSE of the seven localisation techniques when using linear topology:

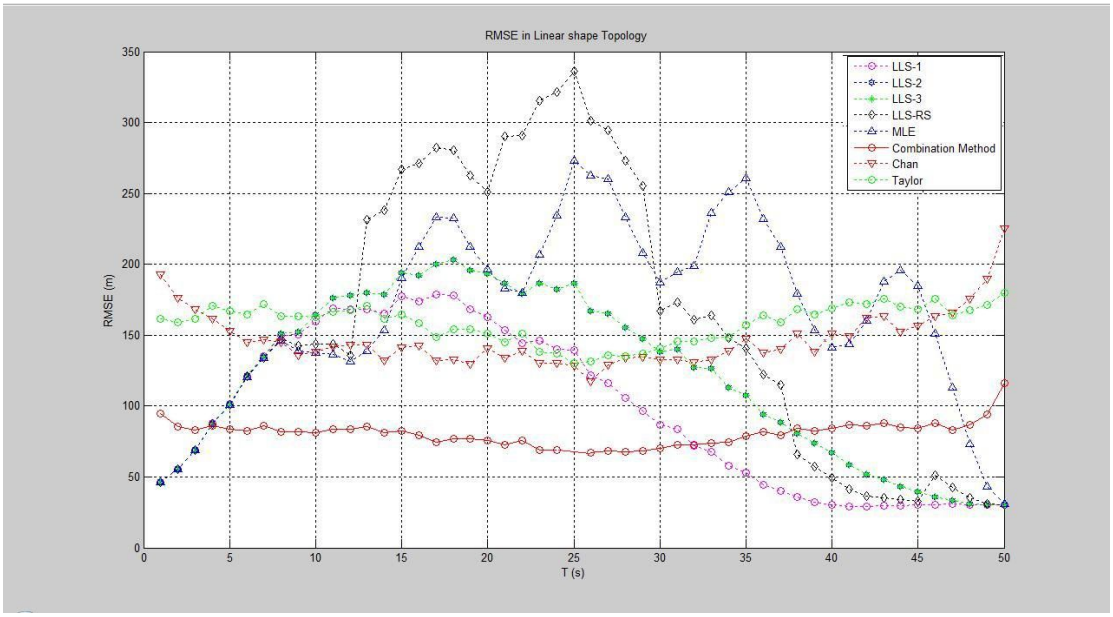

Figure 4.13: RMSE Value in Case of Linear Topology

From Figure 4.13, the linear topology is not a closed shape distribution, so the least linear square methods give a more irregular performance than previous results. On the other hand, the combination, Chan, Taylor methods are again not obviously impacted by the movement of the MS. The combination method shows the best RMSE performance of all the algorithms.

4.5 Summary of the Comparison

From the above figures, we can obtain the following:

- The discrepancy of the various positioning techniques, when a change of a topology occurs, demonstrates the influence of the topology on the accuracy of the underlying positioning method. [11]
- In the simulation in Section 4.4, at a standard sampling interval, the measurements from all BSs are assumed to be available and aggregated to the MS in the localisation technique. Such an approach is commonly employed in previous work that has investigated the performance of cellular/wireless network positioning techniques as testified in the extensive review paper [8].
- Presenting the RMSE values with respect to various topologies shows that the balanced topology provides the best performance with respect to all location techniques, while the linear shape topology reveals the worst performance as its presented values of RMSE are over 340 m compared to less than 30 m in the case of balanced topology. This phenomenon gives that, whenever possible the use of balanced topology should be encouraged. This is mainly due to quality of the obtained measurements which, at least from a geometrical perspective, yield a comprehensive intersection of the underlying circles. [11]
- The Chan and Taylor combination method shows that, on average, it

marginally outperforms the remaining seven topologies regardless of the topology employed. [11]

- The investigation of low values of RMSEs in the above figures reveals that the least square like methods almost approach the minimum RMSE value at the sampling time which corresponds to the moment the vehicle comes close to the central of topology. However this phenomenon is less apparent in the case of Chan, Taylor and combined Chan-Taylor methods where less sensitivity is observed. This is mainly because of the global nature of the three positioning algorithms. [11]
- The results have been obtained assuming low noise perturbation as testified by the low standard deviation shown in Table 4.1. Nevertheless, the influence of noise intensity cannot be precluded. On the other hand, the extra simulations with various noise intensities have shown that the generic trends issued from this analysis are not void when the level noise increases. To see this, a 3D graph is depicted in Figures 4.14 and 4.15 for balanced and linear like topologies. [11] From the two figures, the slop along the “Noise” axis stands the effect of changing the noise on the accuracy. All the algorithms give the linear relationship between RMSEs and Noise adding. But with the comparison of the 4 typical estimators, Combination always gives a stable performance in noise adding scenarios in both of topology.

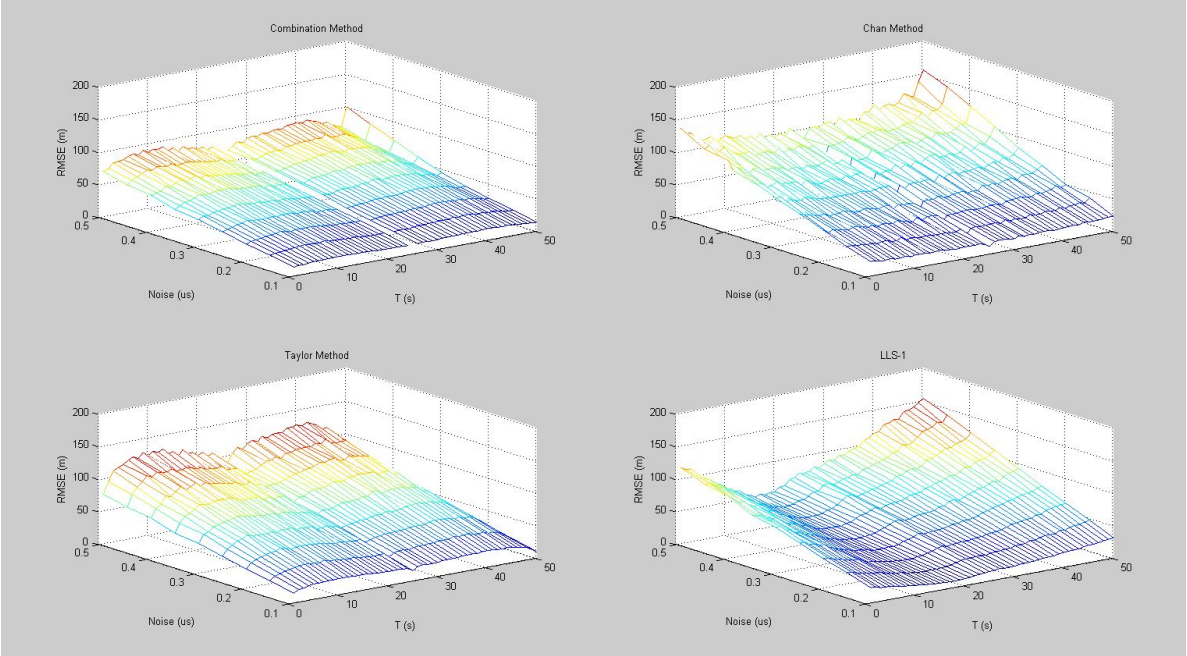

Figure 4.14: Noise Influence in Case of Balanced Topology Structure

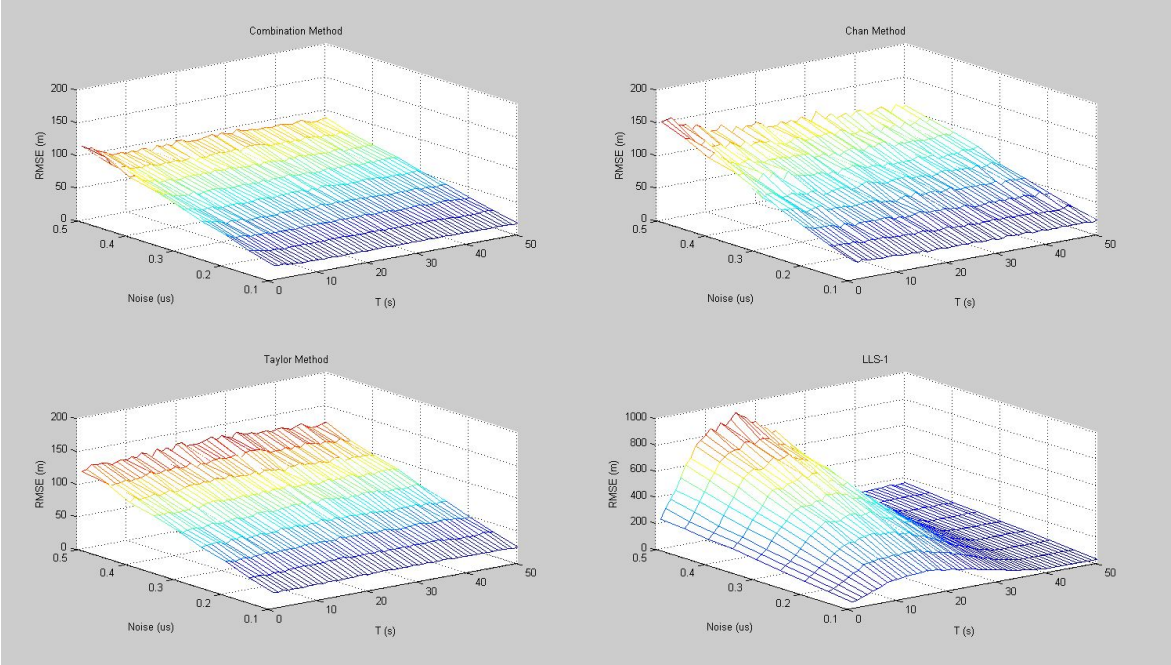

Figure 4.15: Noise Influence in Case of Linear Shape Topology

4.6 Balanced Topology Network with Failure Base Stations

In the previous sections, we discussed how the different types of topology affect the location accuracy. In this section, we concentrate on how the location accuracy is affected when there are failures of BSs in a particular topology network (balanced topology).

The simulation assumes a set of BSs at fixed locations (seven BSs in Figure 4.16). Nevertheless, in cases where blocking occurs in some cells, this yields a different topology.

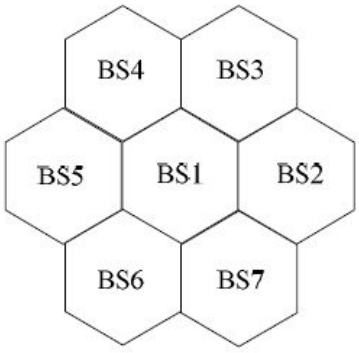

Figure 4.16: Structure of Balanced Topology

The simulation presents the accuracy changes when some of the BSs in Figure 4.16 failed. For instance, if the middle BS in Figure 4.1 fails, this yields a six BSs “circular” topology, which does affect position finding accuracy.

Tables 4.6-4.8 show the average RMSE of each algorithm with a different number of BSs missing contact when σ = 0.1, 0.3 and 0.5us.

Cellular Topology	Average RMSE (m) in Different NBS when Standard Deviations σ = 0.1us						
	NBS=7	NBS =6		NBS = 5			
	No Failure	1th BS Failure	2nd BS Failure	1th & 2nd BS Failure	2nd & 3rd BS Failure	2nd & 4th BS Failure	2nd & 5th BS Failure
Combination	3.63m	17.73m	4.98m	30.71m	4.56m	20.74m	21.61m
LLS-1	16.35m	20.11m	16.74m	29.06m	13.13m	32.29m	33.53m
LLS-2	8.63m	18.32m	10.31m	18.63m	10.75m	9.73m	9.21m
LLS-3	8.63m	17.38m	9.53m	18.20m	8.20m	8.65m	9.21m
LLS-RS	8.63m	20.18m	16.45m	18.93m	24.56m	15.84m	9.21m
MLE	3.94m	19.76m	10.33m	18.84m	20.67m	8.04m	5.44m
Chan	20.51m	38.70m	20.01m	50.17m	25.40m	27.40m	24.88m
Taylor	22.34m	35.79m	21.39m	66.57m	27.00m	29.60m	30.84m

Cellular Topology	Average RMSE (m) in Different NBS when Standard Deviations σ = 0.1us			
	NBS = 4			
	1th & 2nd & 3rd BS Failure	1th & 2nd & 4rd BS Failure	2nd & 3rd & 4th BS Failure	2nd & 3rd & 5th BS Failure
Combination	35.33m	38.62m	3.31m	10.86m
LLS-1	16.92m	18.27m	21.62m	24.41m
LLS-2	17.40m	18.21m	20.42m	25.80m
LLS-3	17.48m	18.14m	10.81m	19.60m
LLS-RS	17.45m	18.24m	27.66m	34.04m
MLE	17.43m	18.23m	25.91m	30.22m
Chan	54.37m	55.16m	21.47m	37.25m
Taylor	67.81m	70.41m	22.89m	43.97m

Table 4.6: RMSE of Each Algorithm with Different Number of BSs Failures when σ = 0.1us

Cellular Topology	Average RMSE (m) in Different NBS when Standard Deviations σ = 0.3us						
	NBS=7	NBS =6		NBS = 5			
	No Failure	1th BS Failure	2nd BS Failure	1th & 2nd BS Failure	2nd & 3rd BS Failure	2nd & 4th BS Failure	2nd & 5th BS Failure
Combination	19.44m	52.31m	22.73m	54.28m	28.47m	58.25m	59.51m
LLS-1	28.86m	46.43m	33.29m	29.92m	27.75m	60.48m	63.10m
LLS-2	26.82m	35.66m	27.12m	25.59m	33.89m	37.48m	35.10m
LLS-3	26.82m	34.60m	26.39m	25.24m	27.88m	24.46m	25.10m
LLS-RS	26.82m	37.09m	43.07m	26.50m	76.48m	44.53m	25.10m
MLE	12.40m	36.72m	31.30m	26.27m	63.61m	64.53m	59.33m
Chan	63.00m	73.64m	71.22m	76.46m	64.25m	72.41m	73.44m
Taylor	67.66m	78.99m	63.83m	77.47m	58.88m	66.86m	75.01m

Cellular Topology	Average RMSE (m) in Different NBS when Standard Deviations σ = 0.3us			
	NBS = 4			
	1th & 2nd & 3rd BS Failure	1th & 2nd & 4rd BS Failure	2nd & 3rd & 4th BS Failure	2nd & 3rd & 5th BS Failure
Combination	55.27m	56.64m	38.54m	40.24m
LLS-1	82.15m	84.13m	63.18m	65.77m
LLS-2	83.80m	84.05m	58.55m	64.58m
LLS-3	84.08m	83.90m	30.89m	45.72m
LLS-RS	83.98m	84.10m	79.65m	78.88m
MLE	83.91m	84.11m	73.86m	74.74m
Chan	77.19m	78.01m	62.33m	67.13m
Taylor	78.89m	78.99m	72.33m	76.76m

Table 4.7: RMSE of Each Algorithm with Different Number of BSs Failures when σ = 0.3us

Cellular Topology	Average RMSE (m) in Different NBS when Standard Deviations σ = 0.5us						
	NBS=7	NBS =6		NBS = 5			
	No Failure	1th BS Failure	2nd BS Failure	1th & 2nd BS Failure	2nd & 3rd BS Failure	2nd & 4th BS Failure	2nd & 5th BS Failure
Combination	33.07m	40.01m	34.56m	51.37m	36.48m	48.81m	50.01m
LLS-1	42.61m	60.77m	51.42m	71.24m	64.73m	154.50m	152.46m
LLS-2	43.13m	54.22m	46.11m	64.37m	58.82m	45.32m	60.71m
LLS-3	43.13m	52.28m	43.13m	57.74m	45.69m	46.99m	49.40m
LLS-RS	43.13m	56.84m	77.29m	137.63m	131.79m	133.48m	133.97m
MLE	20.35m	56.11m	48.69m	114.45m	109.10m	108.23m	110.03m
Chan	102.11m	115.22m	99.99m	120.21m	108.61m	116.43m	117.97m
Taylor	109.48m	120.27m	100.70m	121.85m	119.12m	138.24m	122.64m

Cellular Topology	Average RMSE (m) in Different NBS when Standard Deviations σ = 0.5us			
	NBS = 4			
	1th & 2nd & 3rd BS Failure	1th & 2nd & 4rd BS Failure	2nd & 3rd & 4th BS Failure	2nd & 3rd & 5th BS Failure
Combination	55.53m	60.60m	32.32m	54.31m
LLS-1	115.87m	117.71m	106.74m	113.61m
LLS-2	94.32m	100.07m	98.98m	100.63m
LLS-3	64.76m	69.99m	52.20m	58.70m
LLS-RS	140.47m	144.73m	134.46m	139.63m
MLE	117.47m	128.92m	124.73m	127.40m
Chan	130.13m	141.11m	96.12m	124.91m
Taylor	131.62m	142.93m	128.35m	129.22m

Table 4.8: RMSE of Each Algorithm with Different Number of BSs Failures when σ = 0.5us

In the balanced topology, we took out some of the BSs from the structure, which did affect the quality of location accuracy. From the simulation, we obtained:

- When the central BS (the first BS) failed contact, the accuracy was most affected. To all the techniques, if the centre BS in the topology missing contact, compare with the other BS fails, the accuracy reduce evidently.
- In the balanced topology, without the central BS missing, the failure of adjacent BSs had less influence on accuracy than non-adjacent, because

the failure adjacently does not impact the integral structure of the whole topology. In most of algorithms, from Figure 4.6-4.8, the accuracy reduced more sharply when the 2nd and 5th BSs failure than 2nd and 3rd BSs failure. The exceptions are LLS-3 and LLS-RS, because these two method has a function which can choose the suitable BS to be the reference BS when the structure of network topology changes.

- As discussed in the previous chapter, accuracy performance is affected by the number of BSs employed in the network topology, so that the greater the number of stations, the better is the performance in terms of RMSE values.
- Compared within all the presented methods, Combination method shows a outstanding ability to against the network topology changed, in the other hand, because use the most basic LS method, the LLS-1 is very sensitive with the failures of BSs in the topology structure.

4.7 Conclusion

This chapter highlights the importance of antenna positioning when looking at the accuracy of wireless positioning techniques. Four type of topologies, which can be generated straightforwardly by a regular balanced cellular topology when blocking occurs, have been investigated. Wireless positioning techniques related to TDOA technology were examined. This corresponds to four distinct least square based approaches, maximum likelihood, Chan, Taylor and a combined

Chan-Taylor method. Simulation results were obtained assuming a vehicle moving at a constant speed along the given topology. The results demonstrate the credibility of topology influence on positioning accuracy, and the combined Chan-Taylor shows a marginally increased performance in terms of RMSE and sensitivity to BS positioning.

4.8 Reference

[1] C.C. Docket, Revision of the Commission rules to ensure compatibility with enhanced 911 emergency calling systems, RM-8143, Report No. 94-102, FCC, 1994

[2] B. Brumitt, B. Meyers, J. Krumm, A. Kern, and S. Shafer. EasyLiving: Technologies for intelligent environments, Proceeding of the second international symposium on Handheld and Ubiquitous Computing, Bristol, UK

[3] S. Gezici, I. Guvenc and Z. Sahinoglu, "*On the performance of linear least-squares estimation in wireless positioning systems*," in Communications, 2008. ICC '08. IEEE International Conference on, 2008, pp. 4203-4208.

[4] S. Venkatesh and R. M. Buehrer, "*A linear programming approach to NLOS error mitigation in sensor networks*," in Proc. IEEE Int. Symp. Information Processing in Sensor Networks (IPSN), Nashville, Tennessee, Apr. 2006, pp. 301–308

[5] Z. Li, W. Trappe, Y. Zhang, and B. Nath, "*Robust statistical methods for securing wireless localization in sensor networks*," in Proc. IEEE Int. Symp. Information Processing in Sensor Networks (IPSN), Los Angeles, CA, Apr. 2005, pp. 91–98.

[6] I. Guvenc, S. Gezici, F. Watanabe, and H. Inamura, “*Enhancements to linear least squares localization through reference selection and ML estimation*,” in Proc. IEEE Wireless Commun. Networking Conf. (WCNC), Las Vegas, NV, Apr. 2008, pp. 284–289

[7] S. M. Kay, “*Fundamentals of Statistical Signal Processing: Estimation Theory*”. Upper Saddle River, NJ: Prentice Hall, Inc., 1993

[8] I. Guvenc and Chia-Chin Chong, "*A Survey on TOA Based Wireless Localization and NLOS Mitigation Techniques*," Communications Surveys & Tutorials, IEEE, vol. 11, pp. 107-124, 2009.

[9] Y. T. Chan and K. C. Ho, "*A simple and efficient estimator for hyperbolic location*," Signal Processing, IEEE Transactions on, vol. 42, pp. 1905-1915, 1994.

[10] R. Shimura and I. Sasase, "*TDOA mobile terminal positioning with weight control based on received power of pilot symbol in Taylor-series estimation*," in Personal, Indoor and Mobile Radio Communications, 2006 IEEE 17th International Symposium on, 2006, pp. 1-5.

[11] Hao Li and M. Oussalah, "*Combination of taylor and chan method in mobile positioning*," in Cybernetic Intelligent Systems (CIS), 2011 IEEE 10th International Conference on, 2011, pp. 104-110.

[12] Hao Li and M. Oussalah, “*TDOA Wireless Localization Comparison Influence of Network Topology*”, in Transactions on Networks and Communications (TNC), pp. 104-115

CHAPTER 5: REVIEW OF WIRELESS LOCATION ALGORITHMS IN NLOS SCENARIOS

5.1 Overview

Non-line-of-sight (**NLOS**) [1] [2] is a mobile signal transmission across a path that is partially obstructed. In a mobile wireless location system, if the signal transmitting between the MS and BS is blocked by barriers, this signal has to travel with reflection or diffraction along the NLOS path and the measurement will contain excess delay, shown in Figure 5.1. Compared to the Gaussian noise, the NLOS error is always positive and much more significant than Gaussian noise.

$$\widetilde{d}_i = R_i + n_i + b_i \tag{5.1}$$

d_i is the TOA measurements, n_i is the Gaussian noise and b_i is NLOS bias.

In this situation, if we ignore the NLOS error and directly use the TOA or TDOA to locate, positioning accuracy must be largely reduced. Therefore, NLOS error is of great importance that cannot be neglected. We cannot cancel this error merely by improving the accuracy of the receivers. The NLOS error is related to the signal transmission condition, and has nothing to do with the type of cellular wireless network. In this chapter, some NLOS mitigation techniques are introduced.

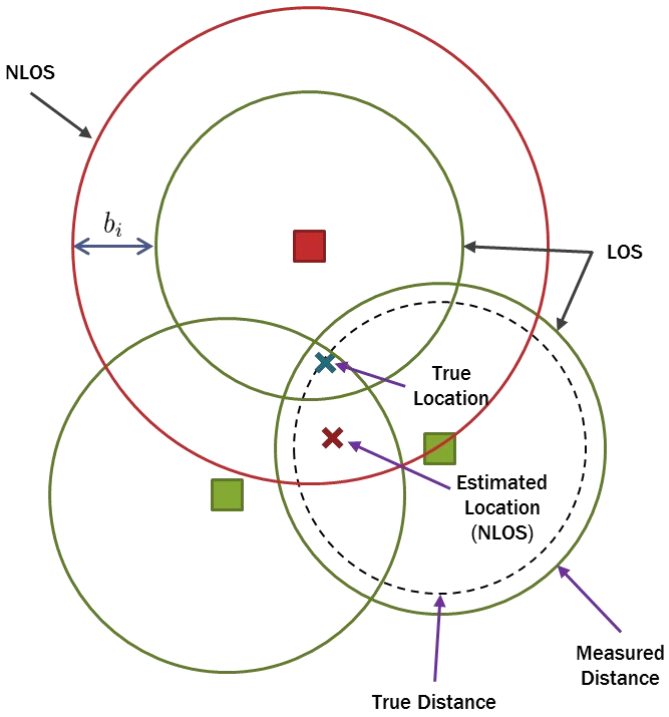

Figure 5.1: NLOS Error Influences TOA Measurements [3]

As the previous chapters' simulations, the NLOS mitigation methods are also simulated with the Monte-Carlo method. With a fixed NLOS, algorithm randomly adds a Gaussian Noise to the distance measurements for each single simulating and repeats 10,000 times to generate a location error level in RMSE.

This chapter is organised as follows: in Sections 5.2 to 5.4, three constrained localisation techniques are represented. Sections 5.5 and 5.6 are dedicated to the robust estimator for NLOS and Section 5.7 provides some concluding remarks.

5.2 Constrained LS Algorithm and Quadratic Program – CLS

Chan's method is not robust to NLOS bias and provides a great positioning error.

CLS [4] [5] [6] introduces a quadratic programming into NLOS environments. The mathematical programming is formulated as follows

$$\hat{\theta}_{cw} = \arg\min_{\theta} \left(A_1\theta - p_1\right)^T \psi^{-1} \left(A_1\theta - p_1\right) \tag{5.2}$$

where, $\left(A_1\theta - p_1\right) \le p_1$

where $A_1 = \begin{bmatrix} x_1 & y_1 & -0.5 \\ x_2 & y_2 & -0.5 \\ \vdots & \vdots & \vdots \\ x_N & y_N & -0.5 \end{bmatrix}$, $p_1 = \frac{1}{2}\begin{bmatrix} k_1 - \hat{d}_1^2 \\ k_2 - \hat{d}_2^2 \\ \vdots \\ k_N - \hat{d}_N^2 \end{bmatrix}$, $\theta = \begin{bmatrix} x \\ y \\ S \end{bmatrix}$

Equation (5.2) is a constrained linear least square algorithm. The quadratic programming (QP) techniques can be used to solve this equation. In the simulation, we can use the “quadprog” function in Matlab. The location result estimated from CLS is to use Equation (5.2) with the function “quadprog” to find a weighted least square solution for the MS, while the constraint θ_{cw} relaxes the equality into an inequality for NLOS scenarios.

5.3 Geometry Constrained Location Estimation – GLE

Geometry constrained location estimation (GLE) is applied on the scenario with only three BSs [7] [8] [9]. The GLE algorithm is based on the least square algorithm plus some additional parameters to incorporate the geometry of the BSs (only three-BS was considered). As we anticipated, the measurements were corrupted by the NLOS error, therefore the conventional least square methods do not perform well with a large NLOS error. So, to constrain the location

estimate within the overlap region (shown in Figure 5.3) of the three geometry circles becomes the primary motivation of the GLE algorithm.

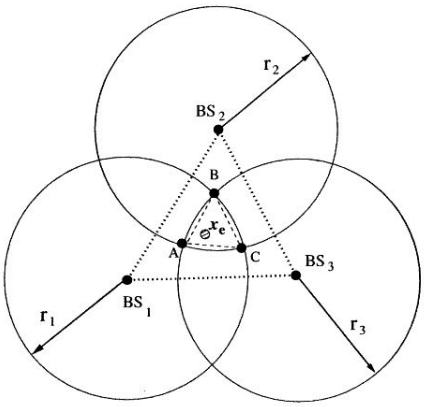

Figure 5.2: General Case of TOA Estimation for NLOS [7]

Assume the intersection points of the three circles being defined as $A = [x_A, y_A]^T$, $B = [x_B, y_B]^T$, $C = [x_C, y_C]^T$. Then, a constrained cost function, which is described as the virtual distance between the MS's position and the three points A, B, and C is defined as:

$$\gamma = \sqrt{\frac{1}{3}\left[\|x-A\|^2 + \|x-B\|^2 + \|x-C\|^2\right]} \tag{5.3}$$

The expected MS position was definitely allocated in the overlap region $\mathbf{x}_e$. In order to construct the constraints from the Three BSs location geometric layout, we chose to allocate the possible location of the MS within the triangular area ABC. The calculation of the expected virtual distance is implemented with different weights (W_1, W_2, W_3) respective to the A, B, and C points. The coordinates for x_e are chosen as

$$x_e = \omega_1 x_A + \omega_2 x_B + \omega_3 x_C \tag{5.4}$$

where the weights are obtained as

$$\omega_i = \frac{\sigma_i^2}{\sigma_1^2 + \sigma_2^2 + \sigma_3^2} \qquad \text{with i = 1, 2, 3} \tag{5.5}$$

σ_1, σ_2, and σ_3 are the corresponding standard deviations obtained from the three TOA measurements.

Since we assume the NLOS measurement variance will be larger. It can be considered that the weights will move the estimator x_e towards to the centre of the NLOS BSs circle. These geometric constraints are incorporated into the least square as Equation (2.22) by updating A_0 and p_0 as follows

$$\psi = \frac{1}{2} p_0 - A_0 * Z_a \tag{5.6}$$

$$A_0 = \begin{bmatrix} X_1 & Y_1 & -0.5 \\ X_2 & Y_2 & -0.5 \\ \vdots & \vdots & \vdots \\ X_N & Y_N & -0.5 \\ \gamma_x & \gamma_y & -0.5 \end{bmatrix} \qquad p_0 = \begin{bmatrix} K_1 - d_1^2 \\ K_2 - d_2^2 \\ \vdots \\ K_N - d_N^2 \\ \gamma_k - \gamma_e^2 \end{bmatrix} \qquad Z_0 = \begin{bmatrix} x \\ y \\ S \end{bmatrix} \qquad S = x^2 + y^2$$

where

$$\gamma_x = \frac{1}{3}(x_A + x_B + x_C) \qquad \gamma_y = \frac{1}{3}(y_A + y_B + y_C)$$

$$\gamma_k = \frac{1}{3}(x_A^2 + x_B^2 + x_C^2 + y_A^2 + y_B^2 + y_C^2)$$

The geometric constraints are also incorporated into other variables as

$$\widetilde{B} = diag(d_1, d_2, d_3, \gamma) \qquad \widetilde{n} = [n_1, n_2, n_3, n_\gamma]^T$$

Then, the two-step (Chan's) method can be employed to solve for the MS location using the variables updated with the geometric constraints.

5.4 Interior Point Optimisation – IPO

The interior point optimisation (IPO) [10] method is an optimisation location estimator in the NLOS scenario. By using Taylor's series approximation in Equation (2.34), a linearized measurement vector is defined as follows

$$h_t = G_t\delta + n_i + b_i \tag{5.7}$$

As shown in Chapter 2, if the NLOS bias is small, it can be neglected; the NLOS bias-free position estimate is given by

$$\tilde{x} = (G_t^T Q^{-1} G_t)^{-1} G_t^T Q^{-1} h_t \tag{5.8}$$

If the bias vector b is known, a more accurate bias-free location estimate is given by

$$\hat{x} = \tilde{x} + Vb \tag{5.9}$$

where $V = -(G_t^T Q^{-1} G_t)^{-1} G_t^T Q^{-1}$

However, in reality, b is unknown and has to be estimated. In order to estimate b, the observed bias metric is defined as

$$z = h_t - G_t\tilde{x} \tag{5.10}$$

which can be simplified to z = Sb + w, where S = I + G_tV, and the bias noise is given by

$$w = G_t(x - \hat{x}) - n \tag{5.11}$$

Then, the following constrained optimisation problem is defined to estimate the NLOS bias errors

$$\hat{b} = \arg\min_b (z - Sb)^T Q_w^{-1} (z - Sb) \quad \text{s.t. } b_i \in B_i \quad i = 1, 2, \ldots, N \tag{5.12}$$

where Bi = [l_i, u_i] are the a-priori information for the range of b_i lower-bounded by $l_i \geq 0$ and upper-bounded by u_i, and Q_w is the covariance matrix of w. In order to solve the constrained optimisation problem, an IPO technique was used.

$$\hat{b} = \arg\min_{b} (z - Sb)^T Q_w^{-1} (z - Sb) \quad \text{s.t. } gi(bi) - si = 0, \text{ and } si > 0,\ i = 1, ..., N$$

where s_i is a slack variable, and $g_i(b_i)$ is a barrier function that satisfies $g_i(b_i) > 0$ $\forall b_i \in [l_i, u_i]$. A generally used smooth second order function that satisfies the requirement is $g_i(b_i) = (u_i - b_i)/(b_i - l_i)$. Then, we solve by minimising the following Lagrangian

$$L(b, \lambda, s) = (z - Sb)^T Q_w^{-1} (z - Sb) - \mu \sum_{i=1}^{N} \ln s_i - \lambda^T (g(b) - s) \tag{5.13}$$

where g(b) and s are obtained upon stacking $g_i(b_i)$ and s_i, respectively, into N × 1 vectors. Note that the logarithmic barrier function $\mu \sum_{i=1}^{N} \ln s_i$ ensures that $s_i = g_i(bi) > 0$ and the bias error is always within [l_i, u_i]. The solution can be obtained by differentiating with respect to b, λ and s, and solving them together to obtain b. Once an estimate of the bias vector b is obtained, the authors employ the bias correction matrix to calculate the bias-free location.

5.5 Robust Estimator for NLOS Location

The M-estimator [11] [12] [13] is employed to eliminate the NLOS errors, and a recursive algorithm is developed to solve the M-estimation normal equations. Compared to conventional algorithms, the proposed algorithm does not rely on a

priori knowledge of the statistical model of the measurement noise. Another advantage is that the proposed algorithm can track the slow movement of the MS due to its recursive nature, which is hard to achieve in other algorithms.

Linear least square estimates can behave badly when the error distribution is not normal, particularly when the errors are heavy-tailed. One remedy is to remove influential observations from the least-squares fit. Another approach, termed robust regression, is to use a fitting criterion that is not as vulnerable as least squares to unusual data.

The most common general method of robust regression is M-estimation, introduced by Huber. This class of estimators can be regarded as a generalisation of maximum-likelihood estimation, hence the term “M” - estimation.

The estimating equations may be written as

$$\sum_{i=1}^{n} w_i \left(y_i - x_i' b \right) x_i' = 0 \qquad (5.14)$$

Solving these estimating equations is equivalent to a weighted least-squares problem, minimising $\sum_{i=1}^{n} w_i^2 e_i^2$. The weights, however, depend upon the residuals, the residuals depend upon the estimated coefficients, and the estimated coefficients depend upon the weights. An iterative solution (called iteratively reweighted least-squares, IRLS) is therefore required:

1. Select initial estimates b, such as the least-squares estimates.

2. At each iteration t, calculate residuals $e^{(t-1)}$ and associated weights $w_i^{(t-1)} = w\left[e_i^{(t-1)}\right]$ from the previous iteration.

3. Solve for new weighted-least-squares estimates

$$b^{(t)} = \left[X' W^{(T-1)} X\right]^{-1} X' W^{(t-1)} y$$

where X is the model matrix, with X_i' as its i^{th} row, and $W^{(t-1)} = \text{diag}\{w_i^{(t-1)}\}$ is the current weight matrix.

Steps 2 and 3 are repeated until the estimated coefficients converge.

We compare the objective functions and the corresponding ψ and weight functions for three M-estimators: the familiar least squares estimator; the Huber estimator; and the Tukey bisquare (or biweight) estimator. The objective and weight functions for the three estimators are also given:

Method	*Objective Function*	*Weight Function*
Least-Squares	$\rho_{\mathrm{LS}}(e) = e^2$	$w_{\mathrm{LS}}(e) = 1$
Huber	$\rho_{\mathrm{H}}(e) = \begin{cases} \frac{1}{2}e^2 & \text{for } \lvert e\rvert \le k \\ k\lvert e\rvert - \frac{1}{2}k^2 & \text{for } \lvert e\rvert > k \end{cases}$	$w_{\mathrm{H}}(e) = \begin{cases} 1 & \text{for } \lvert e\rvert \le k \\ k/\lvert e\rvert & \text{for } \lvert e\rvert > k \end{cases}$
Bisquare	$\rho_{\mathrm{B}}(e) = \begin{cases} \frac{k^2}{6}\left\{1 - \left[1 - \left(\frac{e}{k}\right)^2\right]^3\right\} & \text{for } \lvert e\rvert \le k \\ k^2/6 & \text{for } \lvert e\rvert > k \end{cases}$	$w_{\mathrm{B}}(e) = \begin{cases} \left[1 - \left(\frac{e}{k}\right)^2\right]^2 & \text{for } \lvert e\rvert \le k \\ 0 & \text{for } \lvert e\rvert > k \end{cases}$

Table 5.1: Robust Estimators [11]

The value of "k" for the Huber and bisquare estimators is called a tuning constant; smaller values of k produce more resistance to outliers, but at the expense of lower efficiency when the errors are normally distributed. The tuning constant is generally picked to give reasonably high efficiency in normal cases; in particular, k = 1.345σ for the Huber and k = 4.685σ for the bisquare (which is the standard deviation of the errors) produce 95-percent efficiency when the errors are normal,

and still offer protection against outliers.

5.6 Elliptic NLOS Mitigation Method

The measured distances between the MS and the i[th] BS is denoted as Equation (5.1). As the NLOS error is always positive, we have:

$$d_i = \alpha_i r_i \tag{5.15}$$

where, α_i is a corruption coefficient, $\alpha_i = 1$ means the signal transmitted between the MS and the i[th] BS is in LOS, r_i is the measurement for the distance between BS_i to the MS, and d_i is the true distance between BS_i and the MS. The smaller α_i, the larger the NLOS error effects. Because of the NLOS's positive property, it always has: $0 < \alpha_i \leq 1$.

Form the Cayley - Menger matrix for MS and three BSs topology to locate the MS [4]

$$M(MS \quad BS_1 \quad BS_2 \quad BS_3) = \begin{bmatrix} 0 & d_1^2 & d_2^2 & d_3^2 & 1 \\ d_1^2 & 0 & d_{12}^2 & d_{13}^2 & 1 \\ d_2^2 & d_{12}^2 & 0 & d_{23}^2 & 1 \\ d_3^2 & d_{13}^2 & d_{23}^2 & 0 & 1 \\ 1 & 1 & 1 & 1 & 0 \end{bmatrix} \tag{5.16}$$

Cayley-Menger has a zero determinant, which means:

$$|M(MS \quad BS_1 \quad BS_2 \quad BS_3)| = 0 \tag{5.17}$$

Substituting Equation (5.15) into (5.17) gets:

$$\begin{vmatrix} 0 & \alpha_1^2 r_1^2 & \alpha_2^2 r_2^2 & \alpha_3^2 r_3^2 & 1 \\ \alpha_1^2 r_1^2 & 0 & d_{12}^2 & d_{13}^2 & 1 \\ \alpha_2^2 r_{21}^2 & d_{12}^2 & 0 & d_{23}^2 & 1 \\ \alpha_3^2 r_3^2 & d_{13}^2 & d_{23}^2 & 0 & 1 \\ 1 & 1 & 1 & 1 & 0 \end{vmatrix} = 0 \tag{5.18}$$

Then, we have:

$$1\times(-1)^6\times\begin{vmatrix} \alpha_1^2 r_1^2 & \alpha_2^2 r_2^2 & \alpha_3^2 r_3^2 & 1 \\ 0 & d_{12}^2 & d_{13}^2 & 1 \\ d_{12}^2 & 0 & d_{23}^2 & 1 \\ d_{13}^2 & d_{23}^2 & 0 & 1 \end{vmatrix} + 1\times(-1)^7\times\begin{vmatrix} 0 & \alpha_2^2 r_2^2 & \alpha_3^2 r_3^2 & 1 \\ \alpha_1^2 r_1^2 & d_{12}^2 & d_{13}^2 & 1 \\ \alpha_2^2 r_2^2 & 0 & d_{23}^2 & 1 \\ \alpha_3^2 r_3^2 & d_{23}^2 & 0 & 1 \end{vmatrix} +$$

$$1\times(-1)^8\times\begin{vmatrix} 0 & \alpha_1^2 r_1^2 & \alpha_3^2 r_3^2 & 1 \\ \alpha_1^2 r_1^2 & 0 & d_{13}^2 & 1 \\ \alpha_2^2 r_2^2 & d_{12}^2 & d_{23}^2 & 1 \\ \alpha_3^2 r_3^2 & d_{13}^2 & 0 & 1 \end{vmatrix} + 1\times(-1)^9\times\begin{vmatrix} 0 & \alpha_1^2 r_1^2 & \alpha_2^2 r_2^2 & 1 \\ \alpha_1^2 r_1^2 & 0 & d_{12}^2 & 1 \\ \alpha_2^2 r_2^2 & d_{12}^2 & 0 & 1 \\ \alpha_3^2 r_3^2 & d_{13}^2 & d_{23}^2 & 1 \end{vmatrix} = 0$$

(5.19)

After we expanded (5.19), we have a long equation:

$$-(d_{12}^2 d_{23}^2 d_{13}^2 + d_{12}^2 + d_{23}^2 d_{13}^2) + (d_{12}^2 d_{23}^2 \alpha_3^2 r_3^2 + d_{13}^2 d_{23}^2 \alpha_2^2 r_2^2 - d_{23}^4 \alpha_1^2 r_1^2) -$$
$$(\alpha_2^2 r_2^2 d_{13}^4 - d_{13}^2 d_{12}^2 \alpha_3^2 r_3^2 - d_{13}^2 d_{23}^2 \alpha_1^2 r_1^2) + (d_{12}^2 d_{23}^2 \alpha_1^2 r_1^2 + d_{13}^2 d_{12}^2 \alpha_2^2 r_2^2 - d_{12}^4 \alpha_3^2 r_3^2)$$

$$+(d_{13}^2 d_{23}^2 \alpha_2^2 r_2^2 + d_{12}^2 d_{23}^2 \alpha_3^2 r_3^2 - \alpha_1^2 r_1^2 d_{23}^4) - (d_{23}^2 \alpha_2^2 r_2^2 \alpha_3^2 r_3^2 + d_{23}^2 \alpha_2^2 r_2^2 \alpha_3^2 r_3^2) +$$
$$(d_{23}^2 \alpha_1^2 r_1^2 \alpha_3^2 r_3^2 + d_{13}^2 \alpha_2^2 r_2^2 \alpha_3^2 r_3^2 - \alpha_3^4 r_3^4 d_{12}^2) - (\alpha_2^4 r_2^4 d_{13}^2 - d_{12}^2 \alpha_2^2 r_2^2 \alpha_3^2 r_3^2 - d_{23}^2 \alpha_1^2 r_1^2 \alpha_2^2 r_2^2)$$

$$-(\alpha_2^2 r_2^2 d_{13}^4 - d_{12}^2 d_{13}^2 \alpha_3^2 r_3^2 - d_{13}^2 d_{23}^2 \alpha_1^2 r_1^2) + (d_{13}^2 \alpha_2^2 r_2^2 \alpha_3^2 r_3^2 + d_{23}^2 \alpha_1^2 r_1^2 \alpha_3^2 r_3^2 - \alpha_3^4 r_3^4 d_{12}^2) -$$
$$(d_{13}^2 \alpha_1^2 r_1^2 \alpha_3^2 r_3^2 + d_{13}^2 \alpha_1^2 r_1^2 \alpha_3^2 r_3^2) + (d_{12}^2 \alpha_1^2 r_1^2 \alpha_3^2 r_3^2 + d_{13}^2 \alpha_1^2 r_1^2 \alpha_2^2 r_2^2 - \alpha_1^4 r_1^4 d_{23}^2)$$

$$+(d_{12}^2 d_{23}^2 \alpha_1^2 r_1^2 + d_{12}^2 d_{13}^2 \alpha_2^2 r_2^2 - \alpha_1^2 r_1^2 d_{12}^4) - (\alpha_2^4 r_2^4 d_{13}^4 - d_{12}^2 \alpha_2^2 r_2^2 \alpha_3^2 r_3^2 - d_{23}^2 \alpha_1^2 r_1^2 \alpha_2^2 r_2^2) +$$
$$(d_{13}^2 \alpha_1^2 r_1^2 \alpha_2^2 r_2^2 + d_{12}^2 \alpha_1^2 r_1^2 \alpha_3^2 r_3^2 - \alpha_1^4 r_1^4 d_{23}^2) - (d_{12}^2 \alpha_1^2 r_1^2 \alpha_2^2 r_2^2 + d_{12}^2 \alpha_1^2 r_1^2 \alpha_2^2 r_2^2)$$

$$= 0$$

(5.20)

After simplifying (5.20), we can result:

$$\alpha^T A \alpha + \alpha^T B + C = 0 \tag{5.21}$$

where α is a vector of a corruption coefficient, and A, B, C are defined as follows:

$$A = \begin{bmatrix} -2d_{23}^2 r_1^4 & r_1^2 r_2^2 (d_{13}^2 + d_{23}^2 - d_{12}^2) & r_1^2 r_3^2 (d_{12}^2 + d_{23}^2 - d_{13}^2) \\ r_1^2 r_2^2 (d_{13}^2 + d_{23}^2 - d_{12}^2) & -2d_{13}^2 r_2^4 & r_2^2 r_3^2 (d_{12}^2 + d_{13}^2 - d_{23}^2) \\ r_1^2 r_3^2 (d_{12}^2 + d_{23}^2 - d_{13}^2) & r_2^2 r_3^2 (d_{12}^2 + d_{13}^2 - d_{23}^2) & -2d_{12}^2 r_3^4 \end{bmatrix}$$

$$B = \begin{bmatrix} 2r_1^2 d_{23}^2 (d_{12}^2 - d_{23}^2 + d_{13}^2) \\ 2r_2^2 d_{13}^2 (d_{12}^2 + d_{23}^2 - d_{13}^2) \\ 2r_3^2 d_{12}^2 (-d_{12}^2 + d_{23}^2 + d_{13}^2) \end{bmatrix}$$

$$C = \begin{bmatrix} -2d_{12}^2 d_{23}^2 d_{13}^2 \end{bmatrix}$$

We assume the first BS is the home BS, $\alpha_1 = 1$, which means the signal between the MS and BS_1 is in LOS, so:

$$\alpha = \begin{bmatrix} 1 & \alpha_2 & \alpha_3 \end{bmatrix}^T$$

We also assume that the BSs coordinates are (0,0), (X_2,Y_2), (X_3,Y_3). It follows that

$$\begin{aligned} d_{12}^2 &= (X_2^2 + Y_2^2) \\ d_{13}^2 &= (X_3^2 + Y_3^2) \\ d_{23}^2 &= (X_3 - X_2)^2 + (Y_3 - Y_2)^2 \end{aligned} \tag{5.22}$$

Substituting Equations (5.22) in (5.21), we can create a quadratic equation with respect to α_2 and α_3, with the discriminant classification showing below:

$$\begin{aligned} &\Delta = -16 r_2^4 r_3^4 \left(X_2 Y_3 - X_3 Y_2 \right)^2 \\ &so, \Delta \le 0 \end{aligned} \tag{5.23}$$

A quadratic equation in two variables is always a conic section, and from (5.23), the discriminant is smaller than 0, which means, the equation represents an ellipse. [3]

Since α_2, α_3 are allocated along the ellipse curve, the NLOS state of a BS is tied to the azimuth angle. According to Figure 5.6.1, for example, when a NLOS error becomes dominant in BS3, it tends to the α_2 axis. This angle is useful to recognise the state of NLOS in BSs.

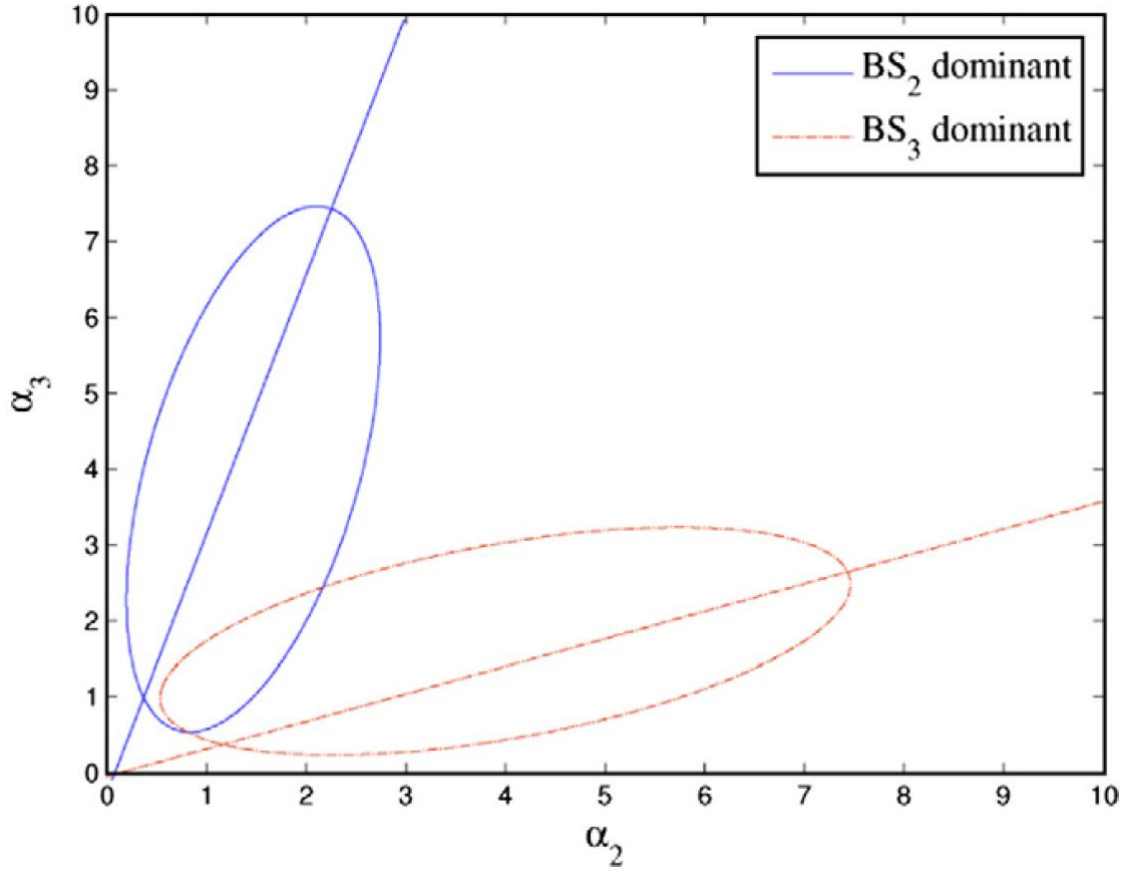

Figure 5.3: Ellipses inclination when one of the BSs NLOS errors is dominant [3]

In order to calculate the azimuth angle, λ, for each BS, we substituted $\alpha_2 = M\cos\lambda$ and $\alpha_3 = M\sin\lambda$ where $M = \sqrt{\alpha_2^2 + \alpha_3^2}$ into Equation (5.21). After we simplify the equation, we can get:

$$f(M,\lambda) = C_1 M^2 + C_2 M + C_3 = 0 \tag{5.24}$$

where

$$C_1 = r_2^2 r_3^2 \sin(2\lambda)(d_{13}^2 - d_{23}^2 + d_{12}^2)$$
$$C_2 = 2r_1^2 d_{23}^2 (d_{13}^2 - d_{23}^2 + d_{12}^2) - 2r_1^4 d_{23}^2 - 2d_{13}^2 d_{23}^2 d_{12}^2$$
$$C_3 = 2\cos(\lambda) r_2^2 (d_{13}^2 (d_{12}^2 + d_{23}^2 - d_{13}^2) + r_1^2 (d_{13}^2 - d_{12}^2 + d_{23}^2))$$
$$+ 2\sin(\lambda) r_3^2 (d_{12}^2 (d_{13}^2 - d_{12}^2 + d_{23}^2) + r_1^2 (d_{12}^2 + d_{23}^2 + d_{13}^2))$$
$$- 2\cos(\lambda) d_{13}^2 r_2^2 - 2\sin(\lambda) d_{12}^2 r_3^2$$

The following step is to find out the α_2 and α_3. We first define two important

points:

$$\alpha_\pi = \alpha_3 : \quad when \quad \alpha_2 = 1$$
$$\alpha_v = \alpha_2 : \quad when \quad \alpha_3 = 1$$

From Equation (5.21) we have:

$$\alpha_v = \alpha_2 = \frac{2r_1^2 r_2^2 (d_{13}^2 + d_{23}^2 - d_{12}^2) + 2r_3^2 r_2^2 (d_{13}^2 - d_{23}^2 + d_{12}^2) + 2r_2^2 d_{13}^2 (d_{12}^2 + d_{23}^2 - d_{13}^2)}{4r_2^4 d_{13}^2}$$

$$\alpha_\pi = \alpha_3 = \frac{2r_1^2 r_3^2 (d_{12}^2 + d_{23}^2 - d_{13}^2) + 2r_3^2 r_2^2 (d_{13}^2 - d_{23}^2 + d_{12}^2) + 2r_3^2 d_{12}^2 (d_{13}^2 + d_{23}^2 - d_{12}^2)}{4r_3^4 d_{12}^2}$$

The estimation has higher location quality when α_π and α_v are near 1. We can assume a threshold which if both α_π and α_v are bigger, then exhaustive search algorithm estimation is sensible. The simulations show that the threshold is α = 0.80.

The correction function is as follow:

$$r_2^2 = r_2^2 - (\sin(\lambda - 10))^2$$
$$r_3^2 = r_3^2 - (\cos(\lambda - 10))^2$$

Figure 5.6.2 shows the flowchart of the ellipse algorithm:

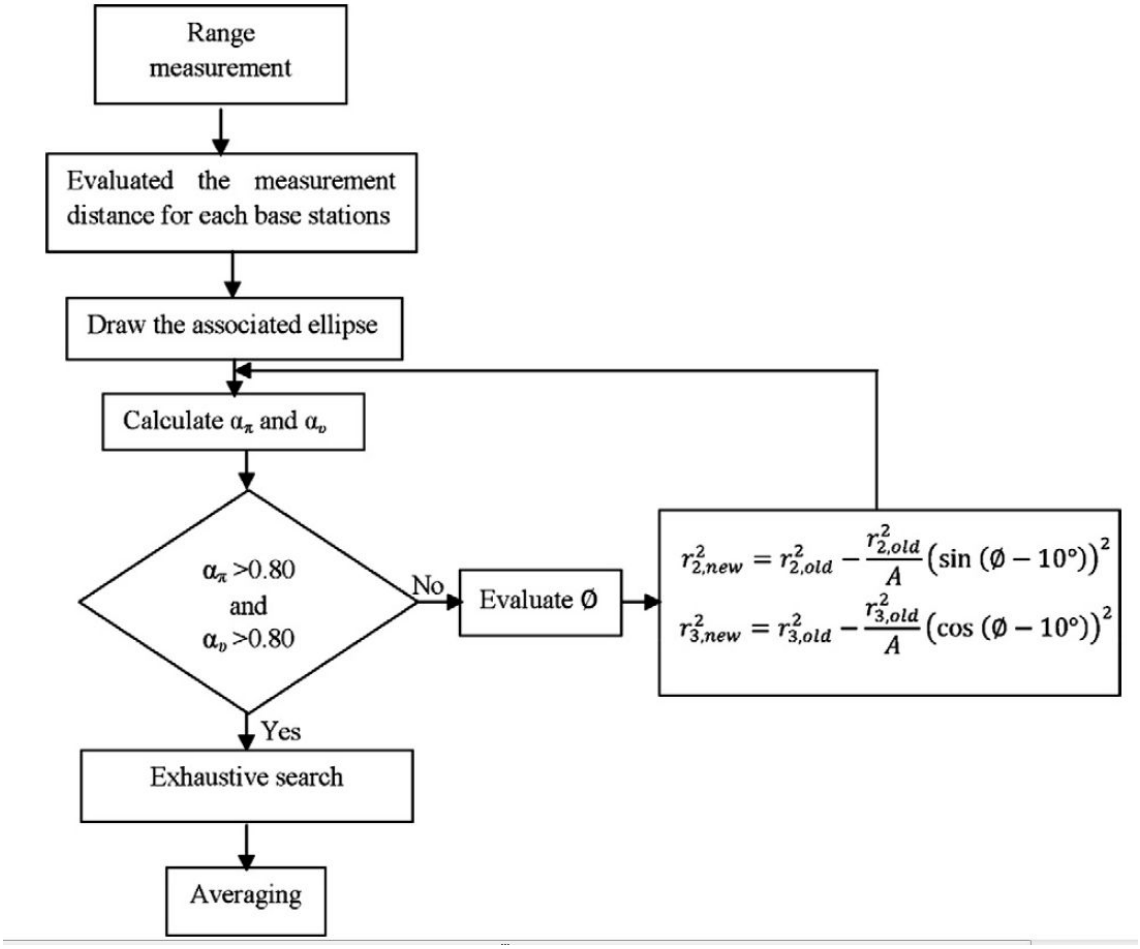

Figure 5.4: Flowchart of Ellipse Mitigation Algorithm [14]

Since we have mitigated the NLOS in the measurements, we could use one of the algorithms explained in the previous chapters for location estimation.

5.7 Algorithms' Limitation of Number of Base Stations with NLOS

In this section, Table 5.2 shows the limitation of each algorithm in different simulation conditions. Some of the algorithms have usage limitations with the suffering of NLOS bias; if the number of NLOS sets added is outside the

limitation, location accuracy is greatly affected.

	Limitation of LOS Sets Required	Influence of More NLOS Bias Sets Added	Influence of Stability with More NLOS Sets Added
CLS	Min=1	Less Sensitive	Less Stable
GLE	Min=2	Very Sensitive	Less Stable
IPO	Min=1	Moderate	Moderate
Robust_LS	Min=2	Sensitive	Stable
Robust_Huber	Min=1	Moderate	Stable
Robust_Bisqaure	Min=1	Sensitive	Stable
Elliptic	Min =1	Less Sensitive	Stable

Table 5.2: Limitation of Each Location Algorithm

5.8 Comparison in Complexity Analysis

When implementing each algorithm in Matlab, different location methods spend different time in calculation. Increasing the number of BSs used for getting the measurements increases execution time. In this section, the comparisons are dedicated to the complexity of each algorithm by analysing the program running speed. The comparison result is shown in Table 5.3 and 5.4.

NLOS Mitigations	Execution Time
CLS	About 5 mins
GLE	About 20 mins
IPO	About 9 hours
Robust_LS	About 15 s
Robust_Huber	About 10 mins
Robust_Bisquare	About 2 mins
Elliptic	About 17 mins

Table 5.3: Execution Time Analysis of Each Location Method

NLOS Mitigations	Complexity
CLS	$O(N^3)$
GLE	$O(N^3)$
IPO	$O(N^3)$
Robust_LS	$O((N-1)^2)$
Robust_Huber	$O((N-1)^2)$
Robust_Bisquare	$O((N-1)^2)$
Elliptic	$O(p*N^{2.373})$ - with p number of iterations

Table 5.4: Complexity Analysis of Each Location Method

Compared with the LOS algorithms, the NLOS mitigation algorithms have longer execution time prevalence. Therefore, it can be summarized as that NLOS algorithms are generally more complex than LOS methods and the reasons for longer execution time are highlighted as follows:

- Complex MATLAB functions are employed in the program – all the algorithms are run by MATLAB. NLOS mitigation methods contain the optimisation or large equation solving functions which slow down the MATLAB running speed, such as “quadprog” function in CLS, “fsolve” in GLE, “minimizing a Lagrangian” in IPO, or large complex iterations in programming.
- Monte-Carlo simulation employed in the program – as we discussed in previous chapters, Monte-Carlo simulation is frequently used in location techniques research. All the algorithms are run independently 10,000 times. Because NLOS mitigations contain complex functions, the program spends more time running out the result for only one time simulation. Therefore, considering the computer’s condition, it will take a long time to run 10,000

times for a Monte-Carlo simulation.

5.9 Conclusion

In Chapter 5, we discussed several algorithms used in the NLOS scenario. Through the introduction and comparisons, we can clearly see the advantages and limitations of each algorithm. In real life, we cannot avoid the NLOS influence when signals are propagating, therefore, a good NLOS mitigation method is very important to wireless location. In the following chapter, I will research the simulation of the comparison among NLOS mitigations, and I will introduce an innovative method for wireless location in a NLOS scenario.

5.10 Reference

[1] S. Gezici and Z. Sahinoglu, “*UWB geolocation techniques for IEEE 802.15.4a personal area networks*,” MERL Technical report, Cambridge, MA, Aug. 2004.

[2] J. Riba and A. Urruela, “*A non-line-of-sight mitigation technique based on ML-detection*,” in Proc. IEEE Int. Conf. Acoustics, Speech, and Signal Processing (ICASSP), vol. 2, Quebec, Canada, May 2004, pp. 153–156.

[3] H. Lal Dehghani, K. Shadi and S. Golmohammadi, "*Non-line-of-sight error mitigation technique for wireless localization in micro-cell networks*," in New Technologies, Mobility and Security (NTMS), 2011 4th IFIP International Conference on, 2011, pp. 1-5.

[4] S. Venkatesh and R. M. Buehrer, “*A linear programming approach to NLOS error*

mitigation in sensor networks," in Proc. IEEE Int. Symp. Information Processing in Sensor Networks (IPSN), Nashville, Tennessee, Apr. 2006, pp. 301–308.

[5] X. Wang, Z. Wang, and B. O. Dea, "*A TOA based location algorithm reducing the errors due to non-line-of-sight (NLOS) propagation*," IEEE Trans. Veh. Technol., vol. 52, no. 1, pp. 112–116, Jan. 2003.

[6] S. Venkatesh and R. M. Buehrer, "*NLOS mitigation using linear programming in ultrawideband location-aware networks*," IEEE Trans. Veh. Technol., vol. 56, no. 5, pp. 3182–3198, Sep. 2007.

[7] C. L. Chen and K. T. Feng, "*An efficient geometry-constrained location estimation algorithm for NLOS environments*," in Proc. IEEE Int. Conf. Wireless Networks, Commun., Mobile Computing, Hawaii, USA, June 2005, pp. 244–249.

[8] Y. Zhao, "*Standardization of Mobile Phone Positioning for 3G Systems*," IEEE Communications Magazine, vol. 40, July 2002, pp. 108-116.

[9] S. Feng and C. L. Law, "*Assisted GPS and Its Impact on Navigation in Intelligent Transportation Systems*," IEEE Intelligent Transportation Systems, 2002, pp. 926-931.

[10] W. Kim, J. G. Lee, and G. I. Jee, "*The interior-point method for an optimal treatment of bias in trilateration location*," IEEE Trans. Veh. Technol., vol. 55, no. 4, pp. 1291–1301, July 2006.

[11] Z. Li, W. Trappe, Y. Zhang, and B. Nath, "*Robust statistical methods for securing wireless localization in sensor networks*," in Proc. IEEE Int. Symp. Information Processing in Sensor Networks (IPSN), Los Angeles, CA, Apr. 2005, pp. 91–98.

[12] P. Petrus, “*Robust Huber adaptive filter*,” IEEE Trans. Signal Processing, vol. 47, no. 4, pp. 1129–1133, Apr. 1999.

[13] R. Casas, A. Marco, J. J. Guerrero, and J. Falco, “*Robust estimator for non-line-of-sight error mitigation in indoor localization*,” Eurasip J. Applied Sig. Processing, vol. 2006, no. 1, pp. 1–8, Jan. 2006.

CHAPTER 6: INNOVATIVE TECHNIQUES FOR NLOS MITIGATION IN WIRELESS LOCATION

6.1 Overview

In Chapter 5, we introduced the non-line-of-sight (NLOS), caused by intermittent blocking of the direct path between the MS and the BSs, which significantly degraded location accuracy. Some classic mitigation algorithms were presented in Chapter 5. In this Chapter 6, we focus on the proposal of a novel NLOS mitigation algorithm.

Chapter 6 is organised as follows: a novel algorithm, named the Gradient Descent Iteration - Combination Algorithm, is introduced in Section 6.2. The simulation results and comparison between each existing algorithm are shown in Section 6.3 with the conclusion presented in Section 6.4.

6.2 Gradient Descent Iteration – Combination (GDIC) Method

6.2.1 Motivation and Structure of the GDIC Algorithm

As we know, in a real communication environment, LOS can be blocked by large buildings or other barriers becoming a NLOS which causes a time extension in TOA [1]. Therefore, the NLOS can be considered as a positive error. This NLOS bias affects distance measurements by adding a positive error, which is much larger than the variance of normal Gaussian noise. If these measurements with a

large positive bias are substituted directly into the location algorithms, the estimating result consequently contains a large error. In order to mitigate this effect, a reduction factor is introduced in this section. Through the iterative process, the large positive NLOS bias is mitigated progressively. In addition, the combination method from Chapter 3 shows a very accurate and stable location quality, hence, this novel algorithm is constructed based on the combination method [2] with NLOS distance measurement mitigation processing.

6.2.2 NLOS Measurements Error Mitigation in GDIC

This method is based on the combination method and gradient descent to mitigate the NLOS effect.

We can assume the

$$R_{i,1} = \alpha_i L_{i,1} \tag{6.1}$$

where, α_i is a corruption coefficient, $L_{i,1}$ is the measurement for the distance between BS_i and the MS, and $R_{i,1}$ is the true distance between BS_i and the MS. Considering that NLOS bias is always a positive error. We have: $0 < \alpha_i \leq 1$.

In this method, we assume there is a TOA measurement without NLOS bias, which means at least one LOS path between the MS to one BS. Let this BS be the servicing BS. The reason for this is to make the iteration converge. Here,

$L_1 = R_1$.

Substitute $\alpha_i L_{i,1}$ to the combination method first part instead of $R_{i,1}$, in Equation (3.8). The combination method is turned to the different performance.

$$\begin{bmatrix} x \\ y \\ R_1 \end{bmatrix} = \left(G_a{}^T Q^{-1} G\right)^{-1} G_a{}^T Q^{-1} h_a$$

$$h = \frac{1}{2}\begin{bmatrix} \alpha_2{}^2 L_{2,1}^2 - X_2^2 - Y_2^2 + X_1^2 + Y_1^2 \\ \alpha_3{}^2 L_{3,1}^2 - X_3^2 - Y_3^2 + X_1^2 + Y_1^2 \\ ..... \\ \alpha_M{}^2 L_{M,1}^2 - X_M^2 - Y_M^2 + X_1^2 + Y_1^2 \end{bmatrix} \quad G_a = \begin{bmatrix} X_{2,1} & Y_{2,1} & \alpha_2 L_{2,1} \\ X_{3,1} & Y_{3,1} & \alpha_3 L_{3,1} \\ ... & ... & ... \\ X_{M,1} & Y_{M,1} & \alpha_M L_{M,1} \end{bmatrix} \tag{6.2}$$

The method to solve the equation uses the same process as the combination method, but now, α_i is unknown. In this case, we can assume the signal between the MS and BS is LOS, ignoring the NLOS effects on each TDOA measurement, which means we assume α_i =1. Then, we can use the weight linear squire to make the initial solution:

$$z_a = \left(G_a{}^T \psi^{-1} G_a{}^T\right)^{-1} G_a{}^T \psi^{-1} h \tag{6.3}$$

where $\psi = E\left[\psi\psi^T\right] = c^2 BQB$;

and $B = diag\{\alpha_2{}^2 L_{2,1}{}^2 + \alpha_2 L_1 \quad \alpha_3{}^2 L_{3,1}{}^2 + \alpha_3 L_1 \quad ..... \quad \alpha_M{}^2 L_{M,1}{}^2 + \alpha_M L_1\}$,

here α_i=1

After this iteration, we get an initial result Za, but we assume there is no NLOS effect, which means this result must contain a large error. This fact will lead to the result that $R_{i,1} \neq \alpha_i L_{i,1}$

From the above, an estimation error function can be shown as:

$$f(\alpha_i) = (\alpha_i L_{i,1} - R_{i,1})^2 \tag{6.4}$$

The quadratic function is with respects to α_i, therefore, it must have a minimum

value (which means that $\alpha_i L_{i,1}$ is closest to the true $R_{i,1}$). Now we can use the gradient descent iteration [3] [4] [5] to update the reduction factor α_i

We can make the deviation for $f(\alpha_i)$, with respect to α_i

$$\frac{\partial f}{\partial \alpha_i} = 2L_{i,1}(\alpha_i L_{i,1} - R_{i,1}) \tag{6.6}$$

Because the $2L_{i,1}$ is constant in each set of measurements, we can ignore its effect in the iteration.

The α_i update function will be:

$$\alpha_i^{k+1} = \alpha_i^k - \mu\left(\alpha_i^k L_{i,1} - R_{i,1}\right) \tag{6.7}$$

μ is a step length of the iteration. Here, we choose $\mu = \frac{1}{2 \times \text{radius of the cell}}$. α_i^k which means the i[th] reduction factor α in the K[th] iteration process. After we update the value of α_i, we substitute the new α_i back into Equation (6.2) to calculate Za, in (6.3). Then, we update $R_{i,1}$ by using the coordinates of the BSs. Additionally, we use the updated $R_{i,1}$ to renew α_i.

The iteration stop condition is $\sum_{i=2}^{M} \left|\alpha_i^k - \alpha_i^{k+1}\right| \le \varepsilon$ – a very small number, here we choose the threshold is 0.001, which because when the simulating radius is 3000m, the error can be accept in 0.1%. And normally, only needs 20 times of iteration to get this threshold. At this stage, we have the accurate α_i, and after $R_i \approx \alpha_i L_i$, we can consider $R_{i,1}$ without NLOS effect. Substituting $R_{i,1}$ in to Equation (2.26), we then follow the rest of the steps to finish the combination method to achieve an accurate estimation result. The flow chart of the GDIC

method is presented as follows:

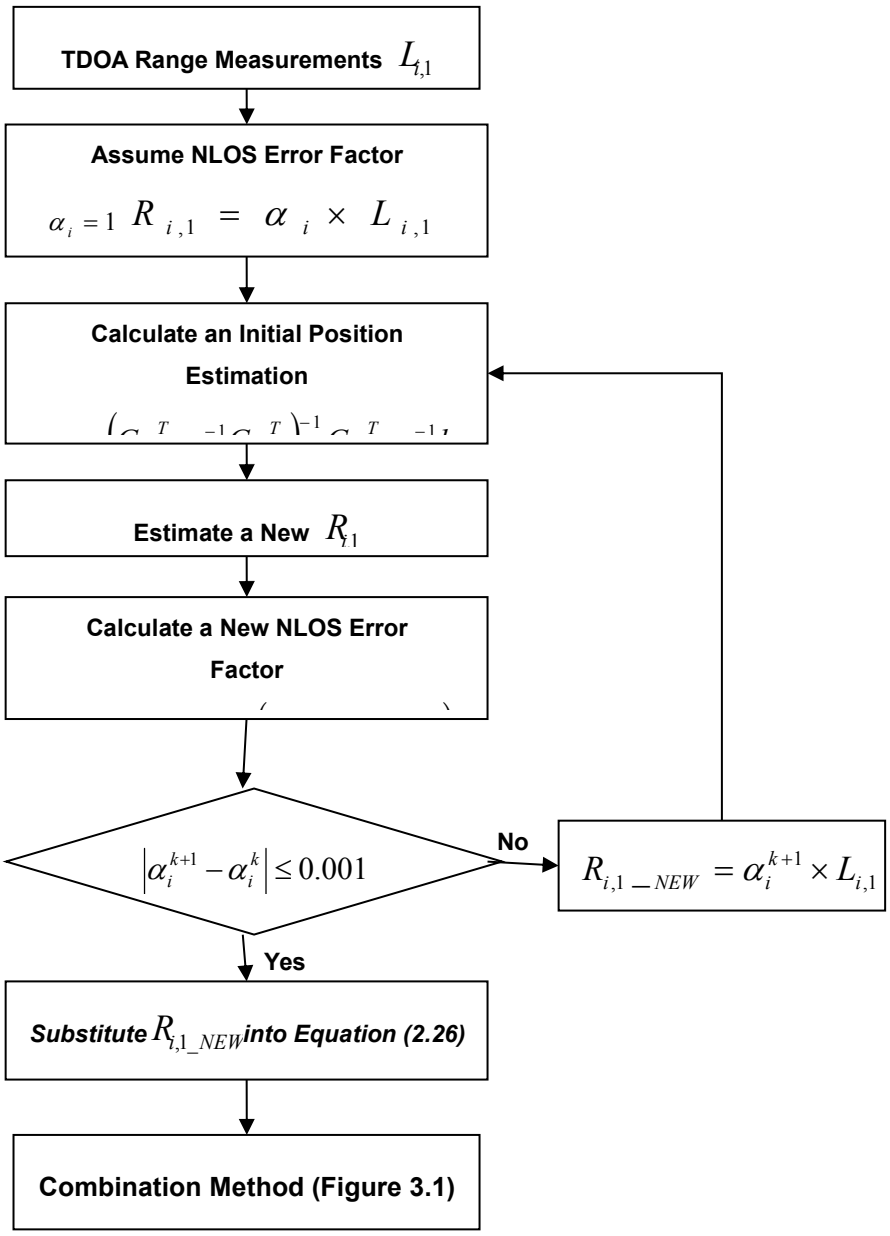

Figure 6.1: Flowchart of GDIC Algorithm

6.2.3 Simulation of Gradient Descent Iteration – Combination

The simulation parameters for demonstrating the location quality level with a

fixed NLOS error factor are described in Table 6.1

Number of BSs	Cell Radius (m)	Standard Deviations σ (us)	NLOS Error Factor α
4, 5, 6, 7	3000m	0.1, 0.15, 0.2, 0.25, 0.3, 0.35, 0.4, 0.45, 0.5us	0.5

Table 6.1: Parameters of the Simulation Setup

α_i = 0.5 which means the NLOS bias was set very large; 50% of the measurements value are NLOS errors. The TDOA measurements are twice as larger as the true value.

NBS	Average RMSE (m) in Different Standard Deviations σ (us)								
	0.1us	0.15us	0.2us	0.25us	0.3us	0.35us	0.4us	0.45us	0.5us
7	21.89m	31.39m	44.96m	54.43m	65.93m	76.37m	87.17m	100.9m	113.5m
6	24.68m	37.47m	49.57m	62.93m	76.54m	86.87m	93.66m	111.5m	125.8m
5	33.64m	49.01m	66.29m	78.28m	92.13m	106.1m	126.6m	132.4m	153.2m
4	40.97m	62.14m	75.95m	98.23m	115.1m	137.5m	151.7m	170.m	178.5m

Table 6.2: Performance of Location Algorithms with NLOS Factor α=0.5

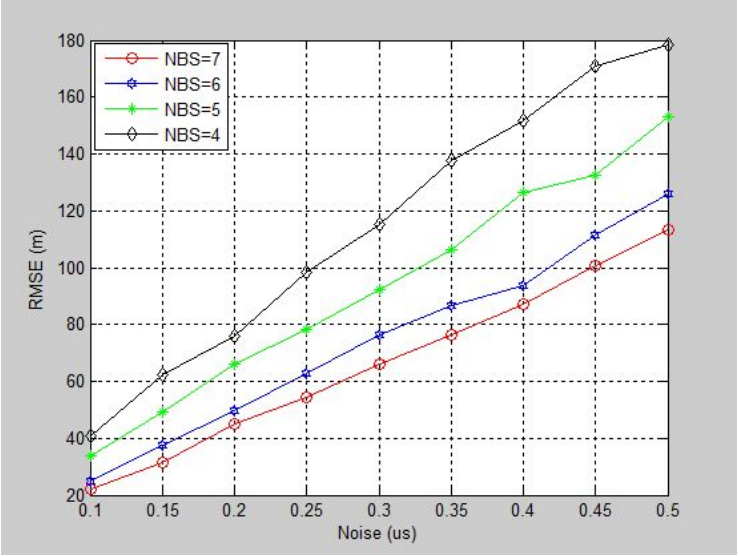

Figure 6.2: RMSE of the GDIC algorithm with NBS = 7, 6, 5, 4, when α = 0.5

Table 6.2 and Figure 6.2 show the GDIC's performance with the seven, six, five and four BSs measurements used. The X-axis states the standard deviation of

Gaussian noise selected from 0.1us to 0.5us. The Y-axis presents the RMSE of the estimation results. The red, blue, green and black lines demonstrate the accuracy difference between the different numbers of sets of measurements from BSs. From the simulation result in Figure 6.2, the conclusion can be obtained as the GDIC algorithm was affected by the number of BS measurements used. The more sets of measurements from the BSs used, the higher accuracy the GDIC method performed. Meanwhile, the GDIC algorithm shows a linear relationship between the standard deviation of noise and location accuracy (RMSE).

Table 6.3 describes the simulation parameters for demonstrating the location quality level change with different NLOS error factors.

Number of BSs	Cell Radius (m)	NLOS Error Factor α	Standard Deviations σ (us)
4, 5, 6, 7	**3000m**	**0.9, 0.8, 0.7, 0.6, 0.5, 0.4, 0.3, 0.2, 0.1**	**0.1**

Table 6.3: Parameters of the Simulation Setup

α_i decreasing means the NLOS bias is getting larger. The smaller α is, the larger the NLOS error is adding to the system.

NBS	NLOS Error Factor α								
	0.9	**0.85**	**0.8**	**0.75**	**0.7**	**0.65**	**0.6**	**0.55**	**0.5**
7	21.81m	21.84m	22.26m	22.71m	23.42m	23.97m	24.58m	24.80m	25.202m
6	25.27m	25.60m	26.02m	27.04m	27.25m	28.50m	29.25m	30.00m	31.20m
5	32.94m	33.11m	34.06m	34.96m	35.16m	35.33m	36.34m	36.55m	37.37m
4	39.03m	40.08m	41.61m	41.73m	43.16m	43.34m	44.53m	45.14m	47.37m

Table 6.4: Performance of Location Algorithms with a Changing NLOS Factor α

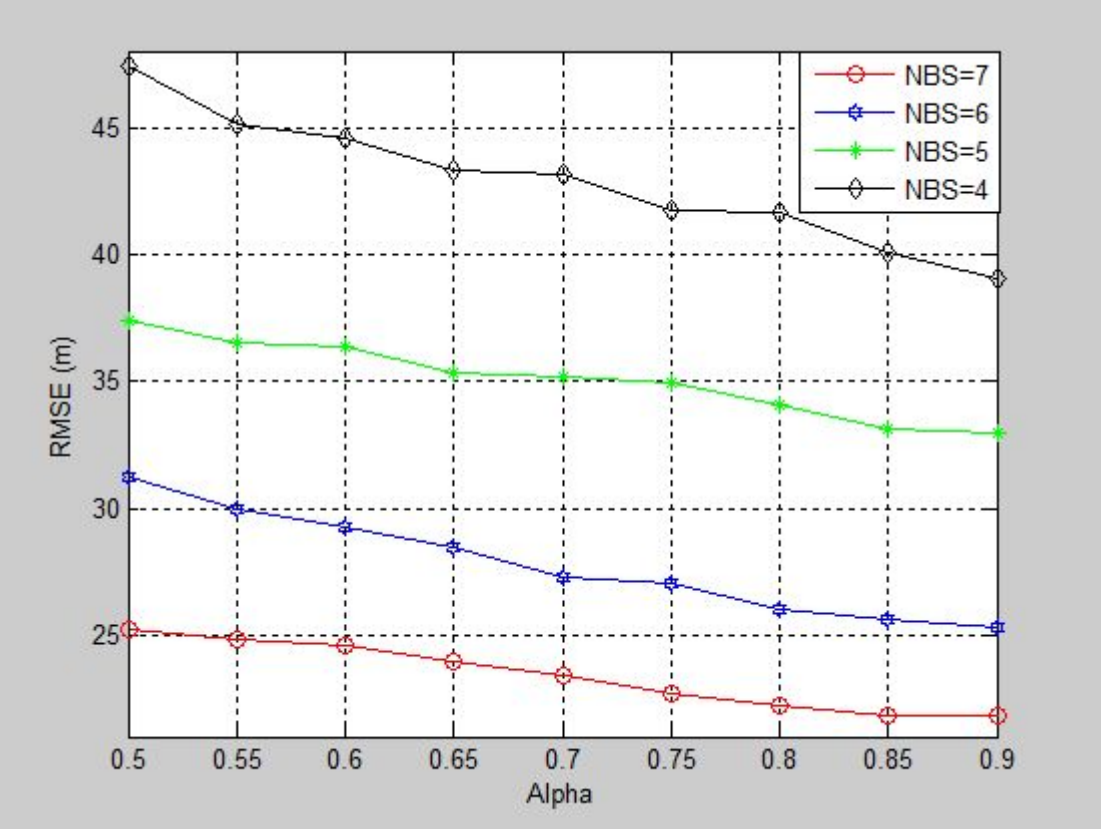

Figure 6.3: RMSE of the GDIC Algorithm with NBS = 7, 6, 5, 4, When α Changes

Table 6.4 and Figure 6.3 show the GDIC performance with the changing NLOS bias added. The X-axis gives an increasing set of NLOS errors added to the measurements. The Y-axis presents the RMSE of the estimation results. The red, blue, green and black lines show the accuracy difference between the different numbers of sets of measurements from BSs. From Figure 6.3, the simulation result can conclude that the GDIC algorithm was affected by the number of BSs measurements used in the topology. The more sets of measurements from the BSs used, the higher accuracy the GDIC method demonstrated. However, the GDIC algorithm was not sensitive to the NLOS error. From the simulation, the GDIC shows an outstanding NLOS error mitigation ability.

6.3 Comparison of GDIC Algorithms with Classic NLOS Algorithms

In this section, a comparison between the GDIC method and the other NLOS mitigation methods is presented. The simulation is demonstrated in three aspects: the comparison in Section 6.3.1 presentes in turn the TOA measurements set suffering a common NLOS bias, Section 6.3.2 gives a comparison of each algorithm suffering from different NLOS errors and in Section 6.3.3, the simulation comparison shows the accuracy changes with different NBS (four, five, six and seven) affected by a common NLOS. All the performance was qualified using RMSE evaluation, and the topology of BSs is a cellular topology.

6.3.1 Simulation of Comparison When α = 0.5

Table 6.5 describes the simulation parameters for demonstrating the location quality level changes with a common NLOS error factor α, and the X-axis is expanded with a set of standard deviations σ.

Number of BSs	Cell Radius (m)	Standard Deviations σ (us)	NLOS Error Factor α
7	3000m	0.1, 0.15, 0.2, 0.25, 0.3, 0.35, 0.4, 0.45, 0.5us	0.5

Algorithms in Comparison Simulation						
CLS	Robust (LS, Huber, Bisquare)	Elliptic	LLS-1	Chan	Taylor	GDIC Algorithms

Table 6.5: Parameters of the Simulation Setup When α = 0.5

In this section, all the distance measurements suffered from a common NLOS bias. The RMSE result is presented in Table 6.6 and Figure 6.4:

NBS=7	Average RMSE (m) in Different Standard Deviations σ (us) When α = 0.5								
	0.1us	0.15us	0.2us	0.25us	0.3us	0.35us	0.4us	0.45us	0.5us
GDIC	21.73m	32.62m	44.76m	54.55m	66.69m	77.32m	87.70m	95.58m	110.3m
CLS	2462m	2443m	2372m	2385m	2436m	2571m	2474m	2444m	2473m
R-HUBER	1521m	1528m	1532m	1537m	1532m	1517m	1528m	1534m	1523m
R-LS	1511m	1522m	1518m	1528m	1524m	1508m	1521m	1527m	1519m
R-BISQURE	1453m	1469m	1471m	1472m	1469m	1465m	1477m	1484m	1481m
CHAN	1140m	1150m	1176m	1204m	1181m	1153m	1184m	1207m	1202m
TAYLOR	2046m	2038m	2014m	2052m	2015m	2017m	2059m	2130m	2079m
LLS-1	4820m	4758m	4819m	4655m	4748m	4971m	4805m	4817m	4826m
ELLIPTIC	321.7m	332.6m	484.7m	354.5m	366.6m	397.3m	387.7m	495.6m	510.3m

Table 6.6: Performance of Each Location Algorithm with 7 BSs When α = 0.5

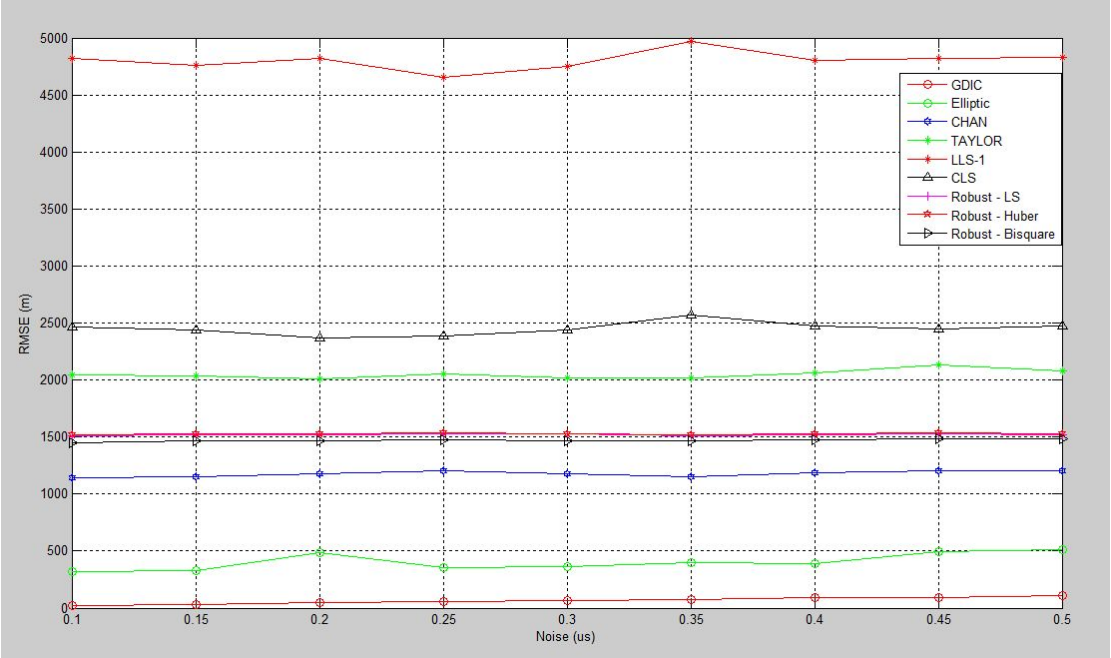

Figure 6.4：RMSE Plotting of Each Location Algorithm with 7 BSs When α = 0.5

From Figure 6.4 and the data in Table 6.6, we can obtain that, in a seven-BS cellular network, when the distance is affected by a common NLOS bias, the “iterative” NLOS mitigations give a better performance than the other algorithms, particularly, the innovative mitigation, GDIC, which shows the best performance both in accuracy and stability. In the RMSE analysis, the classic NLOS mitigations, like CLS, and robust methods, also presented good performances. Although the LLS algorithms performed well in the LOS scenarios, when the measured distances were corrupted by NLOS bias, the least square methods showed their limitations in that location estimation was corrupted with a large error. Meanwhile, the two classic location algorithms, Chan’s and Taylor’s, also show the ability to reduce the NLOS effect.

6.3.2 Simulation of Comparison with Changing NLOS Error Factor α

Table 6.7 describes the simulation parameters for performing the location quality level changes with different NLOS error factors. As described in Section 6.2.2, α stands for the NLOS error factor. The NLOS became larger when α is reduced. α = 1 means there is no NLOS influence.

Number of BSs	Cell Radius (m)	NLOS Error Factor α	Standard Deviations σ (us)
7	3000m	0.9, 0.85, 0.8, 0.75, 0.7, 0.65, 0.6, 0.55, 0.5	0.1 us

Algorithms in Comparison Simulation						
CLS	Robust (LS, Huber, Bisquare)	Elliptic	LLS-1	Chan	Taylor	GDIC Algorithms

Table 6.7: Parameters of the Simulation Setup with a Changing α

In this section, all the distance measurements suffered from a changing NLOS bias, expanding along the X-axis. The RMSE result is presented in Table 6.8 and Figure 6.5:

NBS=7	Average RMSE (m) with Changing α								
	0.5	0.55	0.6	0.65	0.7	0.75	0.8	0.85	0.9
GDIC	21.97m	22.78m	21.81m	22.16m	22.26m	22.44m	21.88m	21.92m	22.20m
CLS	2474m	1691m	1371m	830.2m	588.0m	414.6m	299.4m	210.2m	135.6m
R-HUBER	1530m	1238m	933.1m	807.3m	636.9m	498.4m	374.9m	265.3m	168.8m
R-LS	1519m	1231m	988.1m	802.8m	634.9m	497.9m	373.8m	265.8m	168.7m
R-BISQURE	1465m	1178m	943.2m	765.9m	604.2m	473.5m	354.1m	252.6m	160.6m
CHAN	1167m	924.1m	905.3m	1032m	1144m	1010m	784.51m	543.05m	330.5m
TAYLOR	2022m	1605m	1348m	1132m	916.6m	729.2m	564.5m	405.1m	260.4m
LLS-1	4741m	3569m	2864m	2148m	1663m	1235m	897.7m	614.8m	380.3m
ELLIPTIC	521.6m	465.3m	399.7m	401.3m	376.9m	354.5m	494.7m	329.4m	311.1m

Table 6.8: Performance of Each Location Algorithm with a Changing α

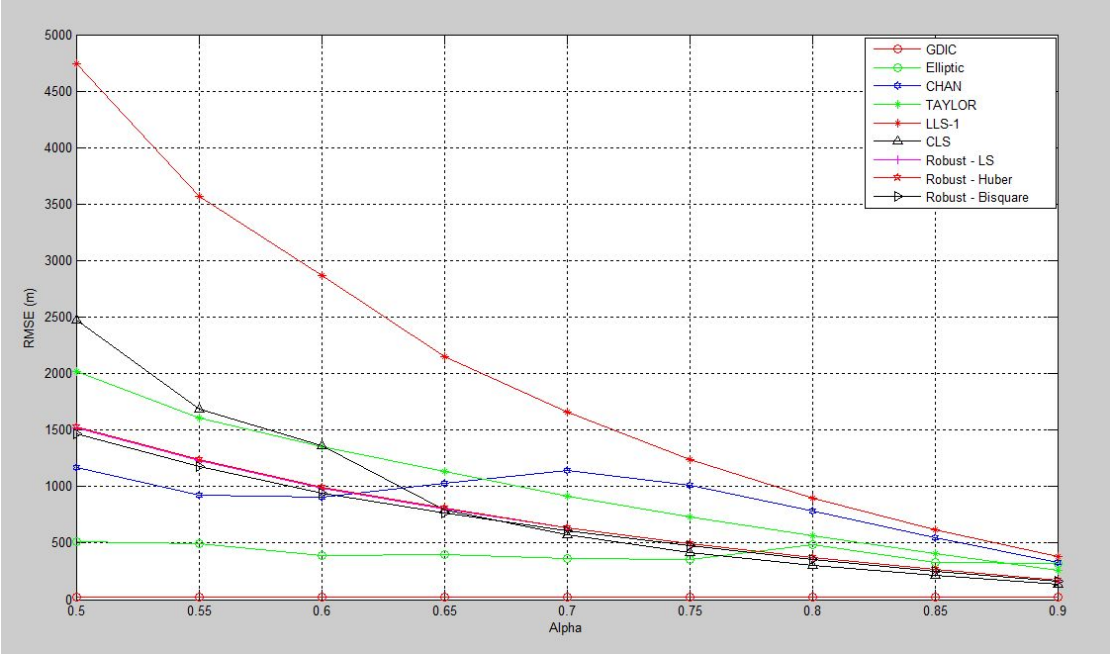

Figure 6.5: RMSE Plotting of Each Location Algorithm with a Changing α

According to the Figure 6.5 and the data in Table 6.8, we can see that the "iterative" NLOS mitigations, GDIC and elliptic, can effectively reduce the impact of the change of NLOS errors. The GDIC NLOS mitigation, again outputs the best performance both in accuracy and stability. In the RMSE analysis, all the other classic NLOS mitigations presented were influenced by the change in NLOS error corruption. When the NLOS error became smaller, all the algorithms could demonstrate good location quality.

6.3.3 Comparison in Complexity Analysis

When implementing each algorithm in Matlab, different location methods spend different time in calculation. Increasing the number of BSs used for getting the measurements increases execution time. In this section, the comparisons are

dedicated to the complexity of each algorithm by analysing the program running speed. The comparison result is shown in Table 6.9.

NLOS Mitigations	Execution Time
CLS	About 5 mins
GLE	About 20 mins
IPO	About 9 hours
Robust_LS	About 15 s
Robust_Huber	About 10 mins
Robust_Bisquare	About 2 mins
Elliptic	About 17 mins
GDIC	About 12 mins

Table 6.9: Execution Time Analysis of Each Location Method

Since the GDIC method is a combination method plus an iteration part for NLOS mitigation, the execution time is longer than some of classic methods. But considered its positioning result, the GDIC still a reliable method in the NLOS scenario.

6.4 Conclusion

This chapter introduced an upgraded combination method, the GDIC method, for NLOS mitigation. Based on the combination method introduced in Chapter 3, GDIC added a gradient descent iteration to mitigate the NLOS effect. The simulations test the performance of classic and innovative estimators under different NLOS environments. The results show that GDIC gives better performance in location quality and stability.

6.5 Reference

[1] J. H. Reed, K. J. Krizman, B. D. Woerner and T. S. Rappaport, "*An overview of the challenges and progress in meeting the E-911 requirement for location service*," Communications Magazine, IEEE, vol. 36, pp. 30-37, 1998.

[2] Hao Li and M. Oussalah, "*Combination of Taylor and Chan method in mobile positioning*," in Cybernetic Intelligent Systems (CIS), 2011 IEEE 10th International Conference on, 2011, pp. 104-110.

[3] A. I. Hanna, I. Yates and D. P. Mandic, "*Analysis of the class of complex-valued error adaptive normalised nonlinear gradient descent algorithms*," in Acoustics, Speech, and Signal Processing, 2003. Proceedings. (ICASSP '03). 2003 IEEE International Conference on, 2003, pp. II-705-8 vol.2.

[4] A. I. Hanna, I. Yates and D. P. Mandic, "*Analysis of the class of complex-valued error adaptive normalised nonlinear gradient descent algorithms*," in Acoustics, Speech, and Signal Processing, 2003. Proceedings. (ICASSP '03). 2003 IEEE International Conference on, 2003, pp. II-705-8 vol.2.

[5] M. Mofarreh-Bonab and S. A. Ghorashi, "*A low complexity and high speed gradient descent based secure localization in wireless sensor networks*," in Computer and Knowledge Engineering (ICCKE), 2013 3th International eConference on, 2013, pp. 300-303.

CHAPTER 7: FIELD TESTING ON A LIVE NETWORK

7.1 Overview

From previous chapters, we introduced an innovative algorithm and the NLOS mitigation method. This section presents a field-testing base on the mobile base stations network in a small and real residential area in Birmingham city. In the test area, experimenter, with a mobile terminal, will walk along an avenue and take the positioning reading by using the combination method.

This chapter is organised as follows: the main experimental device and parameters were introduced in Section 7.2. The experimental process, the calculation for the MS position finding and RMSE are shown in Section 7.3. A conclusion is presented in Section 7.4.

7.2 Experimental Environment and Parameters

7.2.1 Experiment Implementation

The experiment area cell network contains eight BSs, which belong to several mobile network operators. An avenue passes through this BS network. The experimenter walks along the avenue and takes measurements, at a standard sampling intervals, of the signal strength from the BSs around in order to obtain the distance between the MS and BSs. By calculating the positioning of the MS

in each sampling interval, the moving track of the experimenter is obtained.

In order to prevent the effect of system error, Monte-Carlo simulation is employed on this experiment. In each sampling interval, there are 50 sets of distance measurements taken. Additionally, we can compare the experiment positioning results with the true position of the MS to find out the RMSE.

7.2.2 Experiment Device

The mobile signal receiver tool is “SWGPRS023plus”, shown in Figure 7.1. The SWGPRS023+ is a convenient and low-cost hand-held tester for mobile network cells. We employ this device to get the BS’s site reference and the signal strength received.

Figure 7.1： Signal Tester - SWGPRS023+ [1]

7.2.3 Experiment Parameters

In this section, the parameters in the experiment are highlighted. The parameters include a map of the testing field, transmitting information of the BSs, location of the BSs and the moving path of the experimenter.

7.2.3.1 Map of Experiment Field

Figures 7.2 - 7.3 show the maps of the testing field. There are eight BSs set up in this area, which are shown as blue labels in the figures. The red path stands for the MS moving track.

Figure 7.2: Satellite Picture of Testing Field

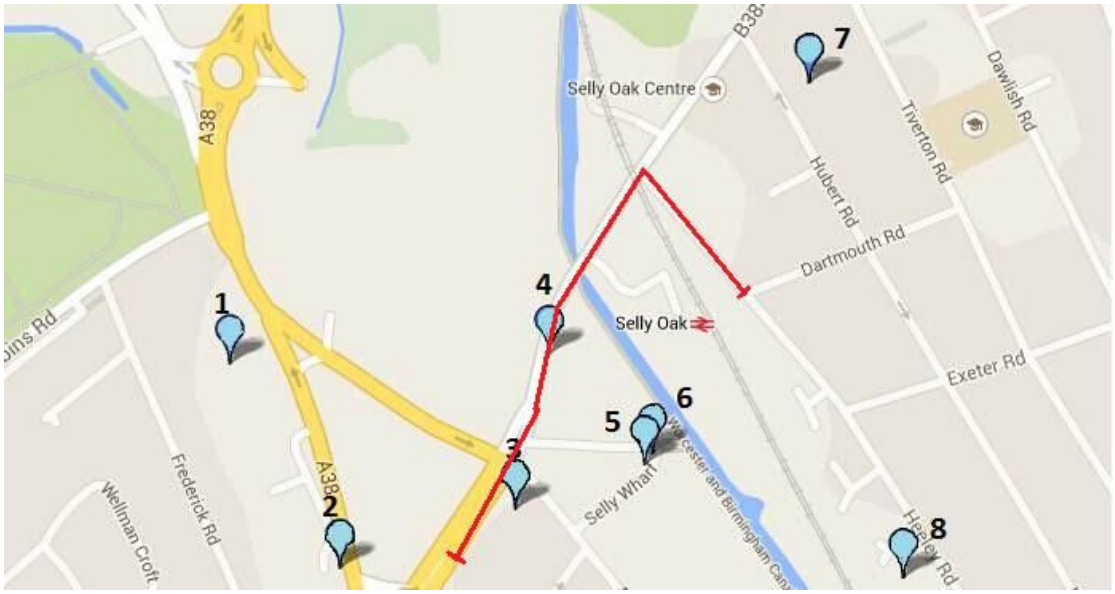

Figure 7.3: Map Layout of Test Field

7.2.3.2 Information of Base Stations

In this section, the information of each BS is presented in Table 7.1. The geographic-location details were measured using an iPhone GPS app. The conversion between geographic and Cartesian coordinates is provided by the software, “Geodetic to Cartesian Converter Online Tool”, as shown Figure 7.4:

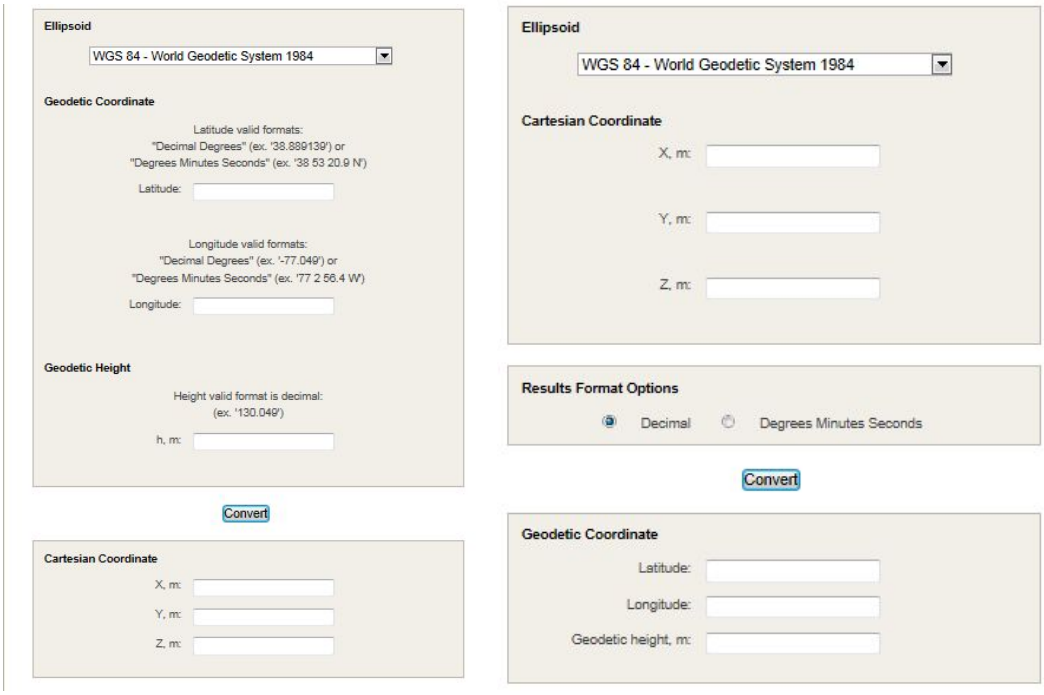

Figure 7.4: Geodetic - Cartesian Converter Online Tool [2]

The following Table 7.1 highlights the BSs' information [3] used for this experiment:

	BS1	BS2	BS3	BS4	BS5	BS6	BS7	BS8
Name of Operator	Airwave	O2	3	Orange	T-MOBILE	Vodafone	O2	O2
Operator Site Ref.	WMI078G	41522	B0061	WMD0736	53092	6059	11330	47674
Station Type	Macrocell	Macrocell	Macrocell	Macrocell	Macrocell	Macrocell	Macrocell	Macrocell
Height of Antenna	30 m	14 m	11 m	15 m	14 m	12 m	11.32 m	16.29 m
Frequency Range	400 MHz	2100 MHz	2100 MHz	1800 MHz	1800 MHz	900 MHz	900 MHz	2100 MHz
Transmitter Power	24 dBW	29 dBW	26.26 dBW	29.5 dBW	26 dBW	23.9 dBW	24 dBW	30 dBW
Latitude (N) Longitude (W)	52°26'29.75" 1°56'31.59"	52°26'23.09" 1°56'26.00"	52°26'26.13" 1°56'17.41"	52°26'30.02" 1°56'16.33"	52°26'27.06" 1°56'11.59"	52°26'27.37" 1°56'11.40"	52°26'38.34" 1°56'03.79"	52°26'22.23" 1°55'58.95"
X	3893970.89893556	3894145.49612461	3894072.27901395	3893976.4816862	3894050.77766566	3894043.30796762	3893778.28937047	3893781.37421528
Y	-132041.330941749	-131941.593057557	-131776.756558464	-131753.102585464	-131666.025811558	-131662.187454391	-131509.403750897	-131418.034766376

Table 7.1: Information of Base Stations

Since the algorithm was built on 2D Cartesian coordinates, the geographic measurements should be converted to Cartesian coordinates.

7.3 Position Finding Process

7.3.1 Radio Propagation Modelling for COST 231-Walfish-Ikegami Model

This model is the Walfisch-Ikegami-Bertoni model, a COST project revised into a COST 231-Walfisch-Ikegami model [4]. The model was built with consideration of the reflection between buildings in urban environments. With the help of Hemani's research [5], the signal propagates in this area is fit for the COST

231-Walfisch-Ikegami model.

The COST 231 model was adapted for a transmitter frequency range from 800 MHz to 2 GHz, and was designed with a BS heighted from 4m to 50 m and cell sizes up to 5 km. The LOS case is approximated by a model using free-space approximation up to 20 m and the following beyond:

$$L_{Loss} = P_{\text{Transmitte r Power}} - P_{\text{Re ceivePower}} = 42.6 + 26 \log(d) + 20 \log(f/1MHz) \quad \text{for } d>20m \tag{7.1}$$

where L represents free space loss, f is the frequency range and d is the propagating distance, which can approximate the distance between the BS and the MS. Therefore, we have the distance measurement as follows:

$$d = 10^{\frac{L_{loss} - 42.6 - 20\log(f/1MHz)}{26}} \tag{7.2}$$

Then, we can get:

$$d = 10^{\frac{P_{\text{Transmitte r Power}} - P_{\text{ReceivePower}} - 42.6 - 20\log(f/1MHz)}{26}} \tag{7.3}$$

Based on Equation (7.3), the experiment only needs to take the measurements of $P_{ReceivePower}$, in order to have the distances to start the location algorithm calculation.

Therefore, the following Table 7.2 gives the inputs and output of this experiment.

Inputs		Output
Known	**Measured**	
Transmitter Power (dBW)	Received Power (dBW)	Distance between
Frequency Range (MHz)		BS and MS (m)

Table 7.2: Input and Output of the Experiment

7.3.2 Position Finding Result

In this experiment, there are 11 sampling intervals during the whole MS movement. In each sampling interval, the experimenter measured the signal strength between the MS to each BS, with each BS repeated 50 times giving 50 sets of distance measurements. The MS position was estimated 50 times based on the experimental data. The current possible position of the MS would be made up by the average of the 50 estimations. The average signal strength and distance measurements are shown in Table 7.3:

Average Signal Strength and Distance Measurements in 1st Sampling Interval								
BS	**BS1**	**BS2**	**BS3**	**BS4**	**BS5**	**BS6**	**BS7**	**BS8**
Signal Strength	-54.3608 dBW	-54.5845 dBW	-54.8022 dBW	-58.8425 dBW	-63.3558 dBW	-59.7964 dBW	-70.4605 dBW	-69.6477 dBW
d	236.5m	104.9m	83.9m	180m	196.9m	203.3m	527.4m	435.1m
Average Signal Strength and Distance Measurements in 2nd Sampling Interval								
BS	**BS1**	**BS2**	**BS3**	**BS4**	**BS5**	**BS6**	**BS7**	**BS8**
Signal Strength	-54.2601 dBW	-60.7565 dBW	-51.1473 dBW	-52.1828 dBW	-60.522 dBW	-56.8206 dBW	-68.6357 dBW	-69.3372 dBW
d	234.4m	181.2m	60.7m	99.8m	153.2m	156.2m	448.7m	423.3m

Average Signal Strength and Distance Measurements in 3rd Sampling Interval								
BS	**BS1**	**BS2**	**BS3**	**BS4**	**BS5**	**BS6**	**BS7**	**BS8**
Signal Strength	-55.4348 dBW	-63.2861 dBW	-53.4907 dBW	-45.4343 dBW	-58.4487 dBW	-54.5635 dBW	-67.4284 dBW	-68.8855 dBW
d	260.1m	226.7m	74.7m	54.9m	127.5m	127.9m	403.2m	406.7m
Average Signal Strength and Distance Measurements in 4th Sampling Interval								
BS	**BS1**	**BS2**	**BS3**	**BS4**	**BS5**	**BS6**	**BS7**	**BS8**
Signal Strength	-57.1624 dBW	-65.6544 dBW	-57.8400 dBW	-35.4123 dBW	-56.2671 dBW	-51.9195 dBW	-65.8693 dBW	-68.2341 dBW
d	303.1m	279.6m	109.8m	22.6m	105.1m	101.2m	351.2m	383.9m
Average Signal Strength and Distance Measurements in 5th Sampling Interval								
BS	**BS1**	**BS2**	**BS3**	**BS4**	**BS5**	**BS6**	**BS7**	**BS8**
Signal Strength	-56.7605 dBW	-67.4880 dBW	-63.6081 dBW	-46.8258 dBW	-62.2985 dBW	-57.9806 dBW	-64.4165 dBW	-69.9852 dBW
d	292.5m	328.9m	183m	62.1m	179.3m	173.1m	308.8m	448.3m
Average Signal Strength and Distance Measurements in 6th Sampling Interval								
BS	**BS1**	**BS2**	**BS3**	**BS4**	**BS5**	**BS6**	**BS7**	**BS8**
Signal Strength	-58.2991 dBW	-68.7595 dBW	-65.1997 dBW	-51.0804 dBW	-62.51.7 dBW	-58.0845 dBW	-62.7190 dBW	-70.9895 dBW
d	335.2m	368.1m	210.7m	90.2m	182.7m	174.7m	265.7m	490m
Average Signal Strength and Distance Measurements in 7th Sampling Interval								
BS	**BS1**	**BS2**	**BS3**	**BS4**	**BS5**	**BS6**	**BS7**	**BS8**
Signal Strength	-60.9607 dBW	-71.9201 dBW	-70.2692 dBW	-60.6207 dBW	-67.5458 dBW	-63.1664 dBW	-57.2017 dBW	-71.1064 dBW
d	424.3m	487m	330.1m	210.7m	283.6m	274m	163m	495.1m
Average Signal Strength and Distance Measurements in 8th Sampling Interval								
BS	**BS1**	**BS2**	**BS3**	**BS4**	**BS5**	**BS6**	**BS7**	**BS8**
Signal Strength	-61.6498 dBW	-72.3188 dBW	-70.6492 dBW	-61.3672 dBW	-67.5512 dBW	-63,2321 dBW	-55.1486 dBW	-70.8013 dBW
d	451m	504.5m	341.4m	225.1m	285.5m	275.6m	135.9m	481.9m
Average Signal Strength and Distance Measurements in 9th Sampling Interval								
BS	**BS1**	**BS2**	**BS3**	**BS4**	**BS5**	**BS6**	**BS7**	**BS8**
Signal Strength	-61.9731 dBW	-72.0309 dBW	-69.8652 dBW	-60.6475 dBW	-65.9748 dBW	-61.5806 dBW	-55.3462 dBW	-69.4830 dBW
d	464.1m	491.8m	318.5m	211.2m	248.3m	238.1m	138.3m	428.8m

Average Signal Strength and Distance Measurements in 10th Sampling Interval								
BS	**BS1**	**BS2**	**BS3**	**BS4**	**BS5**	**BS6**	**BS7**	**BS8**
Signal Strength	-61.4757 dBW	-70.5879 dBW	-67.1444 dBW	-57.7431 dBW	-61.3942 dBW	-56.7553 dBW	-60.2015 dBW	-67.1966 dBW
d	444.1m	432.8m	250.3m	163.3m	165.5m	155.3m	212.6m	350.2m
Average Signal Strength and Distance Measurements in 11th Sampling Interval								
BS	**BS1**	**BS2**	**BS3**	**BS4**	**BS5**	**BS6**	**BS7**	**BS8**
Signal Strength	-61.5895 dBW	-70.4011 dBW	-66.7168 dBW	-57.7776 dBW	-60.2688 dBW	-55.5600 dBW	-61.0455 dBW	-66.4777 dBW
d	448.6m	425.7m	241m	163.8m	149.8m	139.7m	229.1m	328.6m

Table 7.3: Average Signal Strength and Distance Measurements

Based on the experimental data, shown in Table 7.3, we can substitute data for implementing the combination method in Chapters 3 and 6 to find the estimated position of the MS. Then, we can use the Geodetic - Cartesian Converter online tool to convert the Cartesian coordinate into a geographic coordinate and mark on the map to present the estimated moving track of the experimenter. The true position and the estimated position of the MS moving track are shown in Table 7.4.

True Position of Each Sampling Interval		Estimated Position of Each Sampling Interval		Error
Latitude	**Longitude**	**Latitude**	**Longitude**	
52°26′25.08″ N	1°56′19.78″ W	52°26′25.14″ N	1°56′21.56″ W	33.5m
52°26′27.05″ N	1°56′17.56″ W	52°26′27.52″ N	1°56′19.69″ W	42.6m
52°26′27.69″ N	1°56′17.19″ W	52°26′28.53″ N	1°56′17.92″ W	29.3m
52°26′28.52″ N	1°56′16.88″ W	52°26′29.49″ N	1°56′15.50″ W	39.6m
52°26′31.38″ N	1°56′16.15″ W	52°26′32.03″ N	1°56′16.51″ W	21.1m
52°26′32.71″ N	1°56′14.46″ W	52°26′35.13″ N	1°56′14.10″ W	75.1m
52°26′34.08″ N	1°56′12.59″ W	52°26′36.24″ N	1°56′11.73″ W	68.6m
52°26′34.85″ N	1°56′10.76″ W	52°26′36.26″ N	1°56′10.15″ W	45.0m
52°26′34.07″ N	1°56′09.85″ W	52°26′34.86″ N	1°56′08.41″ W	36.4m
52°26′33.11″ N	1°56′08.39″ W	52°26′32.03″ N	1°56′08.30″ W	33.4m
52°26′32.06″ N	1°56′06.97″ W	52°26′31.36″ N	1°56′07.91″ W	27.9m

Table 7.4: Results of Wireless Location Experiment

Based on the experiment results in Table 7.4, we can mark the position of each sampling interval on the map, and build up the moving track of the MS. Figure 7.5 shows both the true and estimated moving paths of the MS on the map. The yellow dots on the map are the true positions of samplings and the red path gives the moving track of the MS along the road. The blue dots and green line are the estimated positions and track of the MS.

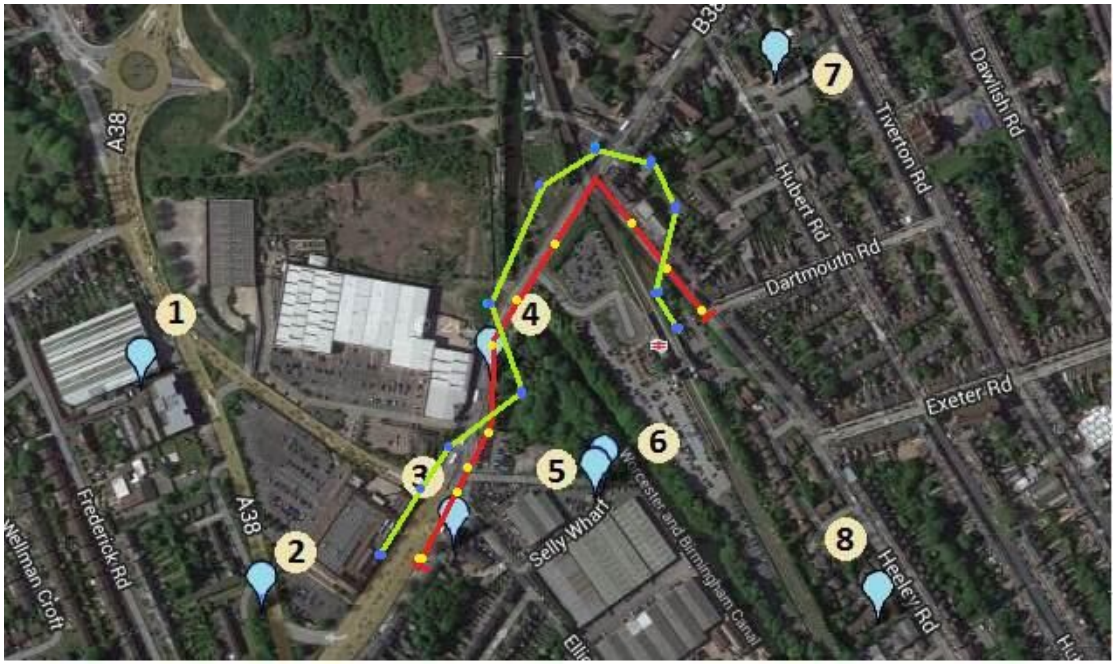

Figure 7.5: True and Estimated Moving Track of MS in Map

From Figure 7.5, although the test result has some errors, the algorithm location quality is good. By using the innovative algorithm introduced in previous chapters, we can approximately trace the MS's movement in a real environment. The errors are caused by the following factors:

- NLOS effect – NLOS bias cannot be avoided, particularly in estimating position in an urban corridor environment. In the experiment, when the experimenter took the measurements for the sixth and seventh sampling, the MS was just moving under a bridge, which caused two whole sets of measurements to be corrupted by a NLOS error. Without a LOS propagation as a reference, the NLOS mitigation method became inefficient. Therefore, the location quality is not as good as in other sets of sampling.
- Network topology irregular – as discussed in Chapter 4, the topology of the

network did affect location accuracy. The topology, shown in Figure 7.5, is irregular. This kind of random shape topology brings the negative influence into predicting the position of an MS which is passing through the network.

- Received signal strength employed – because of the limited conditions, experiment employed RSS for distance measuring. As Chapter 1 discussed, RSS-based positioning accuracy is usually much poorer than using TDOA measuring devices. Especially in an urban environment, with long-distance estimation, RSS-based positioning accuracy becomes worse because such cases correspond to the flat tail area of the log-shaped pass-loss curve.

7.4 Conclusion

In this section, an experiment on the innovative algorithm employed for wireless positioning in the real word is introduced. As shown in the results, the algorithm gives good location accuracy quality which achieves the E911 and E112 requirements.

7.5 Reference

[1]http://www.sequoia.co.uk/siretta-swgprs023-gsm-gprs-signal-strength-tester_p_1475.php

[2] http://www.apsalin.com/convert-geodetic-to-cartesian.aspx

[3] http://sitefinder.ofcom.org.uk/

[4] Hemant Kumar Sharma, Santosh Sahu, Sanjeev Sharma, ”*Enhanced Cost231 W.I.*

Propagation Model in Wireless Network", in International Journal of Computer Applications, April 2011, Number 6 - Article 7

[5] S. Hemani, M. Oussalah and P. Hall, "*GSM mobile positioning using kalman filter for sector antennas*," in Cybernetic Intelligent Systems, 2008. CIS 2008. 7th IEEE International Conference on, 2008, pp. 1-6.

CHAPTER 8: CONCLUSION AND FUTURE WORK

8.1 CONCLUSION

With the substantial increase of location-based services, which includes E911 emergency services where the user is tracked with high accuracy using only the telecom operator's cellular wireless network structure, the emergence of location-based social networking applications in, e.g. MySpace and Facebook, the interest in wireless localisation techniques has grown dramatically in the last 20 years.

In this thesis, several available localisation techniques have been reviewed in Chapter 1. This includes Time-of-Arrival (TOA), Angle-of-Arrival (AOA), Time-Difference of Arrival (TDOA) and Received-Signal Strength (RSS). TOA is highly dependent on a synchronised location system, and the range measurements can be highly accurate. As the difficulty and cost of a synchronised location system is high, TOA systems have gradually been replaced by TDOA systems. The latter is recognised for its high efficiency and precision. Indeed, TDOA only requires a synchronised system with a clock at the transmitter stations. Therefore, TDOA is commonly employed in GSM and CDMA systems, unlike AOA systems where a large antenna array is required. On the other hand, RSS methods, which only rely on the signal strength received from the BSs, are less demanding as they neither require infrastructure

changes nor additional hardware components, presenting a cheap technology for reasonable positioning accuracy levels.

The main importance in wireless location accuracy is the signal propagation channel quality. As we discussed in this thesis, if the signal transmits between the MS and BS along an LOS path, we can approach location estimation with excellent quality, but in an NLOS scenario, NLOS will cause a positive bias, adding to the TOA measurements. Hence, the research mainly contains two sections based on the signal propagation in LOS or NLOS.

Based on the two main directions of study, we reviewed existing location algorithms in the LOS transmitting environment. More specifically, Fang, approximated least square solutions, MLE, and Chan's and Taylor's methods were introduced in Chapter 2. After comparing the algorithms in the same simulation platform, the thesis presents the limitation of each algorithm and the programme running time. As a result, the thesis gives the strengths and weaknesses of the algorithms in each particular situation, and gives the tendentious choice of algorithm used in each particular scenario.

According to the comparison between such approaches, we distinguish the Taylor-based approximation and Chan's-based approach which provide an approximate solution to the underlying hyperbolic equations. Chapter 3 suggests

a linear combination of the two estimators that minimises the variance. For Taylor's estimator, it is acknowledged that when the initial guess is close to the true estimate, then Taylor's approach provides quite high accuracy. Similarly, when the number of BS measurements is greater than four, Chan's algorithm provides an approximate solution, but the accuracy relies on the quality of the a priori information employed to solve the underlying MLE. Consequently, a combination of the two estimators is worth considering. Intuitively, a possible scenario of a combination of the two estimators consists of using Chan's estimator to initialise Taylor's estimator. With a comparison of the innovative combination method and existing algorithms, the new method gives better performance in stability, low variance, and noise mitigation and location accuracy level.

Most of the literature survey investigated the performance of localisation algorithms, regardless of the sensor infrastructure disposition, although in GSM and UMTS networks it is acknowledged that the antenna positioning problem (APP) is a major design issue for any mobile operator. It is universally agreed that several factors influence such design. This includes the (expected) traffic, types of antenna, allocated frequencies, interference, coverage and infrastructure nearby, among others. Unfortunately, less work from a wireless positioning accuracy perspective has been done, although this would

significantly contribute towards the E911, for instance. This motivates the current work where some commonly employed techniques involving TDOA and TOA technology are contrasted and investigated with respect to the geometrical disposition of the antennas. In Chapter 4, we discussed the least square solutions, MLE, Chan's, Taylor's and a newly introduced combination of Chan-Taylor, and compared them when considering several antenna topologies. The latter includes linear, circular, u-shaped and balanced shapes. Such topology can straightforwardly be inferred from regular (optimal) cellular disposition when blocking occurs, disabling some BSs.

After discussing the substance and comparisons between the advantages and disadvantages of both the classic and innovative algorithms in LOS scenarios, we face the practical problem of NLOS, an unavoidable error which dramatically affects location accuracy in a real world application. Chapters 5 and 6 explored NLOS mitigation algorithms to limit the impact of the NLOS bias. Some classic NLOS mitigation methods, like constrained least square, geometry constrained, robust estimator and iterative algorithms, are shown in Chapter 5. Through simulation in complexity analysis comparisons, respectively and together, we can clearly understand the advantages and limitations of each algorithm. Then, in Chapter 6, based on the research of existing algorithms, the combination method, with an NLOS mitigation function, is carried out, named the Gradient

Descent Iteration – Combination (GDIC) method. Compared with existing NLOS mitigation, this new algorithm integrates both the accuracy of iteration methods and the simplicity of constrained methods. In both LOS and NLOS scenarios, GDIC gives a wonderful performance in location accuracy.

After theoretical simulations on various kinds of positioning method, in Chapter 7, a real word experiment was held in Birmingham City. This experiment is based on the combination method and the GDIC method, which are the results of this thesis. The experiment performed wireless location in an MS moving situation in an urban corridor environment. The experiment result presents the reliability of the innovative method persuasively and the development prospect for wireless location technology.

8.2 Future Work

The next steps of research on this topic are dedicated to NLOS-identification technology. As discussed in Chapters 5 and 6, if there are BSs to provide distance measurements, one of the most effective techniques to avoid the NLOS influence is to identify those measurements with NLOS corruption and discard them from the positioning calculation. This part of the research would be prior to the positioning calculation. Therefore, this research should be dedicated to algorithms that can accurately and quickly identify NLOS ability and should work

well with existing location algorithms.

In addition, the wireless indoor techniques are also the one of future research directions which is full of challenges. These techniques have been greatly expected in many applications such as asset tracking and inventory management. Based on the complex indoor environment, the positioning techniques are focus on solving the NLOS problem. So far as we know, some of robust position estimation methods are put forward on the RF-based distance measurements and indoor signal propagation channel modelling. However, the innovative position algorithms are still needed for increasing the indoor positioning accuracy. Furthermore, the indoor positioning research can also try on the technology combination, such as wireless technology combines with optical technology.

How to integrate the outdoor and indoor wireless positioning techniques can be another direction of research. The integration can encourage the industrial to develop the robust detection systems and powerful wireless positioning devices.

Appendix

Combination of Taylor and Chan method in Mobile Positioning

Hao Li M. Oussalah

University of Birmingham, EECE

Edgbaston, B15 2TT, Birmingham, UK

Abstract

Due to increase in location based services, the need for efficient network based location methods has been made of paramount of importance. Among the mobile positioning techniques Time of Arrival (TOA) and Time Difference of Arrival (TDOA) arisen as promising techniques. In order to deal with such technology some theoretical approaches have been put forward to draw the estimation under the technological constraints. Among such approaches, one distinguish the Taylor based approximation and Chan's based approach which provide an approximate solution of the underlying hyperbolic equations. This paper reviews the above approaches and suggests a linear combination of the two estimators that minimize the variance. Simulation platform has been developed to test and compare the performances of these estimators. The result of simulation and actual measurement indicated that the method has high positioning accuracy both in ideal environment and actual measurement.

Keywords: *TOA; TDOA; Position accuracy, linear estimation, fusion*

1. Introduction

Motivated by the E-911 regulation [3] which forces the wireless operators to provide the location of the mobile unit making an emergency call within a circle of radius of no more than 125 meters in at least 67 percent of all cases, the research in mobile positioning, that enables the operators to meet the FCC requirements in cost effective way, has been very active in the last two decades.

Automated position determination will also help in providing emergency road-side services quickly and efficiently. Position location systems may also be very helpful in fleet management and can be used for traffic routing and scheduling of vehicles in real time [1]. There can also be a number of potential applications of position location systems for in-car navigation systems and for direction finding from known position to given destinations. Typically, two streams of approaches contrast depending whether the positioning occurs at mobile station level or base station/operator level.

For the former the location technology based on Time of Arrival (TOA) and Time difference of arrival (TDOA) has been proven to be widely acceptable for wireless location purposes by many operators [1,3,6]. In this course, the travelled time of signal from the mobile station (MS) to the Base Station (BS) is measured to determine, in turn, the distance from MS to BS according to the velocity of

electromagnetic wave .This called the TOA. Strictly speaking, the absolute time of arrival for the signal from the handset to the base stations can be estimated in many ways. If the handset is able to stamp the current time on any outgoing signal, the base station can determine the time that the signal takes to reach the base station. Hence, the distance between the mobile and the base station can be determined. If at least three different receivers can receive the signal from the mobile, the position of the mobile can be found. However, this requires a very accurate timing reference at the
mobile which would need to be synchronized with the clock at the base stations, which adds some burden cost to the handset. Another modified handset technique, based on finding TDOAs has been proposed for CDMA systems [1]. This method uses the pilot tones from different base stations. In CDMA systems, the pilot tone transmitted by each cell is used as a coherent carrier reference for synchronization by every mobile in that cell coverage area. The pilot tone is transmitted at a higher power level than the other channels, thus allowing extremely accurate tracking. Each cell site transmits the same Pseudo Noise (PN) code in its reference channel with a unique code phase. This enables the mobile to differentiate each cell site's pilot tone. The mobile measures the arrival time differences of at least three pilot tones transmitted by three different cells. By intersecting hyperbolas the mobile's position can be estimated.

From the base station perspective, which would provide solutions applicable to all handsets, the time of arrival technique is very commonly employed. This may be done by measuring the time in which the mobile responds to an inquiry or an instruction transmitted to the mobile from the base station. The total time elapsed from the instant the command is transmitted to the instant the mobile response is detected, is composed of the sum of the round trip signal delay and any processing and response delay within the mobile unit. If the processing delay for the desired response within the mobile is known with sufficient accuracy, it can be subtracted from total measured time, which would give us the total round-trip delay. Half of that quantity would be an estimate of the signal delay in one direction, which would give us the approximate distance of the mobile from the base station. If the mobile response can be detected at two additional receivers then the position can be fixed by the triangulation method. However, it is also noticed that such approach is still limited if non-light of sight situations occur because of the multiple signal reflexions.

Another approach consists of using the TDOA. In the latter, the signal can be estimated by two general methods: subtracting TOA measurements from two base stations to produce a relative TDOA, or through the use of cross-correlation techniques, in which the received signal at one base station is correlated with the received signal at another base station. Especially, this can provide increased accuracy when errors due to multiple signal reflections in pairs of TOA measurements are positively correlated because of having a common signal reflector. The more similar the errors in pairs of TOAs are, the more we can gain by changing them into TDOAs. However, this is practical only when we can estimate the TOA by having knowledge of the time of transmission. If we have no timing reference at the transmitter, then this method for estimating TDOAs cannot be used. Once the TDOA estimates have been obtained, they are converted into range difference measurements and these measurements can be converted into nonlinear hyperbolic equations. As these equations are non-linear, solving them is not a trivial operation. Several algorithms have been proposed for this purpose having different complexities and accuracies. Here, we will discuss some mathematical models used by these algorithms.

2. Mathematical Models for Hyperbolic TDOA Equations

Let us consider a general model for the two dimensional (2-D) estimation of a source, consisting of mobile station with Cartesian coordinates (x, y) using M base stations of known location (X_i, Y_i), i=1 to M. Assume without loss of generality that the first base (X_1, Y_1) is the servicing base station so that all TDOA measurements will be measured with respect to the servicing base station. The direct distance R_i from the mobile station to the i^{th} base station is given as

$$R_i^2 = (X_i - x)^2 + (Y_i - y)^2 \quad (1)$$

$$= K_i^2 - 2X_i x - 2Y_i y + x^2 + y^2 \quad (2)$$

With

$$K_i^2 = X_i^2 + Y_i^2 \quad (3)$$

Let $R_{i,1} = R_i - R_1$ be the distance difference to mobile station between the servicing base station and the ith base station. Similarly, one denotes $X_{i,1} = X_i - X_1$ and $Y_{i,1} = Y_i - Y_1$. The covariance of the vector $[R_2 - R_1 \;\; R_3 - R_1 \ldots R_M - R_1]$ is denoted

$$Q = \begin{pmatrix} \sigma_2^2 & 0 & 0 & \ldots 0 \\ 0 & \sigma_3^2 & 0 & \ldots 0 \\ . & & & \\ 0 & 0 & 0 & \ldots \sigma_M^2 \end{pmatrix}$$

The measured TDOA, denoted $\tau_{i,1}$, from the i^{th} base station to the mobile station is such that

$$R_{i,1} = c.\tau_{i,1}, \quad (4)$$

where c stands for the signal propagation speed, corresponding to speed of light, e.g., c = 3.10^8 m/s.

Substituting expressions of R_i and R_1 into $R_{i,1}$ yields

$R_{i,1} = R_i - R_1 = \sqrt{(X_i - x)^2 + (Y_i - y)^2} - \sqrt{(X_1 - x)^2 (Y_1 - y)^2}$ (5) Therefore

$$R_{i,1}^2 = K_i^2 - K_1^2 - 2\left((X_i - X_1)x + (Y_i - Y_1)y + R_{i,1}R_1\right) \quad (6)$$

(6) can be written in matrix form as

$$G_i^T h = F_i \quad (7)$$

With

$G_i = \left[X_i\text{-}X_1 \;\; Y_i\text{-}Y_1 \;\; R_{i,1} \right]^T$, $F_i = -\frac{1}{2}\left(R_{i,1}^2 - (K_i^2 - K_1^2)\right)$, $h = [x \;\; y \;\; R_1]^T$

(8)

System of equations (7), for i=2 to M, yields a nonlinear (hyperbolic) system in (x, y) whose solution gives the position of the mobile station in 2-D space. Especially, when the number of measurements is larger than 3, this leads to a set of redundant equations whose solution requires some optimization based approach, especially when the variance-covariance of the measurements is taken into account.
Two solutions of the above system will be highlighted. The former is based on Taylor linearization [5] while the second is referred to as Chan's method [2].

3 Taylor expansion method

The Taylor-series method linearizes the set of equations in (7) by Taylor-series expansion, then uses an iterative method to solve the system of linear equations. The iterative method begins with an initial guess and improves the estimate at each iteration by determining the local linear least-square (LS) solution. The Taylor-series can provide accurate results and is robust. It can also make use of redundant measurements to improve the PL solution. However, it requires a good initial guess and can be computationally intensive. For most situations, linearization of the nonlinear equations does not introduce undue errors in the position location estimate. However, linearization can introduce significant errors when determining a PL solution in bad geometric dilution of precision (GDOP) situations. GDOP describes a situation in which a relatively small ranging error can result in a large position location error because the mobile is located on a portion of hyperbola far away from both receivers. It has been shown that eliminating the second order terms can lead to significant errors in this situation. The effects of linearization of hyperbolic equations on the position location solution have also been explored elsewhere.
More specifically, With a set of TDOA estimates, the method starts with an initial guess (x_0; y_0) of the unknown mobile position (x, y), and computes the deviations of the position location estimation

$$\delta = \begin{bmatrix} \Delta x \\ \Delta y \end{bmatrix} = \left(G_t^{\,T} Q^{-1} G_t \right)^{-1} G_t^{\,T} Q^{-1} h_t \tag{9}$$

With

$$h_t = \begin{bmatrix} R_{2,1} - \left(R_1 - R_2 \right) \\ R_{3,1} - \left(R_1 - R_3 \right) \\ . \\ R_{M,1} - \left(R_1 - R_M \right) \end{bmatrix} \tag{10}$$

$$G_t = \begin{bmatrix} \frac{X_1 - x}{R_1} - \frac{X_2 - x}{R_2} & \frac{Y_1 - y}{R_1} - \frac{Y_2 - y}{R_2} \\ \frac{X_1 - x}{R_1} - \frac{X_3 - x}{R_3} & \frac{Y_1 - y}{R_1} - \frac{Y_3 - y}{R_3} \\ . & \\ . & \\ \frac{X_1 - x}{R_1} - \frac{X_M - x}{R_M} & \frac{Y_1 - y}{R_1} - \frac{Y_M - y}{R_M} \end{bmatrix} \quad (11)$$

The solution is elaborated as follows:

- Initialize (x, y) as with x= X_0; y= Y_0.
- Use expression (9) to calculate variations Δx and Δy.
- In the next recursion use $x = X_0 + \Delta x$ and $y = Y_0 + \Delta y$
- Repeat the steps above until Δx and Δy get smaller than some threshold α: $|\Delta x| + |\Delta y| < \alpha$

The variance-covariance matrix of the estimate is

$$P_{Taylor} = \left(G_t{}^T Q^{-1} G_t \right)^{-1} \quad (12)$$

The Taylor-series method can provide accurate results, however, it requires a close initial guess (x0; y0) to guarantee convergence and can be computationally intensive.

3. Chan's method

This is a non-iterative solution to the hyperbolic position estimation problem which is capable of achieving optimum performance for arbitrarily placed sensors. When TDOA estimation errors are small, this method is an approximation to the maximum likelihood (ML) estimator

Following Chan's method [2], for a three base station system (M=3), producing two TDOA's, x and y can be solved in terms of R1 from (2.33). The solution is in the form of

$$\begin{bmatrix} x \\ y \end{bmatrix} = \begin{bmatrix} X_{2,1} & Y_{2,1} \\ X_{3,1} & Y_{3,1} \end{bmatrix}^{-1} \left(\begin{bmatrix} R_{2,1} \\ R_{3,1} \end{bmatrix} R_1 + \frac{1}{2} \begin{bmatrix} R_{2,1}^2 + K_1{}^2 - K_2{}^2 \\ R_{3,1}^2 + K_1{}^2 - K_3{}^2 \end{bmatrix} \right) \quad (13)$$

Substituting R_1 in the above equation yields a quadratic equation in R_1, where by choosing a positive and some common sense solution (e.g., solution lying within some radius) yields a correct and a unique solution in terms of (x,y).

In case where we have redundant measurements (more than three dataset), an optimization approach is required to find a single solution, which, in anyway, is only an approximated solution. For this purpose, first an approximation of the solution can be provided by

$$\begin{bmatrix} x \\ y \\ R_1 \end{bmatrix} = \left(G_a{}^T Q^{-1} G \right)^{-1} G_a{}^T Q^{-1} h_a \qquad (14)$$

With

$$G_a = -\begin{bmatrix} X_{2,1} & \mathrm{Y}_{2,1} & \mathrm{R}_{2,1} \\ X_{3,1} & \mathrm{Y}_{3,1} & \mathrm{R}_{3,1} \\ . & & \\ X_{M,1} & \mathrm{Y}_{M,1} & \mathrm{R}_{M,1} \end{bmatrix} \qquad (15)$$

And

$$h_a = \frac{1}{2}\begin{bmatrix} R_{2,1}^2 + K_1{}^2 - K_2{}^2 \\ R_{3,1}^2 + K_1{}^2 - K_3{}^2 \\ . \\ R_{M,1}^2 + K_1{}^2 - K_M{}^2 \end{bmatrix} \qquad (16)$$

Let us denote by $R_{i,1}^0$ the noise free measurement from $R_{i,1}$; namely, $R_{i,1} = R_{i,1}^0 + n_{i,1}$, where $n_{i,1}$ stands for zero mean Gaussian noise, while the noise vector n has a known variance-covariance matrix Q, which allow full noise reconstruction. This yields the following:

$$R_{i,1} = R_i^0 - R_1^0 + n_{i,1} \quad \text{(i=2 to M)} \qquad (17)$$

Or equivalently,

$$R_i^0 = R_{i,1} + R_1^0 - n_{i,1} \quad \text{(i=2 to M)} \qquad (18)$$

Denote

$$B = \begin{pmatrix} R_1^0 & 0 & 0 .. & 0 \\ 0 & R_2^0 & 0 & ..0 \\ . & & & \\ 0 & 0 & ..0 & R_M^0 \end{pmatrix}$$

A second update of estimation in (14) is given by

$$\begin{bmatrix} x \\ y \\ R_1 \end{bmatrix} = \left({G_a}^T \Psi^{-1} G \right)^{-1} {G_a}^T \Psi^{-1} h_a \qquad (19)$$

With

$$\Psi = c^2 B Q B \qquad (20)$$

On the other hand, using the covariance matrix

$$\mathrm{cov}([x \;\; \mathrm{y}\, R_1]^T) \approx (G_a \Psi^{-1} G_a)^{-1}, \qquad (21)$$

One can construct the noise free estimate of x, y and R_1; namely,

$$x = x^0 + v_x, \; \mathrm{y} = y^0 + v_y, \; \mathrm{R}_1 = R_1^0 + v_r, \qquad (22)$$

Where v is zero-mean Gaussian noise with variance-covariance matrix given by expression (21), and [x y R_1] is provided by (19)

Let

$$S = \begin{pmatrix} x^0 - x_1 & 0 & 0 \\ 0 & \mathrm{y}^0 - y_1 & 0 \\ 0 & 0 & R_1^0 \end{pmatrix} \qquad (23)$$

Then, the final estimate is given by

$$\begin{bmatrix} x \\ y \end{bmatrix} = \begin{bmatrix} x_1 \\ y_1 \end{bmatrix} \pm \left(\left(G^T \psi^{-1} G \right)^{-1} G^T \psi^{-1} H \right)^{1/2} \qquad (24)$$

And its associated variance-covariance

$$P_{Chan} = \mathrm{cov}\left([x \;\; \mathrm{y}]^T \right) \approx c^2 (B' G^T S^{-1} G^T B^{-1} Q^{-1} B^{-1} G . S^{-1} G . B')^{-1}$$

(25)

With

$$G = \begin{bmatrix} 1 & 0 \\ 0 & 1 \\ 1 & 1 \end{bmatrix} \qquad (26)$$

$$\psi = 4S(G_a \Psi^{-1} G_a)^{-1} S \qquad (27)$$

$$H = \begin{bmatrix} (x - x_1)^2 \\ (y - y_1)^2 \\ R_1^2 \end{bmatrix} \quad (28)$$

$$G_a' = \begin{bmatrix} 1 & 0 \\ 0 & 1 \\ 1 & 1 \end{bmatrix} \quad (29)$$

$$z_a = \begin{bmatrix} (x - x_1)^2 \\ (y - y_1)^2 \end{bmatrix} \quad (30)$$

$$B' = \begin{bmatrix} x^0 - x_1 & 0 \\ 0 & y^0 - y_1 \end{bmatrix} \quad (31)$$

4. Combination of Chan's and Taylor's hyperbolic estimators

The idea of combining the Taylor's and Chan's estimators looks quite appealing. Indeed, although, it is quite acknowledged that once the initial guess is close to true estimate, then, provided the complexity issue is not a big issue, Taylor's approach provides quite good result. Similarly, when the number of measurements is greater than four, then Chan's algorithm only provides an approximate solution whose accuracy relies on the quality of the *a priori* information employed to solve the underlying maximum likelihood estimator. Consequently, a combination between the two estimators is worth considering. Intuitively, a possible scenario of combination of the two estimators consists of using the Chan's estimator to initialize Taylor's estimator. Nevertheless, one shall consider a combined estimate which minimizes the variance in the light of pioneer work of Franklin and Graybilland [4].

Typically, let Z_1 and Z_2 be the estimates using Taylor and Chan's approach, respectively. The new estimate Z is given as a linear combination of the above two estimates and unbiased; namely,

$$Z = \lambda_1 Z_1 + \lambda_2 Z_2 \quad (32)$$

Using the fact that the estimators are unbiased and the linearity of the expectation, we have

$$E[Z] = \lambda_1 E[Z_1] + \lambda_2 E[Z_2] \quad (33)$$

This yields

$1 = \lambda_1 + \lambda_2$, or, equivalently, $\lambda_1 = 1 - \lambda_2$

The rational behind the preceding is to assume that the two previous estimators only provide approximate estimate of the true solution, which, can be reached asymptotically. This justifies the fact the two estimators have the same mean on average as the combined estimator Z.

As for the variance covariance matrix, using (32), we have

$\mathrm{Var}(Z) = E[(Z - E[Z])^2] = E[(Z - E[Z])^2]$

$$= E\left[\left(\lambda_1 Z_1 + \lambda_2 Z_2 - E\left[\lambda_1 Z_1 + \lambda_2 Z_2\right]\right)^2\right]$$
$$= E\left[\left((\lambda_1 Z_1 - \lambda_1 E\left[Z_1\right]) + (\lambda_2 Z_2 - \lambda_2 E\left[Z_2\right])\right)^2\right]$$

$$= \lambda_1^2 E\left[\left(Z_1 - E\left[Z_1\right]\right)^2\right] + \lambda_2^2 E\left[\left(Z_2 - E\left[Z_2\right]\right)^2\right] \quad (34)$$

This can be rewritten as

$$Var(Z) = \lambda^2.Var(Z_1) + (1-\lambda)^2.Var(Z_2) \quad (35)$$

Especially, given that the output of Z_1 and Z_2 is 2-dimentional (Latitude and Longitude coordinates), a rational is to take the norm of (35), yielding

$$|Var(Z)| = \lambda^2.|Var(Z_1)| + (1-\lambda)^2|Var(Z_2)| \quad (35)$$

To minimize Var(Z), one can set the derivative of |Var(Z)| expression with respect to λ to zero, which yields

$$\lambda = \frac{P_{Taylor}(1,1)^2 + P_{Taylor}(2,2)^2}{P_{Taylor}(1,1)^2 + P_{Taylor}(2,2)^2 + P_{Chan}(1,1)^2 + P_{Chan}(2,2)^2} \quad (36)$$

Consequently, the combined estimator reads as

$$Z = \lambda\begin{bmatrix} x_{Chan} \\ y_{Chan} \end{bmatrix} + (1-\lambda)\begin{bmatrix} x_{Taylor} \\ y_{Taylor} \end{bmatrix} \quad (37)$$

5. Simulation

We reproduce the simulation setting suggested by Zhang et al., in [6]. The simulation conditions are as follows. First, let R=3000m, the number of Base stations (BS) is 4, 5, 6 and 7. The Cartesian coordinates of each BS are as follows: (0,0), $(\sqrt{3}R,\ 0)$, $(\sqrt{3}R/2,\ 3R/2)$, $(-\sqrt{3}R/2,\ 3R/2)$, $(-\sqrt{3}R,\ 0)$, $(-\sqrt{3}R/2,\ -3R/2)$, $(\sqrt{3}R/2,\ -3R/2)$. Basically, when three BS were used, then the first three BS of the above are employed, similarly, if the simulations uses 5 BS, then the first five BS of the above list are employed, etc.

Without non-line-of-sight (NLOS) error, measurement errors are assumed to obey zero mean Gaussian distribution is only considered with varying standard deviation values. Performances of the different positioning methods are compared with respect to Root Mean Square Errors (RMSE).

Figure 1 provides results of the RMSE evaluations as a function of the noise realizations (zero mean Gaussian with standard deviations values 30us, 45us, 60us, 75us, 90us, 105us, 120us, 135us, 150us) using Chan's location method and with different number of base stations (NBS) (4, 5, 6 and 7). Typically, to the initial true mobile position is added a random perturbation generated by Gaussian noise of zero mean and a given standard deviation. Consequently, the obtained time of flight obtained when adding the random

noise to the true time from the initial true mobile position to each of the base station was used as the input for Chan's method as well as other methods (Taylor and combined Taylor-Chan), while the true position is also used to quantify the RMSE evaluation.

As it can be noticed from the above plot, in accordance with the intuition, the RMES increases proportionally to the noise intensity as exemplified by the standard deviation value. On the other hand, the more the number of base stations employed is higher, the better the accuracy of the estimation in terms of RMSE. Figure 2 provides the quality of Chan's estimator in terms of variance-covariance matrix, where the result of the first element of the matrix is displayed, corresponding the latitude coordinate variance estimates. Notice that, as expected, the variance decreases with the number of base stations employed in the estimation process in average.

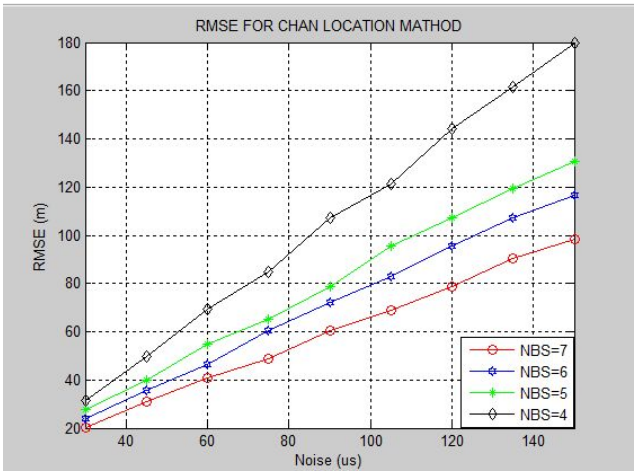

Figure 1. RMSE results when using Chan's location method

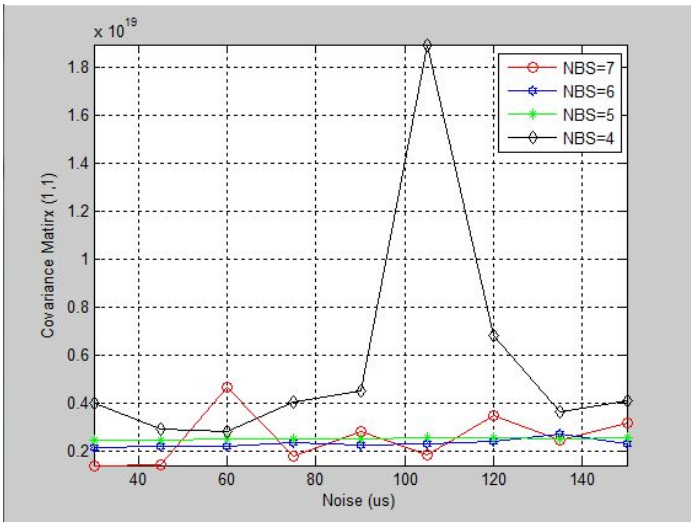

Figure 2. Variance of the first component of Chan's estimate

Similarly, results using Taylor's method and the combined Taylor and Chan's methods are highlighted in figures 3, 4, 5 and 6.

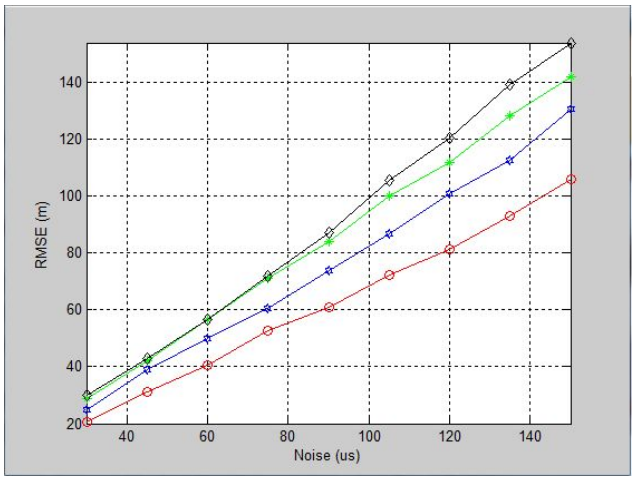

Figure 3. RMSE results when using Taylor's location method

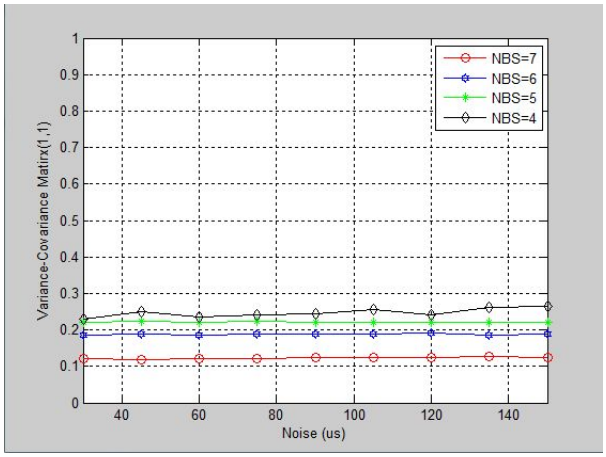

Figure 4. Variance of the first component of Taylor's estimate

Similarly to Chan's method, it is straightforward that Taylor's method results also agree with the intuition when the number of base stations increases and the intensity of noise. Although Taylor's variance result seems more consistent with respect to number of base stations as well as noise intensity as less fluctuations of the behaviour is noticed in contrast to Chan's result. This is largely explained by the iterative nature of Taylor's method which forces the variance components to systematically decrease with respect as noise increases or higher number of base stations were used. A fair comparison between Chan's method and Taylor's estimates in terms of RMSE indicate a slight improvement of Chan's method. This result is however to be taken with cautious as Taylor's method is much sensitive to initialization. For this simulation, the initial guess were taken as the centre of gravity of the various BSs. However, a better initialization would ultimately yield a better result.

Figure 5 provides the outcome of the combination of Taylor and Chan estimator using the approach highlighted in section 4 of this paper.

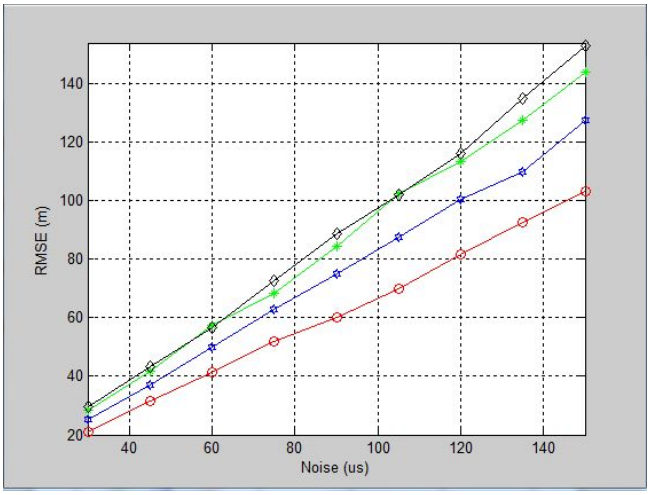

Figure 5. RMSE results when using a combination of Taylor and Chan location method

Intuitively, the outcome always lies within the outcome of Chan's and Taylor's estimators weighted with respect to the inverse of their corresponding variance-covariance matrices. While its associated variance outcome is theoretically always less than its counterpart in case of Chan or Taylor estimator. Strictly speaking, the obtained outcome is natural when the assumption of independence of the two estimators is fully satisfied. However, if one uses, for instance, Chan's estimate to initialize Taylor estimator, although the result of Taylor estimator will be (slightly) improved, the use of the combined filter will be questioned as it violates the independence assumption. On the other hand, the obtained accuracy in terms of RMSE seems acceptable with respect to current level of precision provided by mobile location services.

Conclusion

This paper reviewed two methods employed in mobile positioning; namely, Taylor's method and Chan's method of hyperbolic estimators. A combination of the two estimators has been put forward using a linear combination of the two estimators yielding the minimum variance estimate. A simulation platform using Monte Carlo simulations has been designed to test the performance of the estimators under different noise intensity scenarios and using a range of known base stations. The results shown to be conform to the intuition and widely in agreement with the current accuracy level observed in mobile location services.

REFERENCES

[1] A. Abrardo, G. Benelli, C. Maraffon and A. Toccafondi, Performance of TDOA-based Radiolocation Techniques in CDMA Urban Environments, *Proceedings of the IEEE International Conference on Communication*, 2002 , p. 431 - 435

[2] Y. T., Chan and K.C. Ho, A simple and Efficient Estimator for Hyperbolic Location, *IEEE Transactions on Aerospace and Electronic Systems,* **42**(8), 1994, p. 1905-1915.

[3] C.C. Docket, Revision of the Commission rules to ensure compatibility with enhanced 911 emergency calling systems, *RM-8143, Report No. 94-102, FCC*, 1994

[4] A. Franklin, R. Graybilland and B. Deal, Combining unbiased estimators, *Biometrics*, **15**(4), 1959, pp. 543-550.

[5] R. Shimura and I. Sasase, TDOA mobile terminal positioning with weight control based on received power of pilot symbol in Taylor series estimation, 17th *IEEE International Symposium on Personal, Indoor and Mobile Radio Communications*, 2006, p. 1 - 5

[6] J-W., Zhang, Yu Cheng-lei and Ji Ying-ying. The performance analysis of Chan Location Algorithm in cellular network, *Proceedings of the World Congress on Computer Science and Information Engineerin*g – 2009, p. 339-343.

TDOA Wireless Localization Comparison Influence of Network Topology

Hao Li M. Oussalah
University of Birmingham, School of Electronics, Electrical and Computer Engineering,
Edgbaston, Birmingham, B15 2TT, UK
Hxl441@bham.ac.uk, M.Oussalah@bham.ac.uk

Abstract

The interest to wireless positioning techniques has been increasing in recent decades due to wide spread of location-based services as well as constraints imposed by regulator on cellular operator to achieve an accepted level of cellular accuracy regardless of availability of GPS signals. Nevertheless, failure of some base stations cannot be fully avoided, yielding various cellular topologies, which, in turn would likely influence the accuracy of the positioning. This paper explores four types of cellular topologies: balanced, circular, U-shape and linear, which can be inferred from balanced topology structure. Assuming time difference of arrival technology and, up to some extent, time of arrival technology were employed, least square like methods are contrasted with maximum likelihood, Taylor, Chan and hybrid approaches in a simulation platform.

Keywords: wireless positioning, topology, network, TDOA

1. INTRODUCTION

With the substantial increase of location based services, which include E911 [1] emergency services where user is tracked with high accuracy using only operator's cellular infrastructure, mapping and path finding, targeted advertising, location based social networking such as MySpace, Friendster or Facebook, the interest to wireless localization techniques has grown drastically in the last two decades. In addition, many ubiquitous applications, including systems like EasyLiving [2] and the Rhino Project [3], among others [4], would benefit from a practical location sensing system. RADAR [5] was one of the first systems to use radio frequency (RF) signal intensity for location-sensing. Small et al. [6] and Smailagic et al. [7] looked at how signal intensity varies over time and developed a location-sensing system based on these observations.

Strictly speaking, several localization techniques have been reported in the literature in order to deal with wireless localization, depending on the available technology, which include time-of-arrival (ToA), angle-of-arrival (AOA), time-difference of arrival (TDOA), and received-signal strength (RSS) [8]. Likely the RSS method, where the signal strength from the base station as received in the mobile station is employed as key, which is the less demanding and cheap technology as it does not require any infrastructure change or additional hardware component, which motivates its use in some of above projects like radar [2, 5]. TDOA is recognized for its efficiency and high precision, but requires synchronization among base stations. Indeed, this requires a very accurate timing reference at the mobile which would need to be synchronized with the clock at the base stations. In commonly employed CDMA system [9], TDOA can be implemented using the pilot tones from different base stations, where the pilot tone transmitted by each cell is used as a coherent carrier reference for synchronization by every mobile in that cell coverage area, which enables the mobile to differentiate each cell site's pilot tone. Therefore the mobile measures the arrival time differences of at least three pilot tones transmitted by three different cells.

Most of the literature survey, including the survey of Guvenc and Chong [8], investigated the performance of the localization algorithms regardless the sensor infrastructure disposition. Although in GSM and UMTS network, it is acknowledgeable that the antenna positioning problem (APP) is one of the major design issues for any mobile operators. It is universally agreed that several factors influence such design. This includes, the (expected) traffic, type of antennas, allocated frequencies, interference, coverage, infrastructure nearby, among others. Since earlier work of Anderson and McGeehan [9] in antenna positioning problem, several other works have been published as well as several national and transnational research projects have been initiated. The idea of integrating several aspects of the network design problem is carried out by Reininger and Caminada [10], as part of the ARNO Project. In the latter, the authors partially relate APP and frequency allocation problem by ‘‘optimizing location and parametrization of the base stations on one shot”.

The integration of locating and configuring base stations is carried further to UMTS networks by Amaldi et al. [11], where the problem of selecting the location and configuring the base stations so as to minimize installation costs as well as to meet the traffic demand is considered. In [12] a trade-off is sought between minimum overlap and desirable cell shapes while the quality of radio coverage is controlled in the constraints. Zimmermann et al. [13] as part of EU ARNO project developed a multi-criteria model that involves a minimum cost, minimum interference and optimum cell shapes. This reveals that most of work in this area has rather been performed from operational research perspective where a multi-criteria decision making like approach has been pursued. Unfortunately less work has been achieved from wireless positioning accuracy perspective has been achieved, although this would significantly contribute towards the E911, for instance. This motivates the current work where some commonly employed techniques involving TDOA and ToA technology are contrasted and investigated with respect to the geometrical disposition

of the antennas. More specifically, approximated least square solutions, Maximum likelihood estimation [8], Chan [14], Taylor [15] and a newly introduced combination of Chan-Taylor [16] are compared when considering several antenna topologies. The latter includes linear, circular, U-shape and balanced shapes. Such topology can straightforwardly be inferred from regular (optimal) cellular disposition when some blocking occurs making some BS disabled. The first section of this paper reviews the (eight) main localization techniques employed in this study. Section 3 highlights the simulation platform and comments the obtained results. Finally some conclusive remarks are reported in Section 4.

2. REVIEW OF MAIN TDOA LOCALIZATION TECHNIQUES

Let us consider a general model for the two dimensional (2-D) estimation of a source, consisting of mobile station with Cartesian coordinates (x, y) using M base stations of known locations (X_i, Y_i), i=1 to M. Then the measured distance between the mobile station and the ith base station can be given as:

$$d_i = \sqrt{(X_i - x)^2 + (Y_i - y)^2} + \varepsilon_i = \hat{d}_i + \varepsilon_i = ct_i \quad (1)$$

With $\varepsilon_i \sim \mathcal{N}(\sigma_i^2, 0)$ is the additive white Gaussian noise with variance σ_i^2. $\hat{d}_i$(i=1, M) stands for estimated distance from MS to ith BS, and t_i is the TOA of the signal at the ith BS and c is the speed of light. Consequently, for M measurements, the problem comes down to estimating (x,y) from the following set of equations:

$$\begin{bmatrix} (X_1 - x)^2 + (Y_1 - y)^2 \\ . \\ (X_M - x)^2 + (Y_M - y)^2 \end{bmatrix} = \begin{bmatrix} \hat{d}_1^{\,2} \\ . \\ \hat{d}_M^{\,2} \end{bmatrix} \quad (2)$$

2.1 Least Square and Maximum Likelihood Solutions

Assuming that one base station, say rth BS, acts as a reference, subtracting rth row in (2) from other rows, yields, after some manipulations and defining $K_i = X_i^2 + Y_i^2$ (i=1, M), to matrix equation:

$$AX = \frac{1}{2} B, \quad (3)$$

where

$$A_{[(M-1)\times 2]} = \begin{bmatrix} X_1 - X_r & Y_1 - Y_r \\ X_2 - X_r & Y_2 - Y_r \\ . & . \\ X_M - X_r & Y_M - Y_r \end{bmatrix} \quad ; \quad X = \begin{bmatrix} x \\ y \end{bmatrix} \quad ; \quad B_{[(M-1)\times 1]} = \begin{bmatrix} d_r^2 - d_1^2 - (K_r - K_1) \\ d_r^2 - d_2^2 - (K_r - K_2) \\ . \\ d_r^2 - d_M^2 - (K_r - K_M) \end{bmatrix}$$

(4)

A linear least square solution to (4) yields the following *LLT1* solution:

$$X = \frac{1}{2}(A^T A)^{-1} A^T B \tag{5}$$

Another solution proposed in [17] assumes that each BS acts as a servicing BS, and therefore, concatenates the result yielding M (M-1) equations as described by the new *A*, *B* matrices as:

$$A = \begin{bmatrix} X_2 - X_1 & Y_2 - Y_1 \\ X_3 - X_1 & Y_3 - Y_1 \\ \vdots & \vdots \\ X_M - X_1 & Y_M - Y_1 \\ X_3 - X_2 & Y_3 - Y_2 \\ X_4 - X_2 & Y_4 - Y_2 \\ \vdots & \vdots \\ X_M - X_2 & Y_M - y_2 \\ \vdots & \vdots \\ X_M - X_{M-1} & Y_M - Y_{M-1} \end{bmatrix} \qquad B = \begin{bmatrix} d_1^2 - d_2^2 - K_1 + K_2 \\ d_1^2 - d_3^2 - K_1 + K_3 \\ \vdots \\ d_1^2 - d_M^2 - K_1 + K_M \\ d_2^2 - d_3^2 - K_2 + K_3 \\ d_2^2 - d_4^2 - K_2 + K_4 \\ \vdots \\ d_2^2 - d_M^2 - K_2 + K_M \\ \vdots \\ d_{M-1}^2 - d_M^2 - K_{M-1} + K_M \end{bmatrix} \tag{6}$$

Where the application of (5) yields what we will refer here as *LLT2* solution

A third approach to least square solution was proposed in [18] where the average of all measurements is subtracted from each measurement equation in (2), yielding new matrices:

$$A = \begin{bmatrix} X_1 - \frac{1}{M}\sum_{j=1}^{M} X_j & Y_1 - \frac{1}{M}\sum_{j=1}^{M} Y_j \\ X_2 - \frac{1}{M}\sum_{j=1}^{M} X_j & Y_1 - \frac{1}{M}\sum_{j=1}^{M} Y_j \\ \vdots & \vdots \\ X_M - \frac{1}{M}\sum_{j=1}^{M} X_j & Y_M - \frac{1}{M}\sum_{j=1}^{M} Y_j \end{bmatrix} \qquad B = \begin{bmatrix} \frac{1}{M}\sum_{j=1}^{M} d_j^2 - d_1^2 - \frac{1}{M}\sum_{j=1}^{M} K_j^2 + K_1 \\ \frac{1}{M}\sum_{j=1}^{M} d_j^2 - d_2^2 - \frac{1}{M}\sum_{j=1}^{M} K_j^2 + K_2 \\ \vdots \\ \frac{1}{M}\sum_{j=1}^{M} d_j^2 - d_M^2 - \frac{1}{M}\sum_{j=1}^{M} K_j^2 + K_N \end{bmatrix} \tag{7}$$

Again the application of (5) yields a solution referred to as *LLT3*.

A fourth least square solution is obtained when choosing the rth reference BS as the one that induces the smallest distance among all other distances but yields same generic solution as (3). Such solution was suggested in [19] and is referred to here as *LLT4*.

The previous least square based solutions discard the knowledge about the uncertainty pervading the measurements (e.g., ε_i) as modelled by the associated

variance-covariance matrix, in order to account for such effect, the maximum likelihood solution *MLS* yields as a counterpart of (5) [20]:

$$X = \frac{1}{2}(A^T C^{-1} A)^{-1} A^T C^{-1} B$$

(8)

Where A, B are defined as in (4), while the variance-covariance matrix is given by, assuming without loss of generality $\sigma_1 = \sigma_2 = ... = \sigma_M$:

$$C = 4d_r{}^2\sigma^2 + 2\sigma^4 + diag\left\{4\sigma^2 d_1^2 + 2\sigma^4 \quad \dots \quad 4\sigma^2 d_i^2 + 2\sigma^4 \quad \dots \quad 4\sigma^2 d_M^2 + 2\sigma^4\right\} \qquad (9)$$

2.2 Chan and Taylor methods

In Chan's method [14], one assumes the knowledge of the TDOA with respect to a reference BS, say r, so that the measurements are:

$$d_{i,r} = d_i - d_r = cT_{i,r}$$

(10)

Where the $T_{i,r}$ is the difference of time arrival between ith and rth base stations, and d_i are as in (1). Similarly, one denotes $X_{i,r} = X_i - X_r$, $Y_{i,r} = Y_i - Y_r$). Squaring (10) and substituting in (1) yields after some manipulations to [14]:

$$d_{i,r}^2 + 2d_{i,r}d_r = K_i - K_r - 2X_i x - 2Y_i y \quad (i=1,M,\ i \neq r)$$

(11)

(11) can be put on the form (3) where

$$A_{[(M-1)x3]} = \begin{bmatrix} X_{1,r} & Y_{1,r} & d_{1,r} \\ . & & \\ X_{M,r} & Y_{M,r} & d_{M,r} \end{bmatrix};\ X = \begin{bmatrix} x \\ y \\ d_r \end{bmatrix};\ B_{[(M-1)x1]} = \begin{bmatrix} K_1 - K_r - d_{1,r}^2 \\ . \\ K_M - K_r - d_{M,r}^2 \end{bmatrix}$$

(12)

Where the unknown vector X contains redundant component d_r, and the solution is approached when first assuming low impact of such dependency to the solution, which is then computed in a two-step strategy. Namely, a linear weighted least square is applied first yielding:

$$X = \left(A^T Q^{-1} A\right)^{-1} A_a{}^T Q^{-1} B \quad , \quad \text{with} \quad Q = diag\{\sigma_1, ...\sigma_M\} \quad .$$

(13)

In the second step, the estimate is refined as

$$X = \left(A^T \Psi^{-1} A\right)^{-1} A^T \Psi^{-1} B$$

(14)

With

$\Psi = c^2 BQB$, with $B = diag\{ d_1^0, d_2^0, ..., d_M^0 \}$

(15)

And d_i^0 stands for noise-free estimate of d_i , which is approximated assuming $\mathrm{cov}([x \;\; y \;\; d_r]^T) \approx (A \; \Psi^{-1} \; A)^{-1}$, see [14] for detail.

On the other Taylor's approach [15] to solve (11) in [x, y] starts with an initial guess (x_0; y_0) of the unknown mobile position (x, y), and computes the deviations of the position location estimation:

$$\delta = \begin{bmatrix} \Delta x \\ \Delta y \end{bmatrix} = \left(G_t^T Q^{-1} G_t \right)^{-1} G_t^T Q^{-1} h_t$$

(16)

With

$$h_t = \begin{bmatrix} d_{2,1} - (d_1 - d_2) \\ d_{3,1} - (d_1 - d_3) \\ . \\ d_{M,1} - (d_1 - d_M) \end{bmatrix}, \quad G_t = \begin{bmatrix} \frac{X_1 - x}{d_1} - \frac{X_2 - x}{d_2} & \frac{Y_1 - y}{d_1} - \frac{Y_2 - y}{d_2} \\ \frac{X_1 - x}{d_1} - \frac{X_3 - x}{d_3} & \frac{Y_1 - y}{d_1} - \frac{Y_3 - y}{d_3} \\ . & \\ . & \\ \frac{X_1 - x}{d_1} - \frac{X_M - x}{d_M} & \frac{Y_1 - y}{d_1} - \frac{Y_M - y}{d_M} \end{bmatrix}$$

(17)

In the next iteration, x_0 and y_0 are set to $x_0 + \Delta x$ x and $y_0 + \Delta y$. The whole process is repeated until Δx and Δy are sufficiently small, resulting in the estimated PL of the source (x; y). The Taylor-series method can provide accurate results; however, it requires a close initial guess (x_0, y_0) to guarantee convergence and can be computationally intensive.

In [15], a combination of Chan-Taylor method has been put forward. The proposal assumed a linear combination of the two methods such that the global variance-covariance is minimized. This yield

$$X = \lambda \begin{bmatrix} x_{Chan} \\ y_{Chan} \end{bmatrix} + (1 - \lambda) \begin{bmatrix} x_{Taylor} \\ y_{Taylor} \end{bmatrix},$$

(18)

With

$$\lambda = \frac{P_{Taylor}(1,1)^2 + P_{Taylor}(2,2)^2}{P_{Taylor}(1,1)^2 + P_{Taylor}(2,2)^2 + P_{Chan}(1,1)^2 + P_{Chan}(2,2)^2}$$

(19)

Where P_{Taylor} and P_{Chan} stand for variance-covariance matrices associated to Taylor and Chan methods, respectively.

3. SIMULATION

Similarly to most studies investigating wireless localization techniques, the performances are often evaluated through a set of Monte Carlo simulations. A generic simulation platform is shown in Figure 1. The simulation assumes a set of base station at fixed locations (7 BS in Figure 1). As in practical implementations, the cells have hexagonal shapes in order to restrict the interference between cells as no overlapping region exists. By abuse, we shall refer to such situation a balanced topology. Nevertheless in case where a blocking occurs in some cells, this yields different topology. For instance if the middle BS in Fig 1 is failed, this yields a circular topology. Similarly if the two first cells in the second row of cells in Fig 1 failed, the cells form a U-like shape, so this is referred to U-shape topology. In total, we shall consider here four different topologies: Circular, U-shape, linear and the balanced one as in Figure 1.

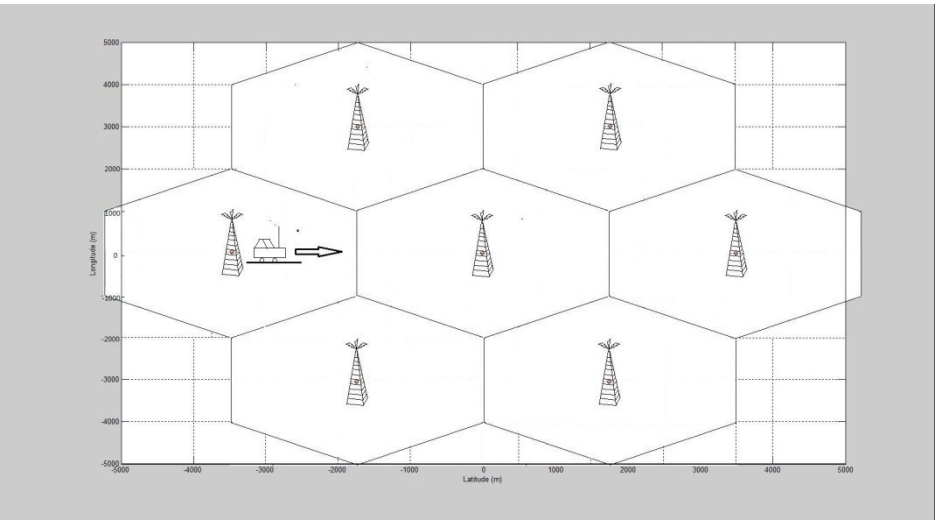

Figure: Generic simulation platform (Balanced topology).

Besides we shall consider a vehicle moving at a constant speed in one direction. We therefore, compute for each of the aforementioned localization technique, the localization accuracy with respect to a set of Monte Carlo simulations. The parameters of the simulations for each topology are described in Table 1. The three other topology structures are represented in Figure 2.

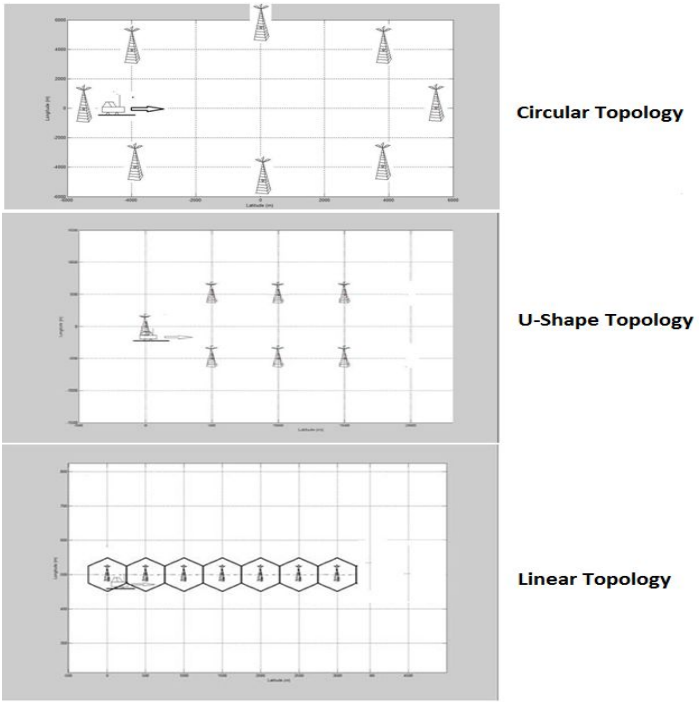

Figure 2: Circular, U-shape and Linear shape topologies

Typically, to the initial true mobile position is added a random perturbation generated by a zero-mean Gaussian noise with a given standard deviation. A pseudo code highlighting the functioning of the simulation is described in Figure 3.

Table 1: Parameters of the simulation setup

BS Topology	Cell Radius	Noise Standard Deviation	MS Starting Position	Moving Distance	Time	Constant Velocity	Freq. of
Balanced	3000 m	0.1 us	[-5000, 0]	10000 m	50 s	200 m/s	Once / second
Circle	3000 m	0.1 us	[-5000, 0]	10000 m	50 s	200 m/s	Once / second
U-Shape	3000 m	0.1 us	[0, 0]	1500 m	50 s	30 m/s	Once / second
Line	3000 m	0.1 us	[0, 450]	3000 m	50 s	60 m/s	Once / second

[MS, RMSE] =LOCATION_ESTIMATION (TOPOLOGY)

RETRIEVE BS_i, Vehicle Movement direction, Std σ, Initial MS0

FOR EACH sampling interval k

FOR EACH Monte Carlo iteration

MS = ComputePosition (MS0, k)

Generate a realization of Noise = (0,σ)

FOR EACH BS

Calculate distance $d_i = \sqrt{(BS_i x - MSx)^2 + (BS_i y - MSy)^2} + Noise$

END FOR

Estimate Position *MS*= *LocationAlgorithm* (*d, BS, Noise*)

END FOR

Calculate RMSE of current MS

END

END

Figure 3: Pseudo-code of simulation

In order to quantify the performance of the eight localization techniques, at each sampling interval along the trajectory of the vehicle, the RMSE of the averaged MS estimation over the 1000 Monte Carlo simulations is calculated for each location technique; namely,

$RMSE(t) = \sqrt{\frac{\sum_{i=1}^{n}\left((x_{True}(t) - x_i(t))^2 + (y_{True}(t) - y_i(t))^2\right)}{n}}$, where $(x_i(t), y_i(t))$ stands for MS (x, y) estimation at i[th] Monte Carlo simulation and t sampling interval, and n=1000.

Figures 4, 5, 6 and 7 summarize the localization errors in terms of RMSE of the eight localization techniques when using balanced, circular, U-shape and linear topology.

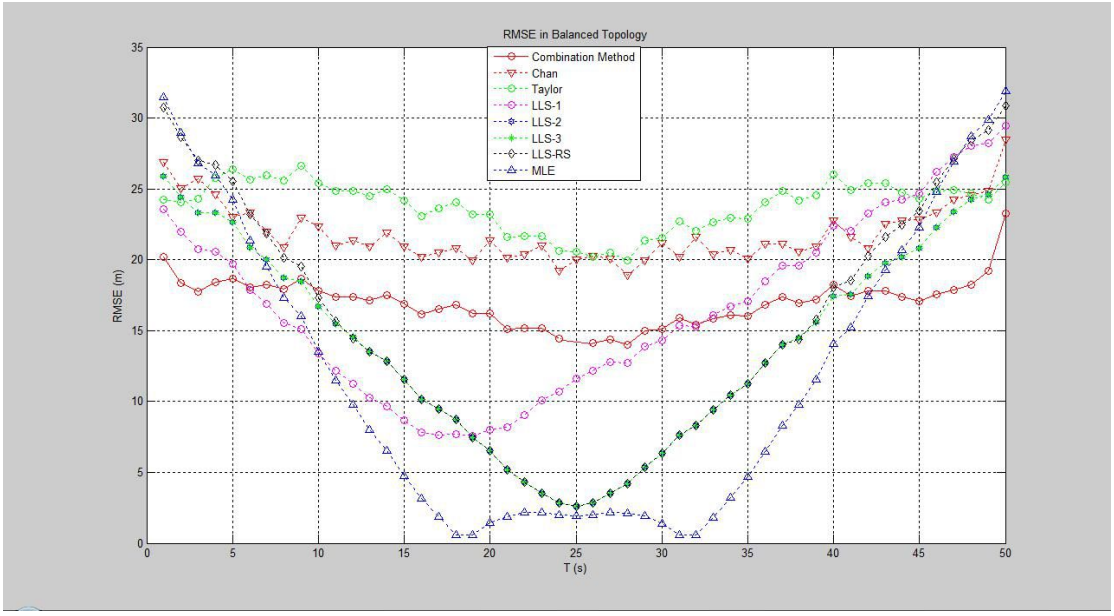

Figure 4: RMSE value in case of Balanced topology

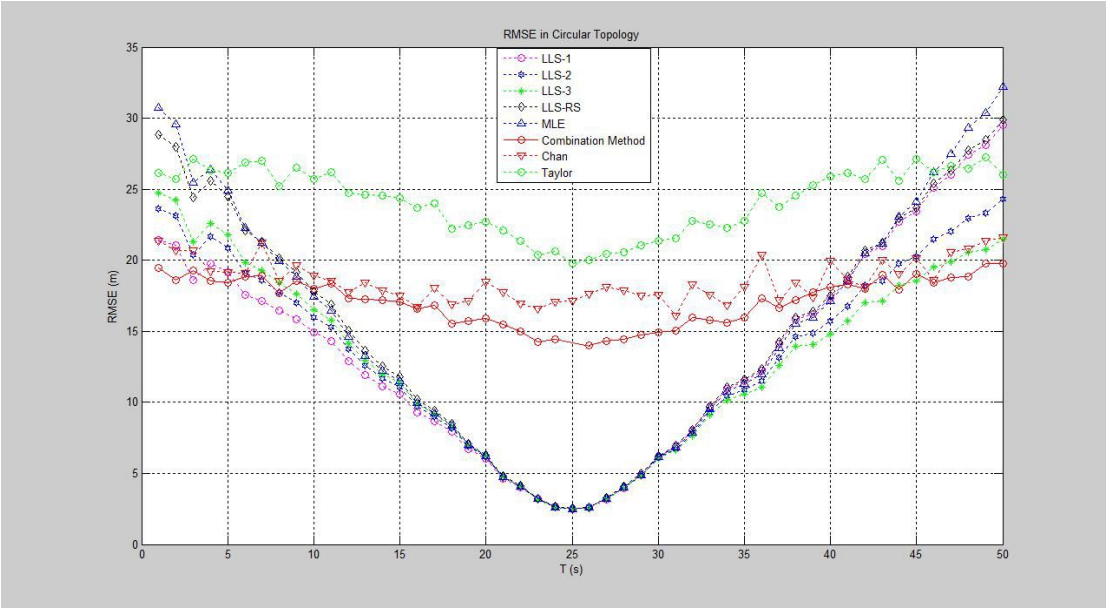

Figure 5: RMSE value in case of Circular topology

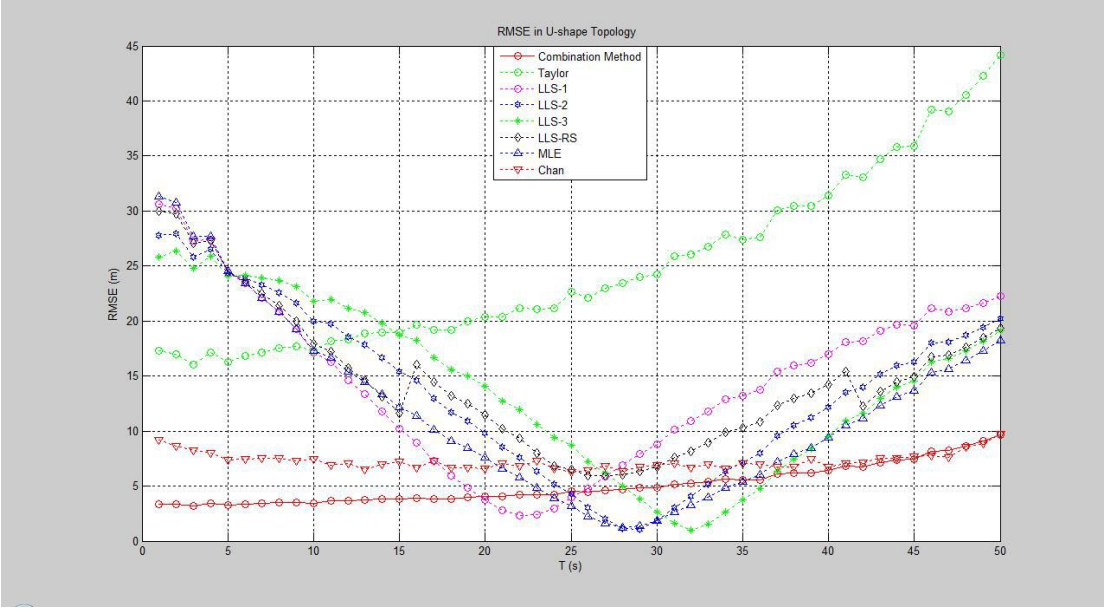

Figure 6: RMSE value in case of U-shape topology

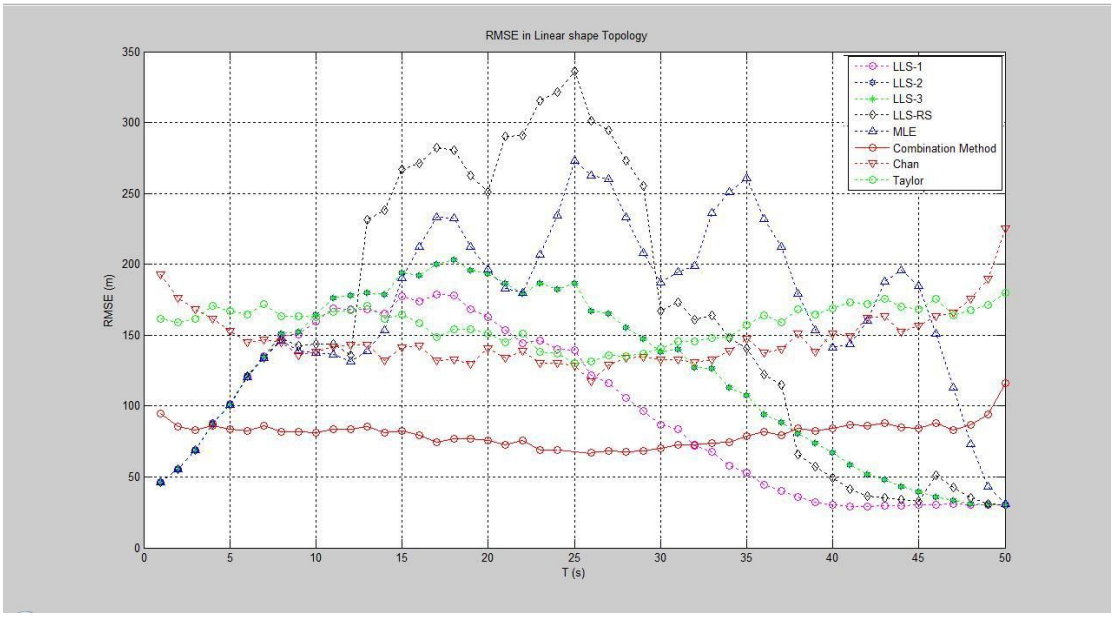

Figure 7: RMSE values in case of Linear shape topology

From the above figures, one can notices the following

- The discrepancy of the various positioning techniques when a change of a topology occurs demonstrates the influence of the topology on the accuracy of the underlying positioning method.
- In the above simulation, at a given sampling interval, the measurements from all base stations are assumed available and aggregated in the localization technique. Although such data cannot be straightforwardly be available in cellular network in practice, where the mobile station is only connected to the base station providing the strongest signal, it is still available from network provider perspective. Besides, such approach is commonly employed in previous work that investigated the performance of cellular/wireless network positioning techniques as testified in the extensive review paper [8].
- Looking at the range of the RMSE values with respect to various topologies reveals that the balanced topology produces the best performance with respect to all positioning techniques, while the linear shape topology yields the worst performance as its associated values RMSE go beyond 340 m as compared to less than 30 m in case of balanced topology. This shows that whenever possible the use of balanced topology should be persuaded. This is mainly due to quality of the obtained measurements, where, at least from geometrical perspective, yields comprehensive intersection of the underlying circles.
- The combination method of Chan and Taylor shows on average that it marginally outperforms the remaining seven topologies regardless the topology employed.

- The investigation of the low values of RMSEs in the above figures reveals that (almost) the least square like methods approach the minimum RMSE value at a sampling time corresponding to the time the vehicle comes close to underlying base station. While such phenomenon is less apparent in case of Chan, Taylor and Combined Chan-Taylor methods where less sensitivity is observed. This is mainly due to the global nature of the above positioning methods.
- The above results have been obtained assuming low noise perturbation as testified by the low standard deviation shown in Table 1. Nevertheless, the influence of the noise intensity cannot be excluded. On the other hand, few extra simulations with various noise intensities have shown that the generic trends issued from this analysis are not void when the level noise increases. To see it, a 3D graph is depicted in Figure 8 and Figure 9 for balanced and linear like topologies.
- So far, the metric employed for comparison is only related to the accuracy of the positioning technique. Nevertheless, one should bear in mind that some techniques are computationally significantly more expensive than others. From this perspective, LLS1 is computationally the most effective one, and also provides good balance between accuracy and computational cost. While Taylor and combined Chan-Taylor are the most expensive ones because of the iterative approach they do involve. Strictly speaking, even for the LLS1, the computational cost increases with the number of measurements available (value of parameter M). This is mainly due to the cost involved by the matrix inversion operation.

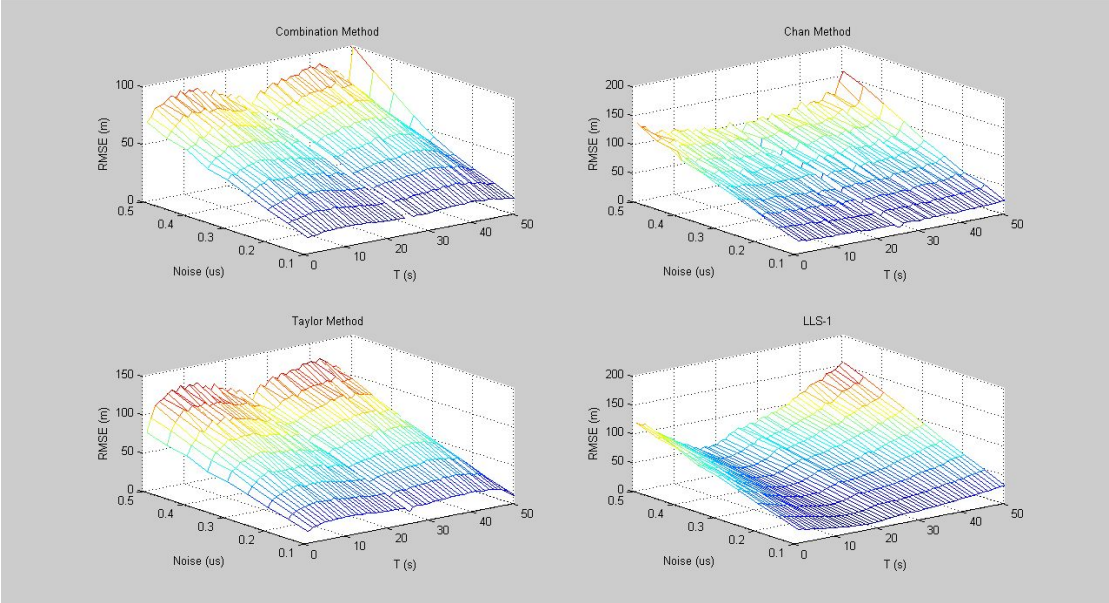

Figure 8: Noise influence in case of Balanced topology structure

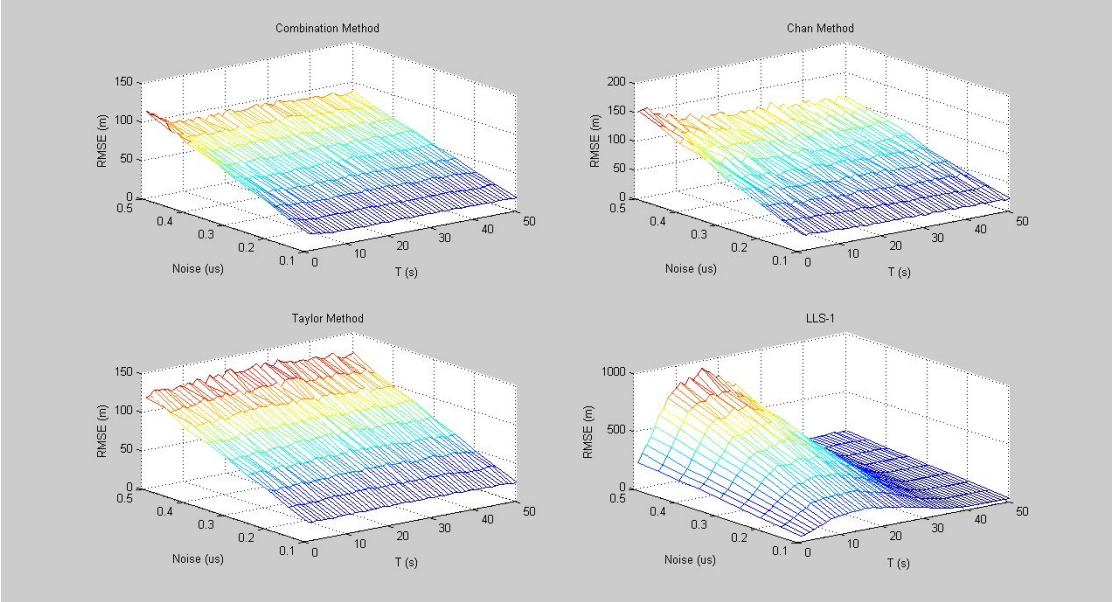

Figure 9: Noise influence in case of Linear shape topology

4. CONCLUSION

This paper highlights the importance of the antenna positioning when looking at the accuracy of the wireless positioning techniques. Four type of topologies, which can straightforwardly be generated by a regular balanced cellular topology when some blocking occurs, have been investigated. Wireless positioning techniques related to TDOA technology have been examined. This corresponds to four distinct least square based approaches, maximum likelihood, Chan, Taylor and a combined Chan-Taylor method. Simulation results have been obtained assuming a vehicle moving at a constant speed along the given topology. The results demonstrate the credibility of the topology influence on the positioning accuracy. Besides, the combined Chan-Taylor shows a marginally increased performance in terms of RMSE and sensitivity to base station positioning.

References

[1] C.C. Docket, Revision of the Commission rules to ensure compatibility with enhanced 911 emergency calling systems, *RM-8143, Report No. 94-102, FCC*, 1994

[2] B. Brumitt, B. Meyers, J. Krumm, A. Kern, and S. Shafer. EasyLiving: Technologies for intelligent environments, Proceeding of the second international symposium on Handheld and Ubiquitous Computing, Bristol, UK

[3] G. Abowd, K. Lyons, and K. Scott. The Rhino project, Aug. 1998.

http://www.cc.gatech.edu/fce/uvid/rhino.html
[4] G. D. Abowd, C. G. Atkeson, J. Hong, S. Long, R. Kooper, and M. Pinkerton. Cyberguide: a mobile context-aware tour guide. Wireless Networks, 3(5):421–433, Oct. 1997.
[5] P. Bahl and V. N. Padmanabhan. Enhancements to the RADAR user location and tracking system. Technical Report MSR-TR-2000-12, Microsoft Research, Feb. 2000
[6] J. Small, A. Smailagic, and D. P. Siewiorek. Determining user location for context aware computing through the use of a wireless LAN infrastructure, Dec. 2000. http://www-2.cs.cmu.edu/˜aura/docdir/small00.pdf
[7] A. Smailagic, D. Siewiorek, J. Anhalt, D. Kogan, and Y. Wang. Location sensing and privacy in a context aware computing environment. Pervasive Computing, 2001
[8] I. Guvenc and CC Chong, A survey on TOA Based Wireless Localization and NLOS Mitigation Techniques, IEEE Communication Surveys and Tutorials, 11 (3), 2009, 107-124.
[9] J. P. McGeehan, and H.R. Anderson. Optimizing Microcell Base Station Locations Using Simulated Annealing Techniques. In: *Proc. of the IEEE Vehicular Technology Conference*,1994, pp. 858–862
[10] P. Reininger, and A. Caminada, .Model for GSM Radio Network Optimisation. In: *2nd Intl. ACM/IEEE MobicomWorkshop on Discrete Algorithms and Methods for Mobile Computing and Communications (DIALM)*, Dallas, December 16, 1998
[11] E. Amaldi, P. Belotti, A. Capone, F. Malucelli, Optimizing base station location and configuration in UMTS networks. Annals of Operations Research 146, 2006, 135–151.
[12] A. Jedidi, A., Caminada, A., Finke, G., 2-Objective optimization of cells overlap and geometry with evolutionary algorithms. LectureNotes in Computer Science 3005, 2004, 130–139.
[13] J. Zimmermann, R. Hons, H. Muhlenbein, ENCON: an evolutionary algorithm for the antenna placement problem. Computers & Industrial Engineering 44, 2003, 209–226
[14] Y. T., Chan and K.C. Ho, A simple and Efficient Estimator for Hyperbolic Location, *IEEE Transactions on Aerospace and Electronic Systems,* **42**(8), 1994, p. 1905-1915.
[15] R. Shimura and I. Sasase, TDOA mobile terminal positioning with weight control based on received power of pilot symbol in Taylor series estimation, 17th *IEEE International Symposium on Personal, Indoor and Mobile Radio Communications*, 2006, p. 1 - 5
[16] Hao Li and M. Oussalah, Combination of Taylor and Chan method in Mobile Positioning, in: Proc. of IEEE CIS 2011 Conference, London, pp…
[17] S. Venkatesh and R. M. Buehrer, “A linear programming approach to NLOS error mitigation in sensor networks,” in Proc. IEEE Int. Symp. Information

Processing in Sensor Networks (IPSN), Nashville, Tennessee, Apr. 2006, pp. 301–308

[18] Z. Li, W. Trappe, Y. Zhang, and B. Nath, “Robust statistical methods for securing wireless localization in sensor networks,” in Proc. IEEE Int. Symp. Information Processing in Sensor Networks (IPSN), Los Angeles, CA, Apr. 2005, pp. 91–98.

[19] I. Guvenc, S. Gezici, F. Watanabe, and H. Inamura, “Enhancements to linear least squares localization through reference selection and ML estimation,” in Proc. IEEE Wireless Commun. Networking Conf. (WCNC), Las Vegas, NV, Apr. 2008, pp. 284–289

[20] S. M. Kay, Fundamentals of Statistical Signal Processing: Estimation Theory. Upper Saddle River, NJ: Prentice Hall, Inc., 1993